

SANDIA REPORT

SAND2015-2889

Unlimited Release

Printed April 2015

Numerical Simulations of Subscale Wind Turbine Rotor Inboard Airfoils at Low Reynolds Number

Myra L. Blaylock

David C. Maniaci

Brian R. Resor

Prepared by
Sandia National Laboratories
Albuquerque, New Mexico 87185 and Livermore, California 94550

Sandia National Laboratories is a multi-program laboratory managed and operated by Sandia Corporation, a wholly owned subsidiary of Lockheed Martin Corporation, for the U.S. Department of Energy's National Nuclear Security Administration under contract DE-AC04-94AL85000.

Approved for public release; further dissemination unlimited.



Sandia National Laboratories

Issued by Sandia National Laboratories, operated for the United States Department of Energy by Sandia Corporation.

NOTICE: This report was prepared as an account of work sponsored by an agency of the United States Government. Neither the United States Government, nor any agency thereof, nor any of their employees, nor any of their contractors, subcontractors, or their employees, make any warranty, express or implied, or assume any legal liability or responsibility for the accuracy, completeness, or usefulness of any information, apparatus, product, or process disclosed, or represent that its use would not infringe privately owned rights. Reference herein to any specific commercial product, process, or service by trade name, trademark, manufacturer, or otherwise, does not necessarily constitute or imply its endorsement, recommendation, or favoring by the United States Government, any agency thereof, or any of their contractors or subcontractors. The views and opinions expressed herein do not necessarily state or reflect those of the United States Government, any agency thereof, or any of their contractors.

Printed in the United States of America. This report has been reproduced directly from the best available copy.

Available to DOE and DOE contractors from

U.S. Department of Energy
Office of Scientific and Technical Information
P.O. Box 62
Oak Ridge, TN 37831

Telephone: (865) 576-8401
Facsimile: (865) 576-5728
E-Mail: reports@adonis.osti.gov
Online ordering: <http://www.osti.gov/bridge>

Available to the public from

U.S. Department of Commerce
National Technical Information Service
5285 Port Royal Rd.
Springfield, VA 22161

Telephone: (800) 553-6847
Facsimile: (703) 605-6900
E-Mail: orders@ntis.fedworld.gov
Online order: <http://www.ntis.gov/help/ordermethods.asp?loc=7-4-0#online>



SAND2015-2889
Unlimited Release
Printed April 2015

Numerical Simulations of Subscale Wind Turbine Rotor Inboard Airfoils at Low Reynolds Numbers

Myra L. Blaylock
Thermal/Fluid Sciences & Engineering Department
Sandia National Laboratories
P.O. Box 969
Livermore, California 94550-MS9957

David C. Maniaci
Brian R. Resor
Wind Energy Technologies Department
Sandia National Laboratories
P.O. Box 5800
Albuquerque, New Mexico 87185-MS1124

Abstract

New blade designs are planned to support future research campaigns at the SWiFT facility in Lubbock, Texas. The sub-scale blades will reproduce specific aerodynamic characteristics of utility-scale rotors. Reynolds numbers for megawatt-, utility-scale rotors are generally above 2-8 million. The thickness of inboard airfoils for these large rotors are typically as high as 35-40%. The thickness and the proximity to three-dimensional flow of these airfoils present design and analysis challenges, even at the full scale. However, more than a decade of experience with the airfoils in numerical simulation, in the wind tunnel, and in the field has generated confidence in their performance. Reynolds number regimes for the sub-scale rotor are significantly lower for the inboard blade, ranging from 0.7 to 1 million. Performance of the thick airfoils in this regime is uncertain because of the lack of wind tunnel data and the inherent challenge associated with numerical simulations. This report documents efforts to determine the most capable analysis tools to support these simulations in an effort to improve understanding of the aerodynamic properties of thick airfoils in this Reynolds number regime. Numerical results from various codes of four airfoils are verified against previously published wind tunnel results where data at those Reynolds numbers are available. Results are then computed for other Reynolds numbers of interest.

ACKNOWLEDGMENTS

Thanks to Matt Barone for consultations and making the data he has available to us. Thanks to Stefan Domino and Srinivasan Arunajatesan for help with Sierra codes.

A special thanks to Nando Timmer for helpful correspondence and access to the wind tunnel data files.

CONTENTS

1. Introduction.....	10
2. Approach.....	14
3. Analysis Tools	16
3.1. RFOIL.....	16
3.2. Fuego	16
3.3. Overflow	18
4. Available Experimental Results	20
4.1 Naming Convention.....	20
4.2 Published Wind Tunnel Data.....	21
5. Simulation Results for 30% Thick Airfoil.....	26
5.1. RFOIL.....	26
5.2. Fuego	27
5.3. Overflow	29
5.4. Compiled Results.....	32
5.5 RFOIL and Overflow for low Reynolds Numbers	38
6. Simulation Results for 25% Thick Airfoil.....	42
6.1. RFOIL.....	42
6.2. Overflow	43
6.3. Compiled Results.....	45
7. Simulation Results for 35% Thick Airfoil.....	50
7.1. RFOIL.....	50
7.2. Overflow	51
7.3. Compiled Results.....	52
8. Simulation Results for 40% Thick Airfoil.....	56
8.1. RFOIL.....	56
9. Discussion.....	58
10. Conclusions and Recommendations	60
11. References.....	62
Appendix A: Convergence test for overflow	64
Appendix B: RFOIL Results	68
DU 91-W2-250Mod.....	68
DU 97-W-300Mod.....	75
DU 99-W3-350	81
Appendix C: Airfoil Coordinates.....	88

FIGURES

Figure 1. Approximate Reynolds numbers (in millions) along the rotor span for a 3 MW rotor compared to a 225 kW (27 m) rotor.	11
Figure 2. Top Left: Close up of the grid created in CUBIT for DU 97-W-300Mod airfoil at $\alpha = 0^\circ$. Bottom Left: Same airfoil at $\alpha = -6^\circ$. Right: Entire grid domain with airfoil in the center.	17
Figure 3. The Overflow grid for DU 97-W-300Mod created with Chimera Grid Tools. The gray region indicates where the turbulence production terms are turned off.	18
Figure 4. NRT 13.5m Reynolds number operating range and airfoil thickness for incoming wind velocities of 5 and 10 m/s.	21
Figure 5. Lift curves from wind tunnel experiments for the DU 91-W2-250 and DU 91-W2-250Mod airfoils.	23
Figure 6. Pitching moment and drag data from wind tunnel experiments for DU 91-W2-250 and DU 91-W2-250Mod.	23
Figure 7. Lift data from wind tunnel experiments done for airfoil DU 97-W-300 and DU 97-W-300Mod.	24
Figure 8. Pitch and drag data from wind tunnel experiments done for DU 97-W-300 and DU 97-W-300Mod.	24
Figure 9. Lift and drag data from wind tunnel experiments for airfoil DU 99-W3-350 and the DU00-W-350 airfoil design.	25
Figure 10. Lift and drag data from wind tunnel experiments for airfoils DU 99-W3-405 and DU00-W-401.	25
Figure 11. Left: RFOIL results for DU 97-W-300Mod produced with $Ma = 0.11$. Right: RFOIL results with a changing Mach number.	26
Figure 12. RFOIL pitching moments and drag polars for DU 97-W-300Mod.	27
Figure 13. Left: Lift curve for the DU 97-W-300Mod airfoil using various turbulence models in Fuego. The black dash-dotted line is the experimental data (using the DU97-W-300 airfoil [18]) The red dot represents the simulation run on a fine mesh. Right: The drag polar for the LRSST case is compared with the experimental results [20].	28
Figure 14. Velocity magnitude around a DU 97-W-300Mod at $\alpha = 0, 6,$ and -6° using the current SST turbulence model in Fuego ($Re = 3 \times 10^6, Ma = 0.11$).	28
Figure 15. Overflow lift and drag polars for $Re = 3$ million with the transition location specified (red stars) and without (red circles) and RFOIL results with and without zig-zag tape (blue), both using DU97-W-300Mod, compared to experimental (solid black) data using DU97-W-300 [20].	30
Figure 16. Lift curve of the DU 97-W-300Mod airfoil using Overflow steady state runs with $Ma = 0.11$	30
Figure 17. Lift curve of the DU 97-W-300Mod airfoil using Overflow steady state and time accurate (OFTA) runs which have Mach numbers that vary with the Reynolds numbers.	31
Figure 18. Overflow pitching moment results and drag polars for the DU 97-W-300Mod airfoil.	31
Figure 19. Mach number from Overflow for the DU 97-W-300Mod airfoil at $Re = 0.7$ million for $\alpha = -2^\circ$ (left) and $\alpha = 16^\circ$ (right).	32
Figure 20. RFOIL lift results with $Ma = 0.11$ and $Ma = 0.21$, Fuego results with $Ma = 0.11$, and Overflow results with $Ma = 0.21$ are compared to wind tunnel values [20].	33

Figure 21. Left: For $Re = 3 \times 10^6$, RFOIL drag results with and without the correction factor of 1.09, Fuego results with $Ma = 0.11$, and Overflow results with $Ma = 0.21$ are compared to [20] wind tunnel values. Right: Comparison of drag results of DU 97-W-300Mod at $Re = 1 \times 10^6$ from RFOIL, corrected RFOIL, and Overflow to wind tunnel results [16].	33
Figure 22. Left: Lift to drag ratio for DU 97-W-300Mod at $Re = 3 \times 10^6$ for corrected and uncorrected RFOIL, Overflow, and Fuego compared to DU97-W-300 wind tunnel data [20]. Right: Comparison of lift to drag ratios at $Re = 1 \times 10^6$ from RFOIL, corrected RFOIL, and Overflow to wind tunnel results [16].	34
Figure 23. Comparison of the RFOIL, Overflow, and Fuego lift curves to the wind tunnel data for $Re = 7 \times 10^6, 3 \times 10^6, 2.5 \times 10^6, 2 \times 10^6, 1 \times 10^6$, and 0.7×10^6 for the DU 97-W-300Mod airfoil.	35
Figure 24. Comparison of the RFOIL, Fuego, and Overflow drag polars to the wind tunnel data for $Re = 7 \times 10^6, 3 \times 10^6, 2.5 \times 10^6, 2 \times 10^6, 1 \times 10^6$, and 0.7×10^6 for the DU 97-W-300Mod airfoil.	36
Figure 25. Comparison of the RFOIL, Fuego, and Overflow lift to drag ratios to the wind tunnel data for the DU 97-W-300Mod airfoil.	37
Figure 26. Comparison of Overflow and RFOIL pitching moment to experimental data [18] for DU 97-W-300Mod.	38
Figure 27. Comparison of RFOIL to Overflow lift curves for DU 97-W-300Mod airfoil at lower Reynolds numbers.	39
Figure 28. Comparison of RFOIL to Overflow lift to drag ratio and drag polar for DU 97-W-300Mod airfoil at lower Reynolds numbers.	40
Figure 29. Comparison of RFOIL to Overflow pitching moments for DU 97-W-300Mod airfoil at lower Reynolds numbers.	40
Figure 30. RFOIL DU 91-W2-250Mod lift curve for a wide range of Reynolds number values.	42
Figure 31. RFOIL DU 91-W2-250Mod pitching moment and drag for a wide range of Reynolds number values.	43
Figure 32. Overflow lift curve data for DU 91-W2-250Mod airfoil at Re ranging from 7 to 0.7 million. "OFTA" indicates that the time accurate mode was used.	44
Figure 33. Overflow pitching moment and drag data for DU 91-W2-250Mod airfoil. "OFTA" indicates that the time accurate mode was used.	44
Figure 34. Comparison of RFOIL and Overflow lift curves to the wind tunnel data for the DU 91-W2-250Mod airfoil. "OFTA" indicates that the time accurate mode was used for the Overflow runs.	45
Figure 35. Left: For $Re = 3 \times 10^6$, RFOIL drag results with and without the correction factor of 1.09, and Overflow results are compared to wind tunnel data [20]. Right: the same for $Re = 1 \times 10^6$. "OFTA" indicates that the time accurate mode was used in Overflow.	46
Figure 36. Left: For $Re = 3 \times 10^6$, RFOIL lift to drag results with and without the correction factor of 1.09, and Overflow results are compared to wind tunnel data [20]. Right: the same for $Re = 1 \times 10^6$. "OFTA" indicates that the time accurate mode was used in Overflow.	46
Figure 37. Comparison of RFOIL and Overflow drag polar data to the wind tunnel data for the DU 91-W2-250Mod airfoil. RFOIL results both with and without the 1.09 correction factor are shown. "OFTA" indicates that the time accurate mode was used for Overflow.	47
Figure 38. Comparison of RFOIL and Overflow lift to drag ratio to the wind tunnel data for the DU 91-W2-250Mod airfoil. RFOIL results both with and without the 1.09 correction factor are shown. "OFTA" indicates that the time accurate mode was used for Overflow.	48

Figure 39. Comparison of RFOIL and Overflow pitching moment to the wind tunnel data for the DU 91-W2-250Mod airfoil. “OFTA” indicates that the time accurate mode was used for Overflow.	49
Figure 40. Left: Lift curve comparisons of RFOIL to wind tunnel results for the Adjusted DU99-W3-350lm airfoil at $Re = 3 \times 10^6$ [21] and the DU 99-W3-350 at $Re = 7 \times 10^6$ [18]. Right: Drag polar for $Re = 7 \times 10^6$ (DU 99-W3-350 [18]).	50
Figure 41. RFOIL DU 99-W3-350 lift curve for a wide range of Reynolds number values.	50
Figure 42. Lift curve for the DU 99-W3-350 airfoil at $Re = 7$ and 1 million. Both cases are run in the time accurate mode.	51
Figure 43. Pitching moment and drag polar for the DU 99-W3-350 airfoil.	51
Figure 44. Comparison of RFOIL and Overflow lift curves to the wind tunnel data for the DU 99-W3-350 airfoil.	52
Figure 45. Comparison of RFOIL and Overflow drag polars to the wind tunnel data for the DU 99-W3-350 airfoil.	53
Figure 46. Comparison of RFOIL and Overflow lift to drag ratios to the wind tunnel data for the DU 99-W3-350 airfoil.	54
Figure 47. Comparison of RFOIL and Overflow pitching moments to the wind tunnel data for the DU 99-W3-350 airfoil.	55
Figure 48. RFOIL data for DU 99-W3-405 compared with wind tunnel data at $Re = 7 \times 10^6$ [18] and $Re = 3 \times 10^6$ [21].	56
Figure 49. RFOIL DU 99-W3-405 lift curve for a wide range of Reynolds number values.	56
Figure 50. $Re = 3 \times 10^6$, $Ma = 0.11$, Low Mach Preconditioning on: example of good convergence	64
Figure 51. $Re = 7 \times 10^5$, $Ma = 0.11$, Low Mach Preconditioning on: example of poor convergence	64
Figure 52. $Re = 7 \times 10^5$, $Ma = 0.11$, Low Mach Preconditioning off	65
Figure 53. $Re = 7 \times 10^5$, $Ma = 0.05$, $DT = 0.05$	65
Figure 54. Left: $Re = 7 \times 10^5$, $Ma = 0.11$, $DT = 0.1$, no low Mach preconditioning, no sub-iterations (Corresponding to Figure 51)Right: . $Re = 7 \times 10^5$, $Ma = 0.05$, $DT = 0.05$ (Corresponding to Figure 53)	66
Figure 55. $Re = 2 \times 10^6$, $Ma = 0.11$, $DT = 0.1$, low Mach preconditioning turned on, no sub-iterations	66
Figure 56. $Re = 7 \times 10^5$, $Ma = 0.026$, Low Mach Preconditioning on, Time accurate with $DTPHYS = 0.001$, $DT = 0.001$, 18 Newton Sub-iterations	67

TABLES

Table 1. Proposed airfoils for the new NRT blade.	14
Table 2. DU Airfoil Map	20
Table 3. Airfoil Coordinates	89

NOMENCLATURE

α	Angle of attack
c	Chord length
C_D (CD)	Coefficient of drag
C_L (CL)	Coefficient of lift
CM (CM)	Pitching moment coefficient
CFD	Computational Fluid Dynamics
DOE	Department of Energy
DT	Time step
Ma	Mach number
NRT	National Rotor Testbed
RANS	Reynolds Averaged Navier-Stokes
Re	Reynolds number based on chord length
SNL	Sandia National Laboratories
SWiFT	Scaled Wind Farm Technology

1. INTRODUCTION

Sandia National Laboratories (SNL) and The U.S. Department of Energy (DOE) are designing a modern, research-quality wind turbine rotor for use at the new Scaled Wind Farm Technology (SWiFT) site at Texas Tech University in Lubbock, Texas. Designated as the National Rotor Testbed (NRT) [1], the new rotor will be a public resource used to accelerate important rotor innovation and to conduct complex flow and turbine-to-turbine interaction research that will increase the efficiency of wind power plants and lower the cost of electricity. The blades are expected to provide a publicly available baseline blade design which will enable increased participation in future blade research as well as accelerated hardware manufacturing and testing for demonstration of innovation.

The SWiFT facility is unique in that it utilizes wind turbines that are large enough to represent the physics relevant to utility-scale machines, yet small enough to be extremely cost effective when compared to the megawatt scale counterparts. It features 1980s-era heavily modified [1] Vestas V27 225-kilowatt turbines with 27-meter (m) diameter rotors. Although the aerodynamic and structural technologies used in the original rotors of the V27 enabled a cutting-edge product in their own time, today's modern turbines (with capacity ratings of 1.5 to 3 megawatts and rotor diameters of 70 to 120 m) are able to take advantage of the fruits of an additional 20 plus years of wind turbine rotor technology research. Modern rotors are designed to a new level of optimal aerodynamic and structural efficiency, but they have their own challenges: acoustics, controls, sensing, aerodynamics, and structural dynamics. The goal of the NRT is to provide a greater understanding of these challenges as well as wind plant complex flow issues. It is envisioned that the NRT blades will be primarily used to study two phenomena in the near term: wake deficit recovery as a function of atmospheric conditions and turbine-turbine interaction effects due to wake impingement on a downstream rotor. Findings from turbine-turbine interaction research performed on these machines will be used to guide improvements in overall wind plant efficiency. The subscale nature of the NRT blades at SWiFT will enable high-fidelity measurements and sensing along with accurate simulation of the larger rotors, which is logistically simpler and more cost effective than relying on equivalent megawatt-scale test turbines. After the blades have been manufactured, they will replace the existing rotors on the DOE turbines at SWiFT.

Features of the new NRT blades do not represent the optimal design for a V27 size rotor, but instead are determined by functional scaling of relevant parameters and design drivers from a representative megawatt-scale rotor. It is important to note that, unlike many scaled tests, Reynolds number is not the parameter that will be kept constant for the rescaling of the NRT blades. Instead it is more relevant to recreate dynamic loads and match the circulation of the rotor. The lift curve slope and angle of attack margin are also important. The rotor will be highly instrumented, so the airfoils must be thick enough so that there is room for the hardware.

The thickness of inboard airfoils for these utility scale rotors are typically as high as 35-40%. The thickness and the proximity to three-dimensional flow of these airfoils present design and analysis challenges, even at the full scale. However, more than a decade of experience with the airfoils in numerical simulation, in the wind tunnel, and in the field has generated confidence in

their performance. The DU-series of airfoils is in common use in commercial, utility-scale machines today. This paper looks at four in particular: DU 91-W2-250Mod, DU 97-W2-300Mod, DU 99-W3-350, and DU 99-W3-405. Experimental polar data for these airfoils are shown in Section 4. All of these except for the DU 99-W3-405 will be considered in the design of the NRT blades. These airfoils were designed specifically for application on the inboard region of wind turbine blades.

Reynolds numbers for megawatt-, utility-scale rotors are generally above 1-2 million, maximum 6-8 million. The range in size of these utility-scale rotors is 80-120 m in diameter. When used on a sub-scale rotor, Reynolds number regimes are significantly lower for the inboard blade. Performance of the thick airfoils in this regime is uncertain because of the lack of wind tunnel data and the inherent challenge associated with associated numerical simulations. Figure 1 shows an example spanwise distribution of Reynolds numbers for a 3 MW rotor operating at rated wind speed compared to an example spanwise distribution of Reynolds numbers for a 27m, 225 kW rotor operating at rated wind speed.

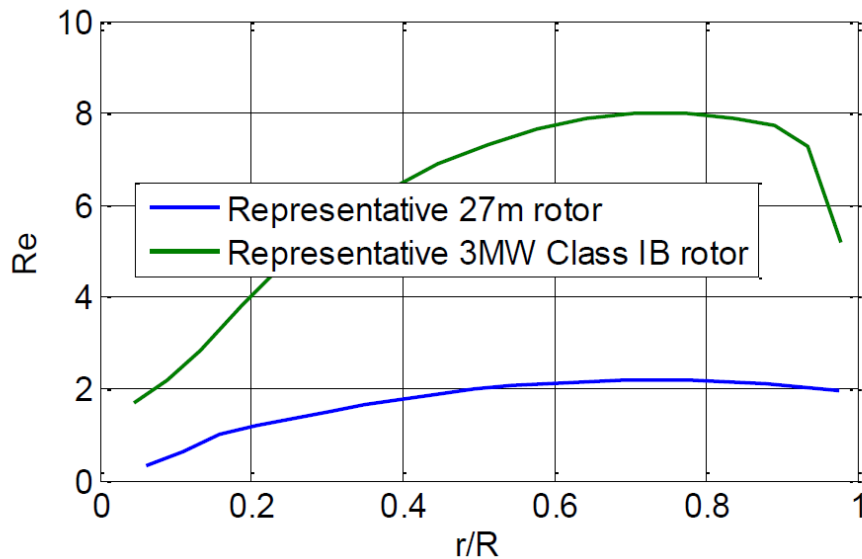


Figure 1. Approximate Reynolds numbers (in millions) along the rotor span for a 3 MW rotor compared to a 225 kW (27 m) rotor.

There are several challenges to the design of the scaled blades. Because Reynolds numbers in the range of 500,000-1,000,000 are below the normal operating range of these DU airfoils, few wind tunnel tests and simulations have been done in this regime. At low Mach numbers simulations of the Navier-Stokes equations become more stiff. This requires greater time for convergence or scaling of the eigenvalues. The thick airfoils at higher angles of attack produce significant laminar separation bubbles on both the upper and lower surface [2]. This more detached flow also causes more eddies and time dependent flow features. In these cases, Unsteady Reynolds average Navier-Stokes (URANS) is more appropriate than Reynolds average Navier-Stokes (RANS).

For this paper a variety of simulation tools are explored in order to find the best method of producing accurate results, first in 2D and also looking ahead to the next step which will be 3D

simulations. The simulation results will improve understanding of the aerodynamic properties of thick airfoils in this Reynolds number regime. The integrated boundary layer panel method code RFOIL as well as two Reynolds average Navier-Stokes computational fluid dynamics (CFD) codes, Fuego and Overflow, will be compared to experimental data for Reynolds numbers where data is available. The results for the lower Reynolds numbers of interest will be shown for all cases, even when wind tunnel data is not available.

2. APPROACH

While it is the goal of this project to use airfoils with reliable wind tunnel data whenever possible, it is probable that this will not always be the case. One example would be looking at transition airfoils along the blade between two known airfoils. In the absence of wind tunnel tests, capable analysis tools are needed to support simulations that enable improved understanding of the aerodynamic properties of thick airfoils in this Reynolds number regime.

Three thick airfoils designed at TU-Delft specifically for wind turbine blades will be considered for the inboard section of the rotor: DU 91-W2-250Mod, DU 97-W-300Mod, and DU99-W3-350. These thick DU airfoils (25-35%) were not designed for low the Reynolds number operation (0.7-1.5M) that will be seen by the NRT scaled rotor, so testing in this regime has been limited. If used improperly, the inboard airfoils on the proposed design could harshly limit aerodynamic performance due to influence of Reynolds number on stall characteristics and maximum lift conditions ($C_{L,max}$). To better understand the effects of low Reynolds numbers without having to run more wind tunnel tests, CFD simulations will be run. With these results we can maximize our confidence in whatever inboard airfoils are chosen such that the performance of the NRT rotor is as predictable as possible. Most of the work has concentrated on DU 97-W-300Mod since there is more experimental data available in the literature for this airfoil. The DU 99-W3-405 airfoil was also modeled and results are shown here for completeness, although it is no longer being considered for use in the NRT blade. Table 1 lists the span location and Reynolds number range for each airfoil.

Table 1. Proposed airfoils for the new NRT blade.

NRT 13.5m			Reynolds number in millions	
Airfoil Thickness	Span Start	Span End	Re Low	Re High
35%	<18%	18%	--	~1.0
30%	18%	35%	0.7-1.0	1.2-1.75
25%	35%	55%	1.0	1.75-1.8
21%	55%	75%	1.0	1.6-1.75
18%	75%	99%	0.43-1.0	0.7-1.6

The following codes were used to compute airfoil performance: RFOIL, Sierra Fuego, and Overflow. Suitability of these codes was determined by first comparing their results against previously published wind tunnel data. Next, the most suitable candidates are used to compute performance data for the lower Reynolds numbers of interest for the few cases where the wind tunnel data is not available. While RFOIL produces accurate results for lift and drag, it cannot be used for future 3D simulations. As an extra check on the CFD values, RANS results are compared with RFOIL at the lower Reynolds numbers which do not have experimental data.

3. ANALYSIS TOOLS

The simulations capabilities in this report were chosen for their potential applicability to this unique problem of thick airfoils combined with lower Reynolds number regime. Two sets of CFD codes are compared to help determine which should be used in the full scale exploration of the SWiFT blade. The first is Fuego, the low-Mach component of Sandia National Laboratories Sierra suite of codes. The second is Overflow, which was developed by NASA. Results from the panel code RFOIL will also be presented.

3.1. RFOIL

RFOIL [3] is a modification of the panel code XFOIL [4]. It is widely used for airfoil design, and has an incredibly quick turnaround time for producing output such as lift, drag, pitching moment, and pressure profiles. The modifications incorporate effects from rotating blades such as the Coriolis force and centrifugal force as well as cross flow velocity profiles. Despite these enhancements which do increase the accuracy for inboard airfoils, for our full blade design investigation we will most likely need to use a fully 3D CFD code in order to fully understand the important inboard 3D effects as well as any flow anomalies that occur when transitioning from one airfoil to the next along the span of the blade. RFOIL is still critical for providing validation of the CFD codes for scenarios that do not have wind tunnel data as well as providing transition locations on the airfoils that are needed for more accurate RANS calculations.

3.2. Fuego

The computational fluid mechanics code, Fuego [5] was used to perform simulations of the flow around a DU 97-W-300Mod airfoil over a range of angles of attack. Fuego is a Sandia National Laboratories' developed code which is part of the Sierra suite of codes. It was designed to simulate turbulent reacting flow and heat transfer [5] on massively parallel computers. The code was adapted for compressible flow and combustion, and is well suited for low Mach number flows. The discretization scheme used in Fuego is based on the control volume finite element method [6], where the partial differential equations of mass, momentum, and energy are integrated over unstructured control volumes.

Three different versions of Menter's SST $k-\omega$ turbulence model [7] as well as a one equation $k-\omega$ model were tested. They have slightly different boundary conditions for the kinetic energy at the wall (k_{wall}) and for the specific dissipation at the wall (ω_{wall}) [8]. The first model ("SST" in Figure 13 , does not use a near wall turbulent kinetic energy transport equation and sets:

$$k_{wall} = \frac{\mu_\tau^2}{\sqrt{\beta_1}}$$
$$\omega_{wall} = \frac{\mu_\tau}{\sqrt{\beta_*} \kappa y_+}$$

The second SST model uses a value of k_{wall} based on a modified production and dissipation source term for the near wall turbulent kinetic energy transport equation. In this case,

$$\omega_{wall} = \frac{\mu_{\tau}}{\sqrt{\beta_*} \kappa y_+}$$

where

$$\mu_{\tau} = \sqrt{\tau_{wall} / \rho}$$

The third version is a low Reynolds number SST (LRSST), which is the “standard” Menter SST two-equation model with:

$$k_{wall} = 0$$

$$\omega_{wall} = \frac{6\nu}{\beta_1 y_+^2}$$

More detail for all four cases can be found in the Fuego Theory Manual [8]. Scripts were written for the Sierra meshing tool, CUBIT, that allow the production of grids with airfoils at specific angles of attack. Because flow through the domain in Fuego is specified by inflow boundary conditions on the left of a rectangular domain and outflow boundary conditions on the right (instead of specifying an angle of inflow as is done in other flow solvers), an o-grid or c-grid with a uniform hex-mesh surrounding the airfoil is imbedded in a rectangular domain with a non-uniform hex-mesh. A new mesh must be generated for each angle of attack (see Figure 2). The grid domain is square with 100 chord lengths per side. This allows the far field walls to be $50c$ from the airfoil. The spacing near the walls of the airfoil has a $y^+ \approx 1.0$. The meshes have approximately 280,000 nodes. A finer mesh of ~ 1 million nodes was also created and run for one case with an angle of attack of 0° .

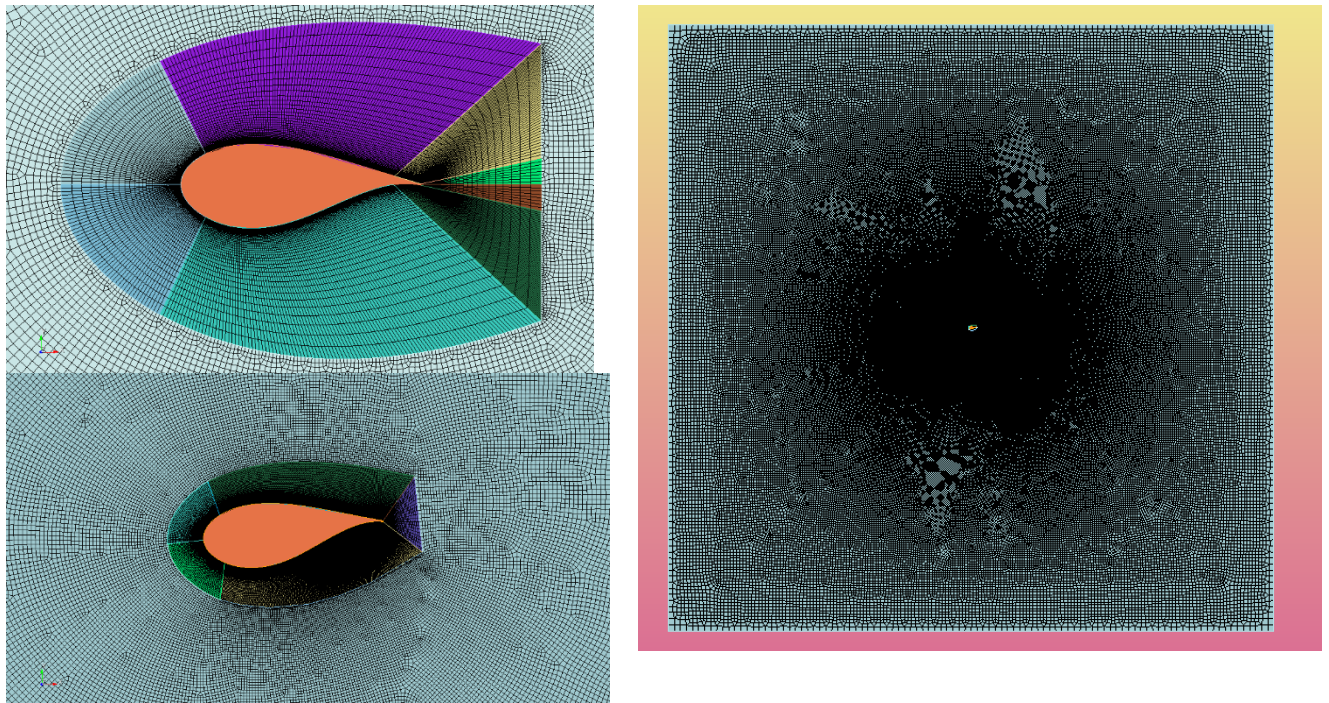


Figure 2. Top Left: Close up of the grid created in CUBIT for DU 97-W-300Mod airfoil at $\alpha = 0^\circ$. Bottom Left: Same airfoil at $\alpha = -6^\circ$. Right: Entire grid domain with airfoil in the center.

3.3. Overflow

The second set of software tested was the unsteady RANS flow solver Overflow [9-11]. The cases were run with a laminar flow in a specified region at the leading edge of the airfoil and then switched to fully turbulent using the Menter's SST $k-\omega$ turbulence model [7] at a specified location. The simulations were performed with second order time accuracy and dual time stepping. The force and moment coefficients were calculated using the FOMOCO utilities [12].

The meshes were created using Chimera Grid Tools [13-15]. They are all a C-grid which extends 30 chord lengths from the airfoil. For the DU 97-W-300Mod airfoil, there are 445,000 nodes with 637 around the airfoil, 96 in the wake, and 179 normal to the airfoil. The other airfoils have similar meshes. Overflow runs with 3 identical planes of the 2D grid. To trip the flow from laminar to turbulent, turbulence production terms in the gray region of Figure 3 are turned off so the transition to turbulence occurs where the turbulence terms are activated in the orange section. The transition locations are calculated with RFOIL.

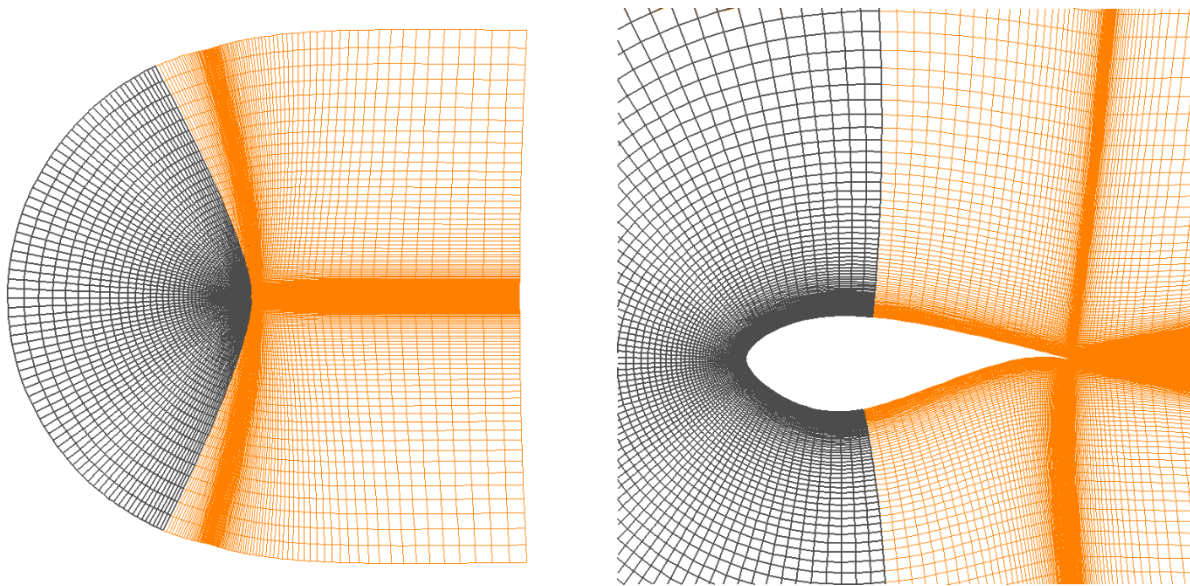


Figure 3. The Overflow grid for DU 97-W-300Mod created with Chimera Grid Tools. The gray region indicates where the turbulence production terms are turned off.

4. AVAILABLE EXPERIMENTAL RESULTS

4.1 Naming Convention

There are four DU airfoils discussed in this paper with thicknesses of: 25, 30, 35, and 40%. This section explains the naming convention used for these airfoils in the rest of the paper. The naming conventions were requested by the designer of the original airfoils [16]. Table 2 lays out the naming convention used here compared with other published works as well as which experimental data is available.

For the 25% thick airfoil, the DU 91-W2-250Mod airfoil was used. This is the same as the “DU 91-W2-250.lm” found in the file “DOWEC-NREL-5MW blade airfoil data-v2.xls” that was made available on the NREL forum site [17]. The spreadsheet gives details of the airfoil used in the DOWEC offshore wind turbine research project [18] which was also the bases for the NREL 5MW offshore reference wind turbine design. The ‘LM’ versions were modified during the design of the blades for the DOWEC study to have thinner aft sections of the airfoils. There is also published wind tunnel data for the DU 91-W2-250 airfoil. The two airfoils are very similar, so the simulation results from the DU 91-W2-250Mod will also be compared to the DU 91-W2-250 wind tunnel data.

For the 30% thick airfoil we will be using the DU 97-W-300Mod. This is the same airfoil as the “DU 97-W-300.lm” found in [18]. The DU 97-W-300Mod was tested at multiple Reynolds numbers, between 1 million and 10 million, in the cryogenic wind tunnel of the DNW in Cologne, Germany [19]. This data has been published down to a Reynolds number of 2.9 million. For lower Reynolds numbers, the wind tunnel data for the DU 97-W-300 has been used for comparison. Again, the two airfoils are quite similar, so the simulation data from DU 97-W-300Mod will be compared to wind tunnel results from both.

For the 35% thick airfoil we will be using the DU 99-W3-350. This is the same as the “Adjusted DU 35” in [18]. There is also published data for DU 00-W-350, however, the airfoils are different enough that the results from the simulations should not be cross compared. This airfoil might be used for span locations less than 18%.

For the 40% thick airfoil we will be using the DU 99-W3-405. This is the same as the “Adjusted DU4050” from [18]. There is also published data for DU00-W-401, but again the airfoils are different enough to prevent simulation comparisons. It was decided to not use the DU 99-W3-405 airfoil on the new NRT blade after the investigation using RFOIL revealed its limited performance at low Reynolds numbers of the NRT usable range. It is still in this paper for completeness.

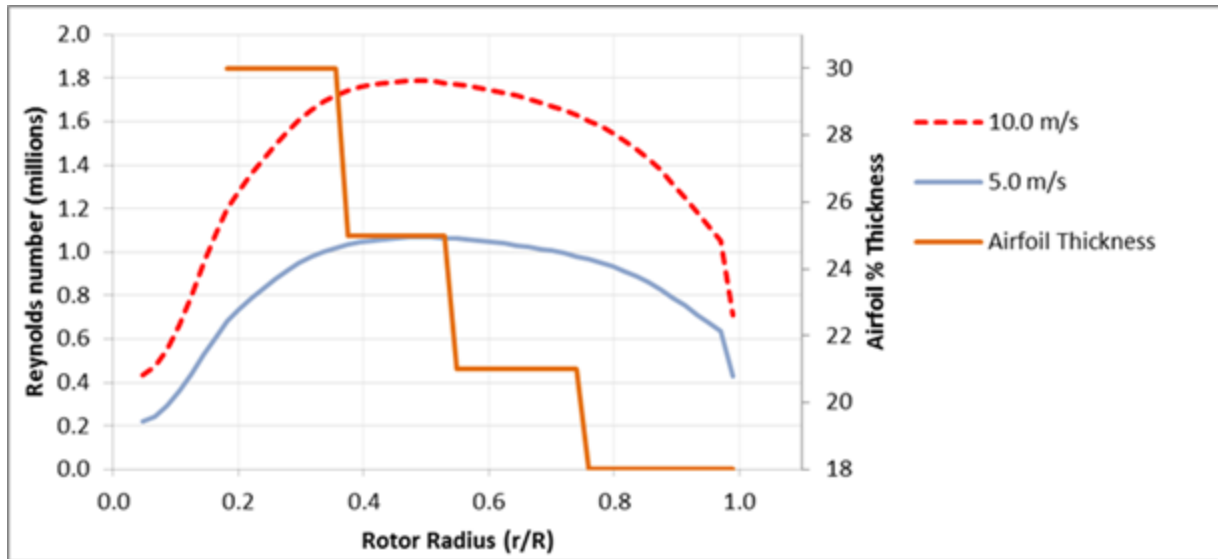


Figure 4. NRT 13.5m Reynolds number operating range and airfoil thickness for incoming wind velocities of 5 and 10 m/s.

Table 2. DU Airfoil Map

Naming in This Report	DOWEC [18]	Wind Tunnel papers [19-21]	Available Wind Tunnel Data (Re $\times 10^6$)
DU 91-W2-250		DU 91-W2-250	0.7, 1, 1.5,2,3
DU 91-W2-250Mod	DU 91-W2-250.LM		7
DU 97-W-300		DU 97-W-300	0.7,1,2,2.5,3
DU 97-W2-300Mod	DU 97-W-300.LM	DU 97-W-300Mod	7
DU 99-W-350		DU 99-W-350	3
DU 99-W3-350	Adjusted DU 35		7
DU 00-W-401		DU 00-W-401	3
DU 99-W3-405	Adjusted DU4050		7

4.2 Published Wind Tunnel Data

There are published experimental data sets for the DU 91-W2-250Mod at Re = 7 million [18] and the DU 91-W2-250 has available data at Re = 1.5 [21], 2 [20], and 3 [20, 21] million. Re = 0.7, and 1 million data for DU 91-W2-250 was also made available to us through personal correspondence with W.A. Timmer [16]. Figure 5 shows the lift curves for the wind tunnel experiments for the DU 91-W2-250 and DU 91-W2-250Mod airfoils. Figure 6 shows the pitching moment and drag polar for the same airfoils.

The DU 97-W-300Mod has published data at $Re = 7$ million [18] and for the DU 97-W-300 at $Re = 1$ [20], 2 [20, 21], 2.5 [21], and 3 million [20, 21]. $Re = 0.7$ million data for DU 97-W-300 was also made available to us through personal correspondence with W.A. Timmer [16]. Figure 7 shows the lift curve for these data while Figure 8 shows the pitching moment and drag.

There is wind tunnel data for DU 99-W3-350 at $Re = 7$ million [18] and for DU00-W-350 at $Re = 3$ million [21]. The lift curves and drag data for DU 99-W3-350 and DU00-W-350 are shown in Figure 9. Because of the noticeable difference in the lift near stall, these two airfoils are not directly compared.

There is wind tunnel data for the DU 99-W3-405 at $Re = 7$ million [18] and for DU00-W-401 at $Re = 3$ million [21]. Figure 10 shows the lift and drag data for these two airfoils. Like the 35% thick airfoils, these are different enough that they should not be directly compared.

The wind tunnel tests for these airfoils were run at two locations: the low-speed low-turbulence wind tunnel of the Faculty of Aerospace Engineering of Delft University and Laminar Wind Tunnel of the Institut für Aerodynamik und Gasdynamik der Universität Stuttgart. Both of these tunnels have a turbulence level that is less than 0.1% [20, 21]. RFOIL tends to match experimental results better in a low turbulence level wind tunnel like these better than in wind tunnels with a higher turbulence level [21].

These data are used to validate and compare the CFD codes at the Reynolds numbers where data is available. The tools which fits the data the best will be used to predict the forces on the airfoils at the lower Reynolds numbers of interest to the NRT where wind tunnel data is not available.

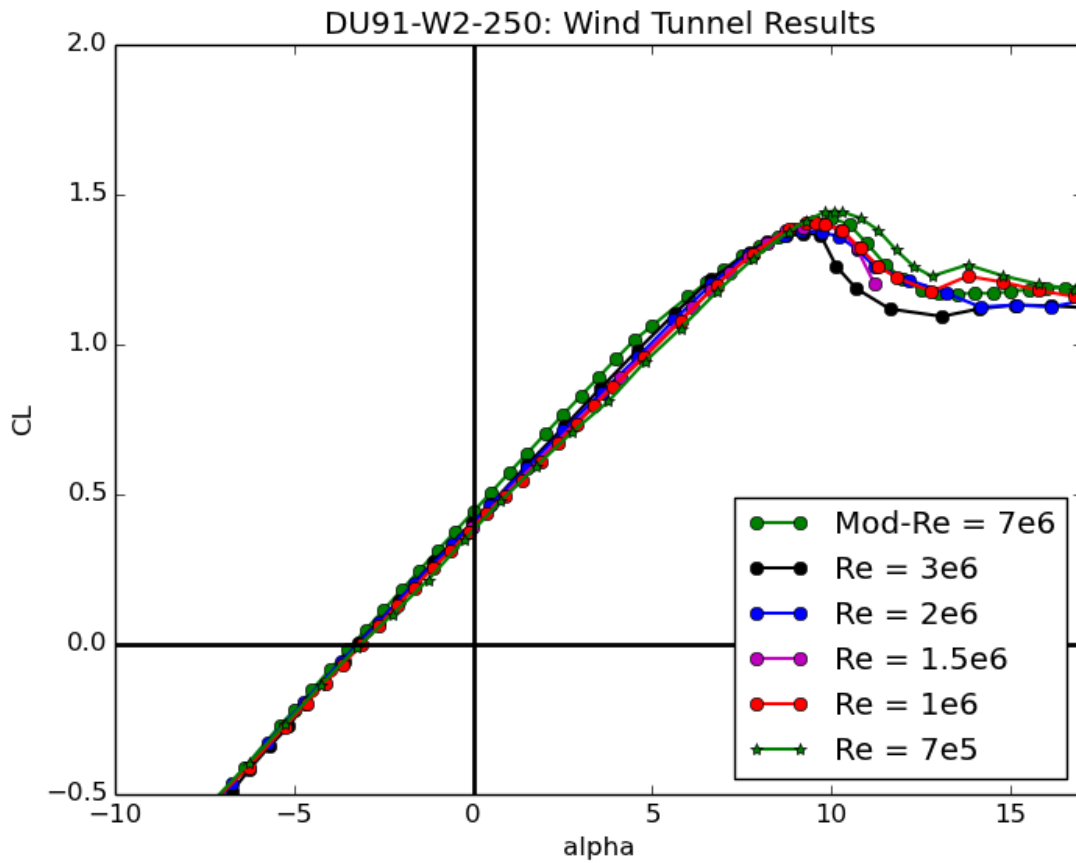


Figure 5. Lift curves from wind tunnel experiments for the DU 91-W2-250 and DU 91-W2-250Mod airfoils.

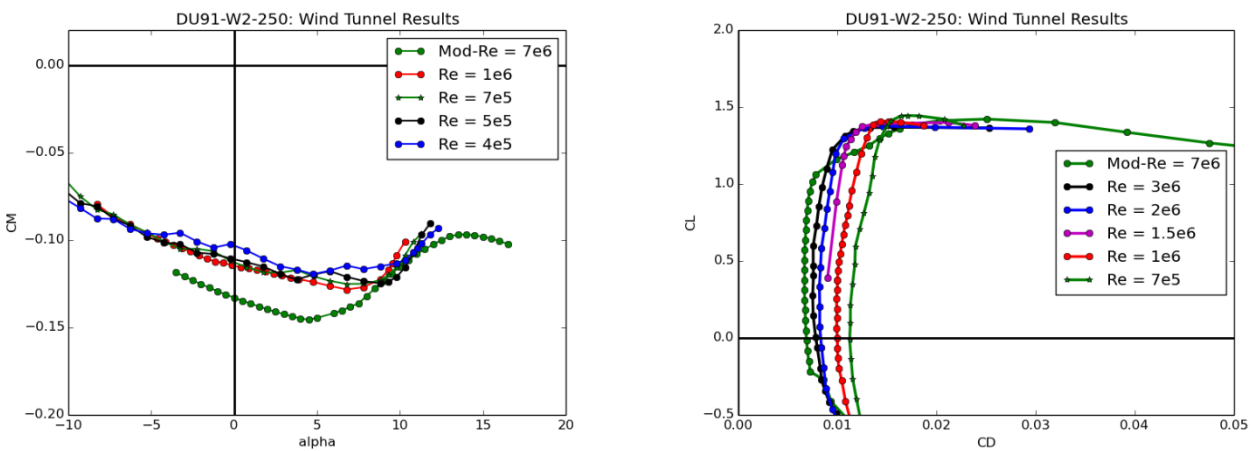


Figure 6. Pitching moment and drag data from wind tunnel experiments for DU 91-W2-250 and DU 91-W2-250Mod.

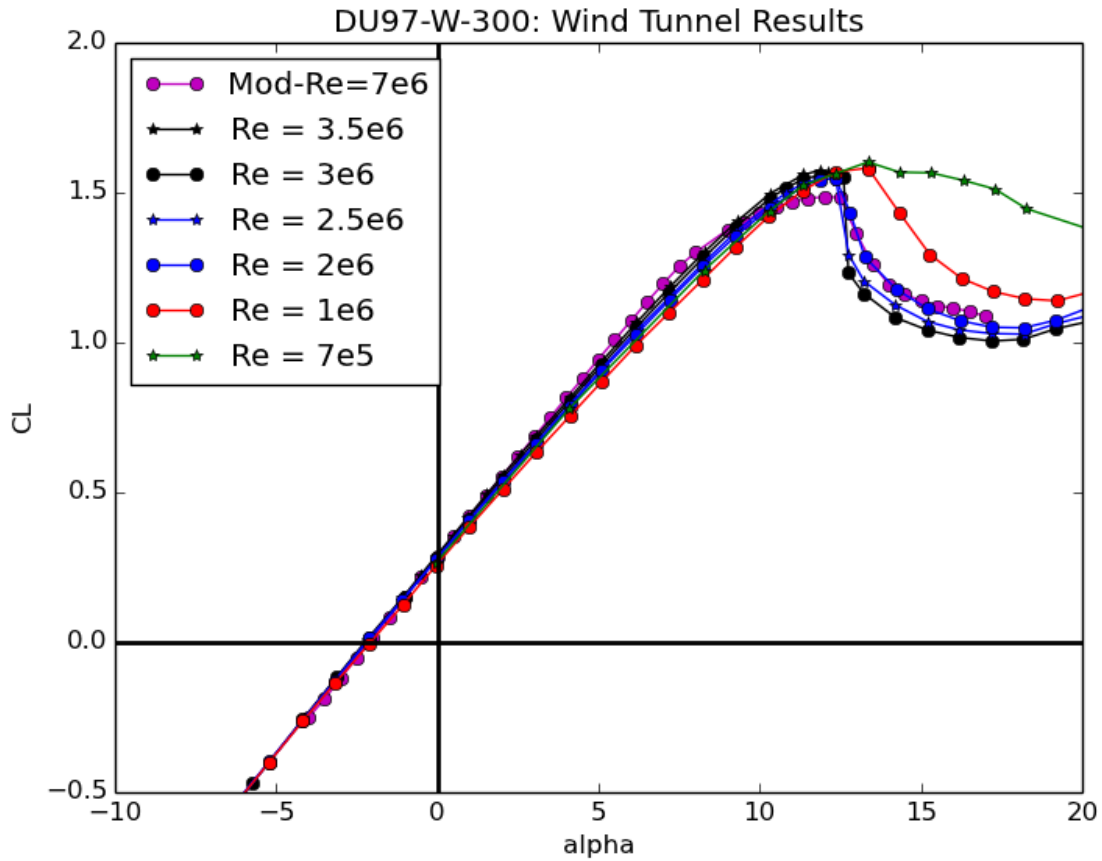


Figure 7. Lift data from wind tunnel experiments done for airfoil DU 97-W-300 and DU 97-W-300Mod.

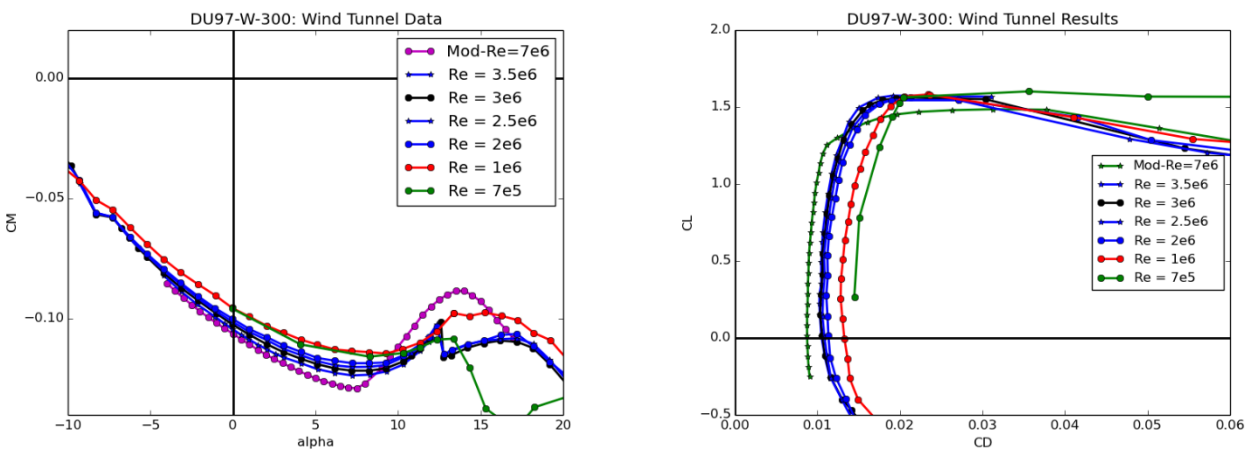


Figure 8. Pitch and drag data from wind tunnel experiments done for DU 97-W-300 and DU 97-W-300Mod.

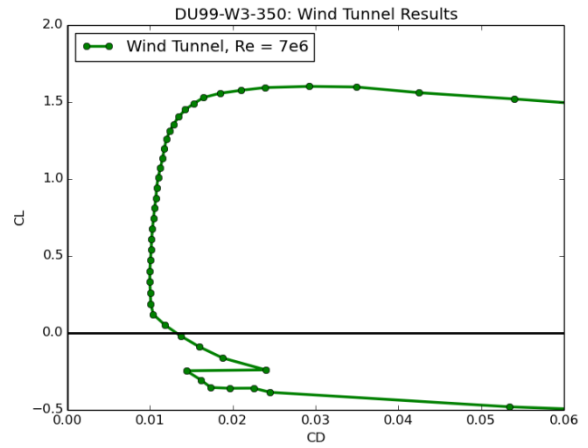
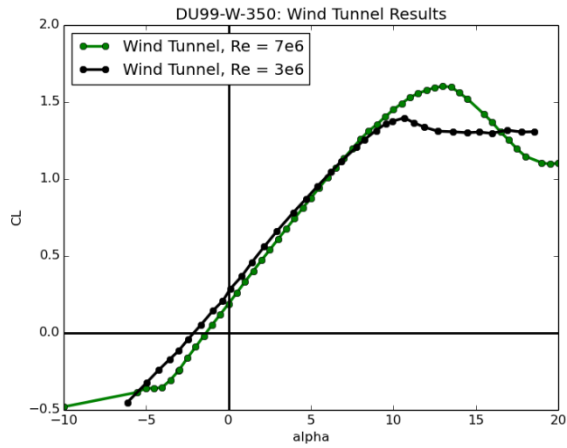


Figure 9. Lift and drag data from wind tunnel experiments for airfoil DU 99-W3-350 and the DU00-W-350 airfoil design.

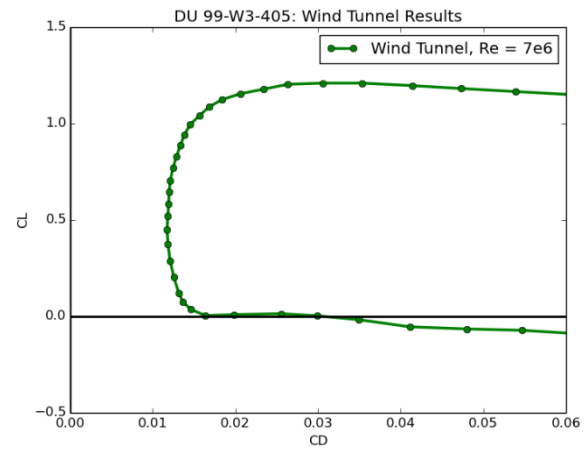
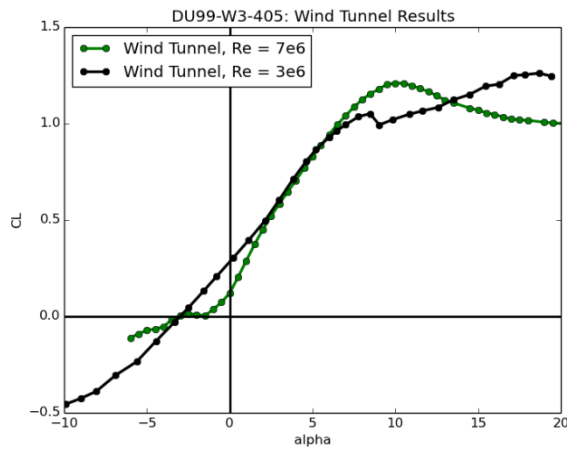


Figure 10. Lift and drag data from wind tunnel experiments for airfoils DU 99-W3-405 and DU00-W-401.

5. SIMULATION RESULTS FOR 30% THICK AIRFOIL

This report starts with the examination of the DU97-W-300Mod because it has the most available published experimental data of all the airfoils considered here. Lessons learned and techniques developed are applied to the other airfoils. Fuego results were computed for this airfoil only.

5.1. RFOIL

Originally, all simulations were run for all Reynolds numbers with a Mach number of $Ma = 0.11$ for simplicity. However, the Overflow results at the lower Reynolds numbers were not converging (See Appendix A.). A second approach was to vary the Mach number for each Reynolds number. In order to quickly determine the effects that changing the Mach number has on the lift curves at different Reynolds numbers, RFOIL [3] was used to produce results with various parameters. The Mach number for these tests ranged from $Ma = 0.05$ to $Ma = 0.213$ (from reported velocities of 25 m/s to 75 m/s [20]). Assuming all else was held constant, this means that the Mach numbers are $Ma = 0.05, 0.071, 0.1065, 0.142, 0.213$ for Reynolds numbers of $Re = 0.7, 1, 1.5, 2,$ and 3 million, respectively.

It is clear from the wind tunnel data shown in Section 4 that dropping the Reynolds number from 7 million to 1 million has a relatively small effect on the lift curve, mostly noticeable after $C_{L,max}$. Viscosity is on for all cases, and the turbulence amplification factor is set to an $N_{crit} = 9.0$. The Mach number is a constant $Ma = 0.11$ in the left hand side of Figure 11, but is changed for every Reynolds number in the right hand side of Figure 11. Since there is only a small change between these two results, it was determined that there would be no ill effects when Overflow was run with varying Mach number, which helped convergence at low Reynolds numbers. It is also more realistic compared to the setup of the experimental wind tunnel tests. Figure 12 shows the pitching moment and drag polar for this airfoil produced by RFOIL with Reynolds numbers ranging from 7 million to 0.7 million and changing Mach numbers.

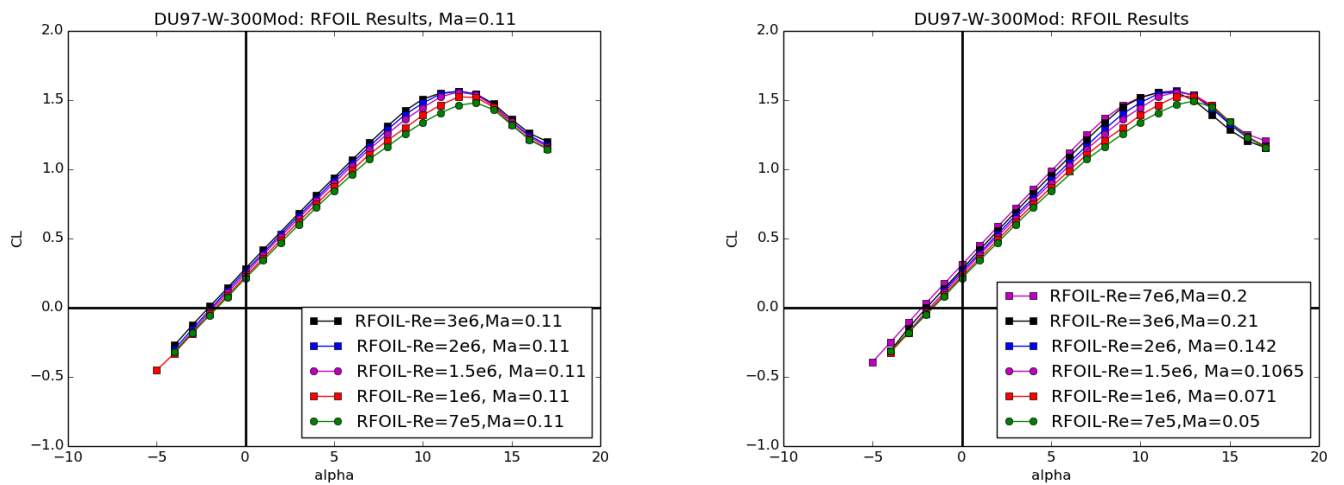


Figure 11. Left: RFOIL results for DU 97-W-300Mod produced with $Ma = 0.11$. Right: RFOIL results with a changing Mach number.

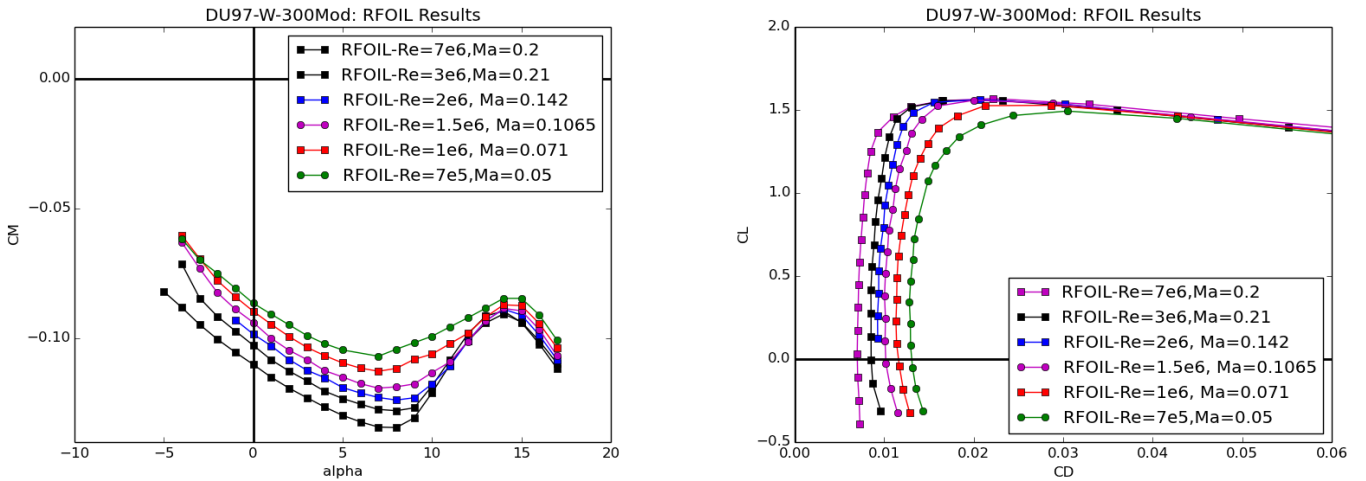


Figure 12. RFOIL pitching moments and drag polars for DU 97-W-300Mod.

5.2. Fuego

Flow over the DU 97-W-300Mod airfoil was simulated at angles of attack of $\alpha = -9, -6, -3, 0, 3, 6$ and 9° using the Sierra low-Mach code, Fuego. A Reynolds number of $Re = 3 \times 10^6$ was used in order to compare with published results, and the incoming velocity was set to 3835 cm/s ($Ma = 0.11$). All solid surfaces are considered viscous walls, and all cases were run fully turbulent. As discussed in section 3.2, several turbulence models were tested which include Menter's Shear Stress Transport (SST), a low Reynolds number SST (LRSST), SST using near wall calculations, and a one equation $k-\omega$ model. Scripts [22] were modified to post-process the data and calculate the lift and drag on the airfoil. The lift values were compared against experimental data taken from [20]. All of the lift values from the Fuego simulations are consistent with each other, but are lower by up to ~ 0.5 from the experimental and RFOIL data.

A grid study using a much finer mesh with ~ 1 million nodes for the SST models was conducted for $\alpha = 0^\circ$ and showed that the grid does not make a noticeable difference. The one equation $k-\omega$ model was slightly closer to the RFOIL data, but still significantly off, and it is expected that the SST models would perform better than the $k-\omega$ model for this type of problem because it captures the physics in the free stream better than a $k-\omega$ model alone.

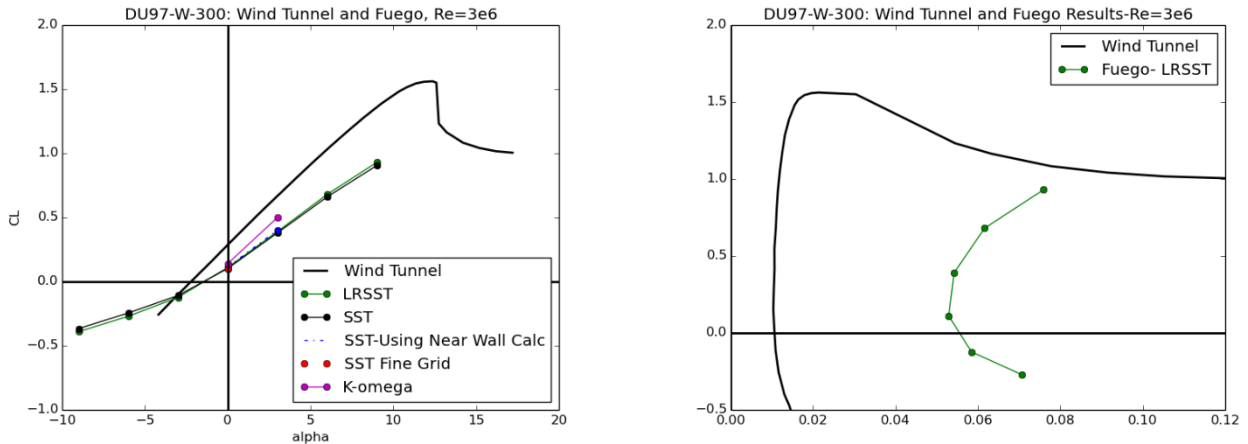


Figure 13. Left: Lift curve for the DU 97-W-300Mod airfoil using various turbulence models in Fuego. The black dash-dotted line is the experimental data (using the DU97-W-300 airfoil [18]) The red dot represents the simulation run on a fine mesh. Right: The drag polar for the LRSST case is compared with the experimental results [20].

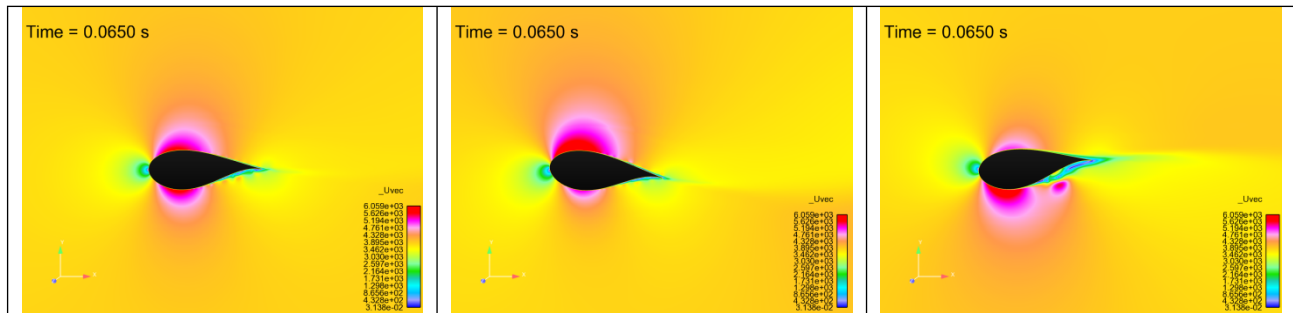


Figure 14. Velocity magnitude around a DU 97-W-300Mod at $\alpha = 0, 6, \text{ and } -6^\circ$ using the current SST turbulence model in Fuego ($Re = 3 \times 10^6, Ma = 0.11$).

The lift and drag results did not match the experimental data [20], and flows did not seem to be converging. Dr. Stefan Domino, a Sierra programmer, looked into the problem and was able to find and correct errors for several versions of SST in Fuego. He reported that the new implementation in Fuego converges to machine precision for test cases including the backstep flow and others. There were both some implementation issues as well as subtleties on some of the nonlinear terms (the cross diffusion term) which were contributing to the problem.

Tests of the turbulence models were made with 2D grids of both the DU 97-W-300Mod airfoil as well as the NACA 0012 airfoil. The NACA 0012 airfoil flow at $\alpha = 15^\circ$ matches the pressure distribution and lift reported in Gregory & O'Reilly [23]. However, the thicker DU 97-W-300Mod results matched the previous runs without the turbulence model corrections, but not the experimental data. Barone and Berg's results with this airfoil [24] using the Spalart-Allmaras and $k-\omega$ turbulence models were able to match the experimental results only by tripping the flow from laminar to turbulent at the location predicted by XFOIL. When the boundary layer remains laminar near the leading edge, a large suction (negative C_p) peak develops that increases lift.

Immediate development of a turbulent boundary layer, as in the current Fuego results, will prevent this peak from developing and lift will be under-predicted. It is believed that this is the cause of much of the discrepancy between the Fuego lift and drag results and the experimental data. While it is possible to set the transition location using Fuego, it is rather difficult due to meshing and implementation constraints. Because of this, it was decided to test the results against another flow solver, Overflow.

5.3. Overflow

Overflow was first run for the DU97-W-300Mod airfoil using the fully turbulent Menter's SST $k-\omega$ turbulence model throughout the domain. However, this produced results which had consistently lower lift over the full range of angles of attack, similar to what is seen in the Fuego results. Overflow has the option of turning off the turbulence production terms in specified regions of the flow. This simulates the flow transitioning from laminar to turbulent flow at given location along the airfoil, allowing the transition location of the flow in the simulation to be specified at a given x/c location on both the suction and pressure sides of the airfoil. If this method is not used, the flow becomes turbulent sooner than is seen in the experimental results, and results in a lower value for the lift. As can be seen in Figure 15, the simulations where the boundary layer transition is specified match well with the experimental data [20] up to stall, while the cases without the specified transition location under predicts the lift and over predicts the drag. RFOIL results both with and without zig-zag tape are also shown for comparison. The zig-zag tap would force the flow to transition to turbulence farther forward, matching the case where the transition location is not specified in Overflow. The Overflow transition locations for both the upper and lower surface of the airfoil were taken from RFOIL runs with specific Reynolds number and angle of attack. The RFOIL results which specify the transition locations are presented in Appendix B. The Overflow results with a forced transition location are used for the remainder of this paper.

To begin with all cases were run in steady-state mode, with a time step of $DT = 0.1$, and had a Reynolds number ranging from ranging from 0.7 million to 3 million. All cases were run with $Ma = 0.11$ and had the transition location specified at the appropriate location for that Reynolds number. As can be seen in Figure 16, the lift curves at lower Reynolds numbers are not as one would expect. They were checked carefully, and it was found that these Reynolds number cases were not converged. Several iterations of changing different flow parameters were tried until convergence was met. A closer look at the residuals and convergence criterial can be found in Appendix A. The Mach number was set to match the experimental setup ranging from $Ma = 0.071$ to $Ma = 0.21$ depending upon the Reynolds number. For the cases in which $Re = 0.7$ million, convergence was reached only when they were run in time accurate mode. This is indicated in figure legends as "OFTA". Figure 17 shows the lift curves with the final parameters. Figure 18 shows the pitching moment and drag polars for the range of $Re = 3, 2, 1.5, 1$ and 0.7 million. The Mach number is varied for each Reynolds number. The transition location is specified for all cases. Figure 19 shows Overflow results of the Mach number in the flow field for two different angles of attack.

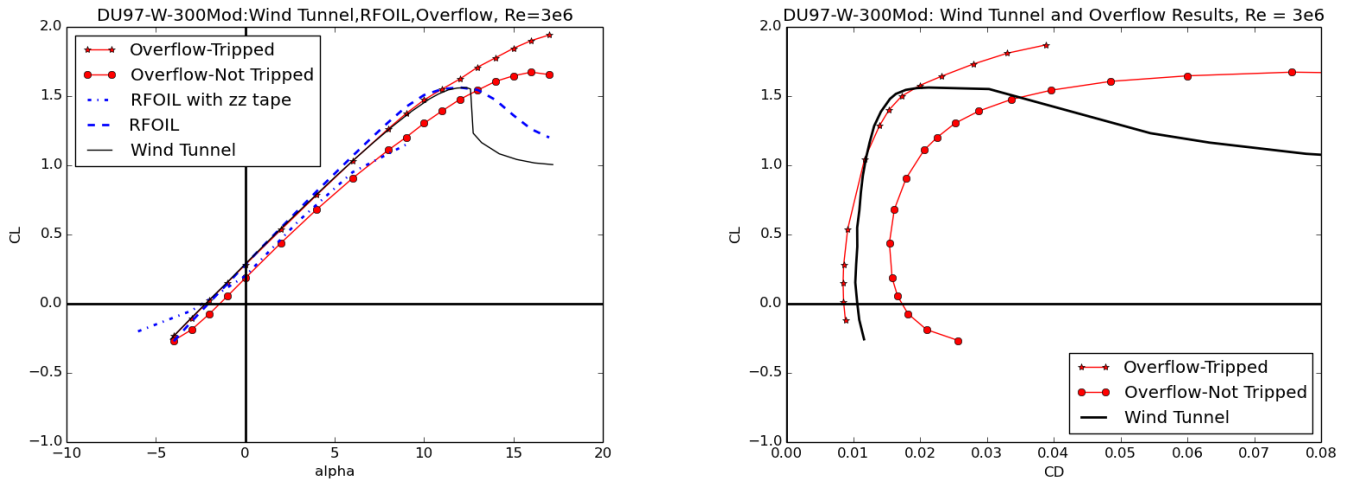


Figure 15. Overflow lift and drag polars for $Re = 3$ million with the transition location specified (red stars) and without (red circles) and RFOIL results with and without zig-zag tape (blue), both using DU97-W-300Mod, compared to experimental (solid black) data using DU97-W-300 [20].

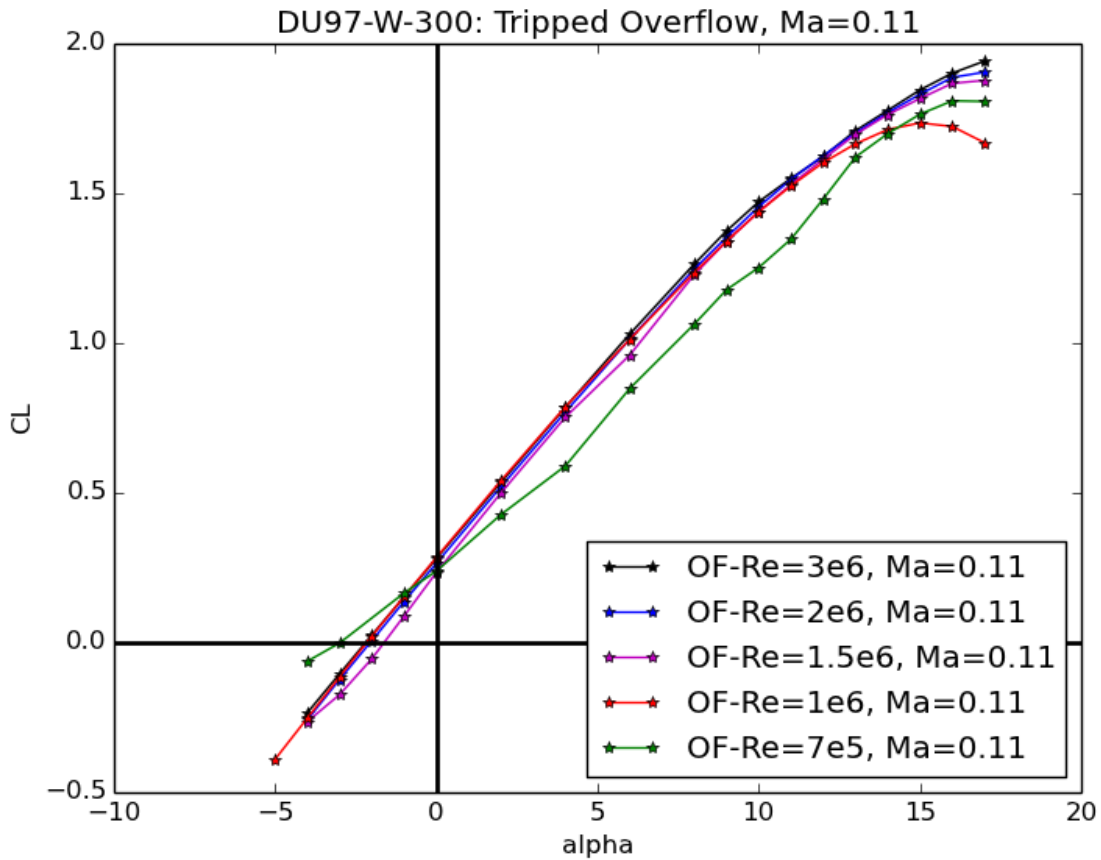


Figure 16. Lift curve of the DU 97-W-300Mod airfoil using Overflow steady state runs with $Ma = 0.11$.

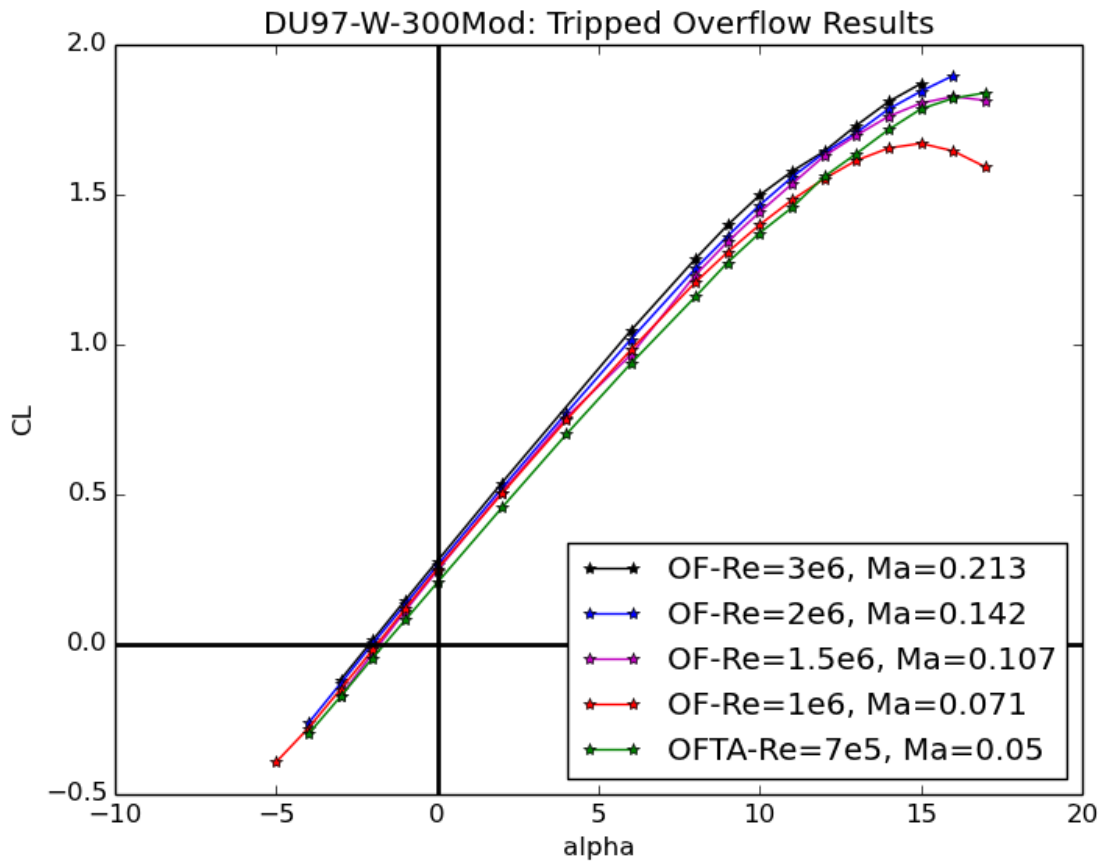


Figure 17. Lift curve of the DU 97-W-300Mod airfoil using Overflow steady state and time accurate (OFTA) runs which have Mach numbers that vary with the Reynolds numbers.

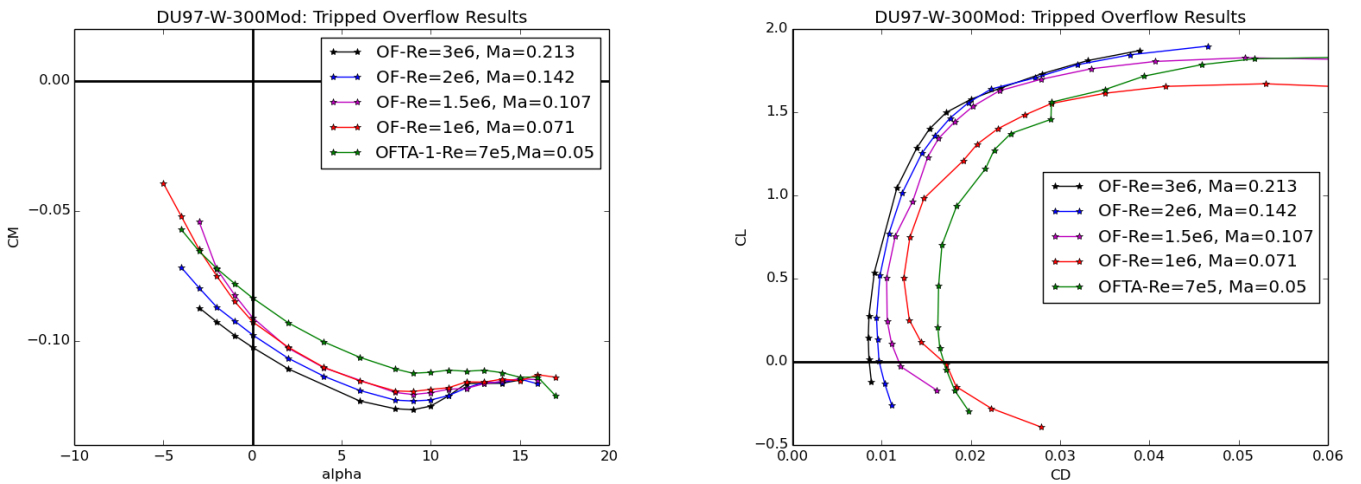


Figure 18. Overflow pitching moment results and drag polars for the DU 97-W-300Mod airfoil.

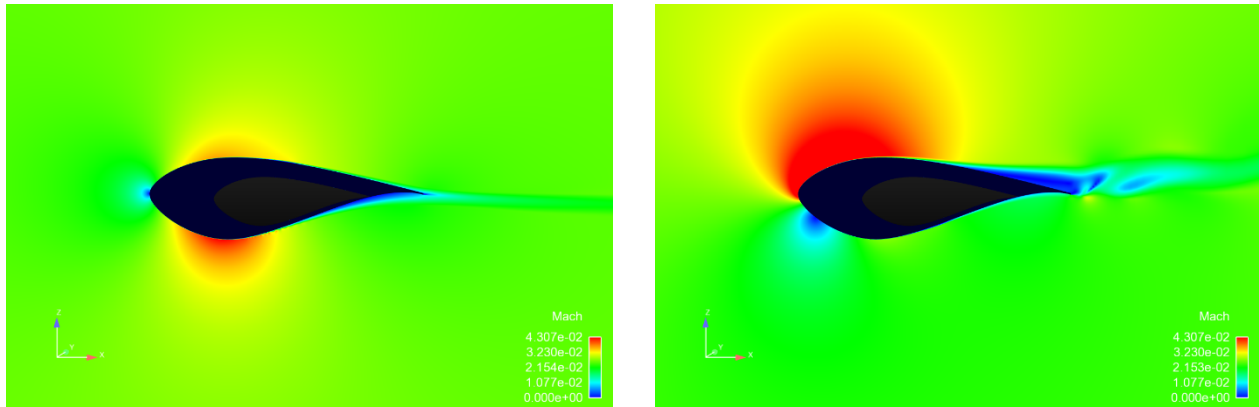


Figure 19. Mach number from Overflow for the DU 97-W-300Mod airfoil at $Re = 0.7$ million for $\alpha = -2^\circ$ (left) and $\alpha = 16^\circ$ (right).

5.4. Compiled Results

In order for a direct comparison, lift curves, drag polars, and pitching moments from all codes are plotted alongside the wind tunnel results. There are Fuego results only for $Re = 3 \times 10^6$, so the comparison to wind tunnel, RFOIL, and Overflow at this Reynolds number is shown in Figure 21. Fuego underestimates the lift value for all angles of attack, probably due to the early onset of the turbulent boundary layer. Fuego also overpredicts the drag values and under predicts the lift to drag ratios. Because of this, simulations for other airfoils were not run with Fuego.

It has been found previously that RFOIL results consistently underpredict drag by 9% and that multiplying the drag results by a factor of 1.09 will improve the accuracy [25]. This is consistent with what was found in this study as well. Figure 21 and Figure 22 compare both the corrected and uncorrected RFOIL drag values to the wind tunnel data as well as the Overflow and Fuego results. For the higher Reynolds number ($Re = 3 \times 10^6$) the Overflow drag values still match the experimental data better than the other methods. However for the lower Reynolds number ($Re = 1 \times 10^6$), the corrected RFOIL data are closer to the wind tunnel results.

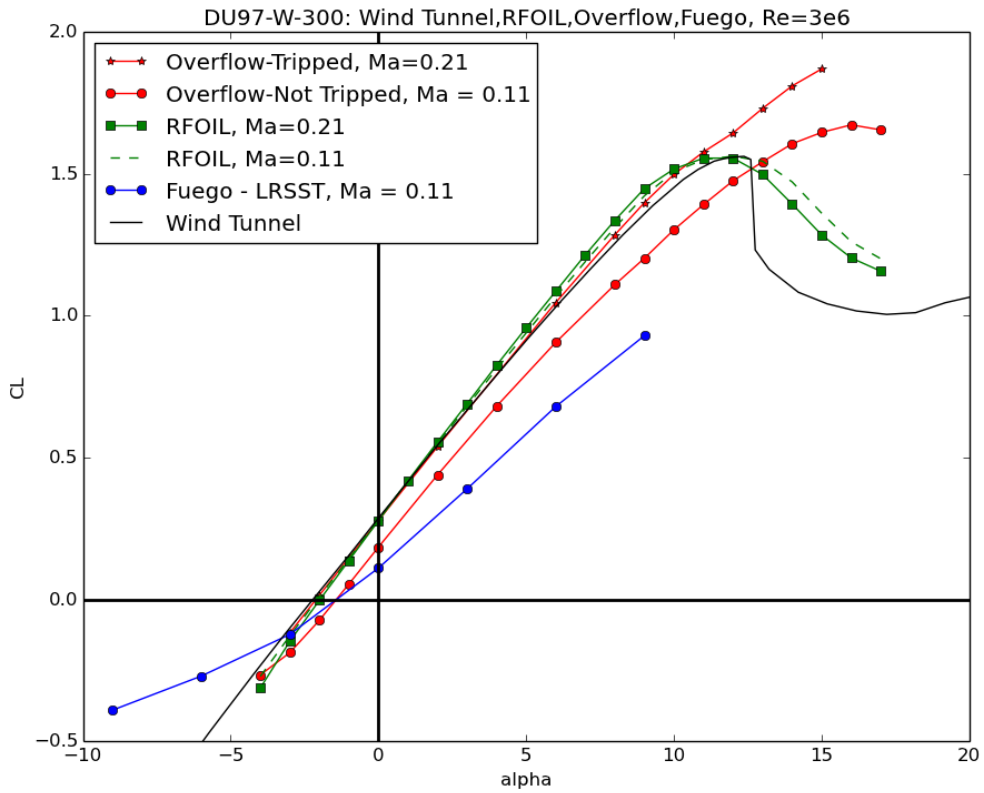


Figure 20. RFOIL lift results with $Ma = 0.11$ and $Ma = 0.21$, Fuego results with $Ma = 0.11$, and Overflow results with $Ma = 0.21$ are compared to wind tunnel values [20].

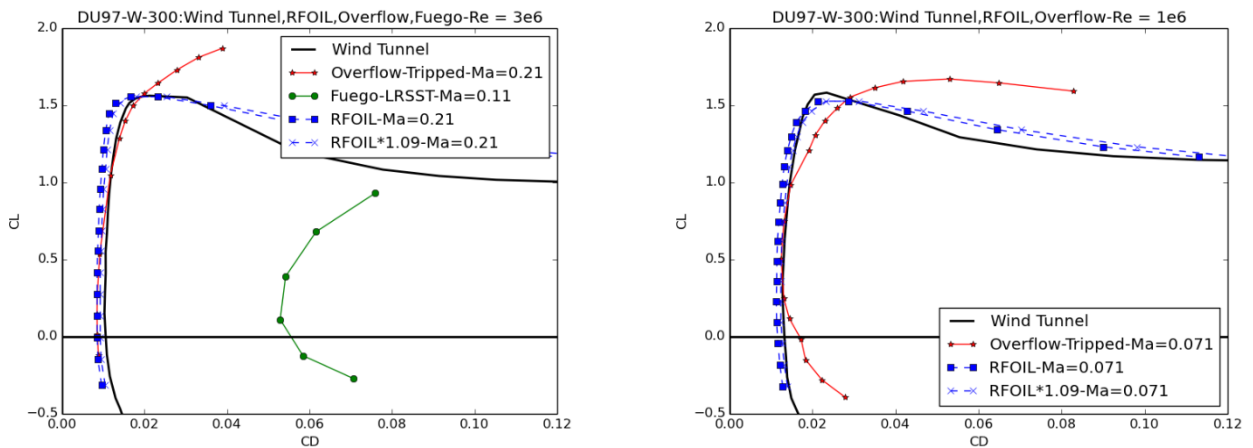


Figure 21. Left: For $Re = 3 \times 10^6$, RFOIL drag results with and without the correction factor of 1.09, Fuego results with $Ma = 0.11$, and Overflow results with $Ma = 0.21$ are compared to [20] wind tunnel values. Right: Comparison of drag results of DU 97-W-300Mod at $Re = 1 \times 10^6$ from RFOIL, corrected RFOIL, and Overflow to wind tunnel results [16].

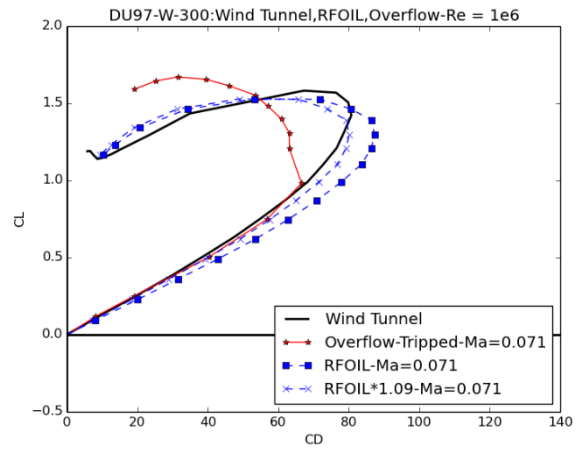
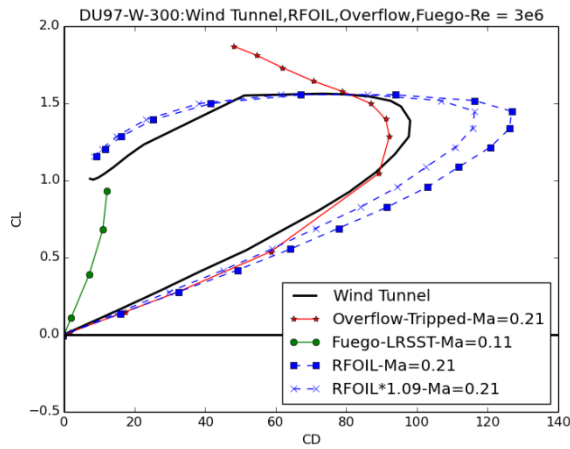


Figure 22. Left: Lift to drag ratio for DU 97-W-300Mod at $Re = 3 \times 10^6$ for corrected and uncorrected RFOIL, Overflow, and Fuego compared to DU97-W-300 wind tunnel data [20]. Right: Comparison of lift to drag ratios at $Re = 1 \times 10^6$ from RFOIL, corrected RFOIL, and Overflow to wind tunnel results [16].

The lift to drag ratio comparisons are shown in Figure 22 for DU97-W-300Mod at $Re = 3 \times 10^6$ and 1×10^6 . For $Re = 3 \times 10^6$, Overflow with specified transition locations match the wind tunnel [21] maximum C_l/C_d better than both Fuego and RFOIL. For $Re = 1 \times 10^6$ the RFOIL results are more accurate.

DU97-W-300Mod: Wind Tunnel,RFOIL and Overflow Results

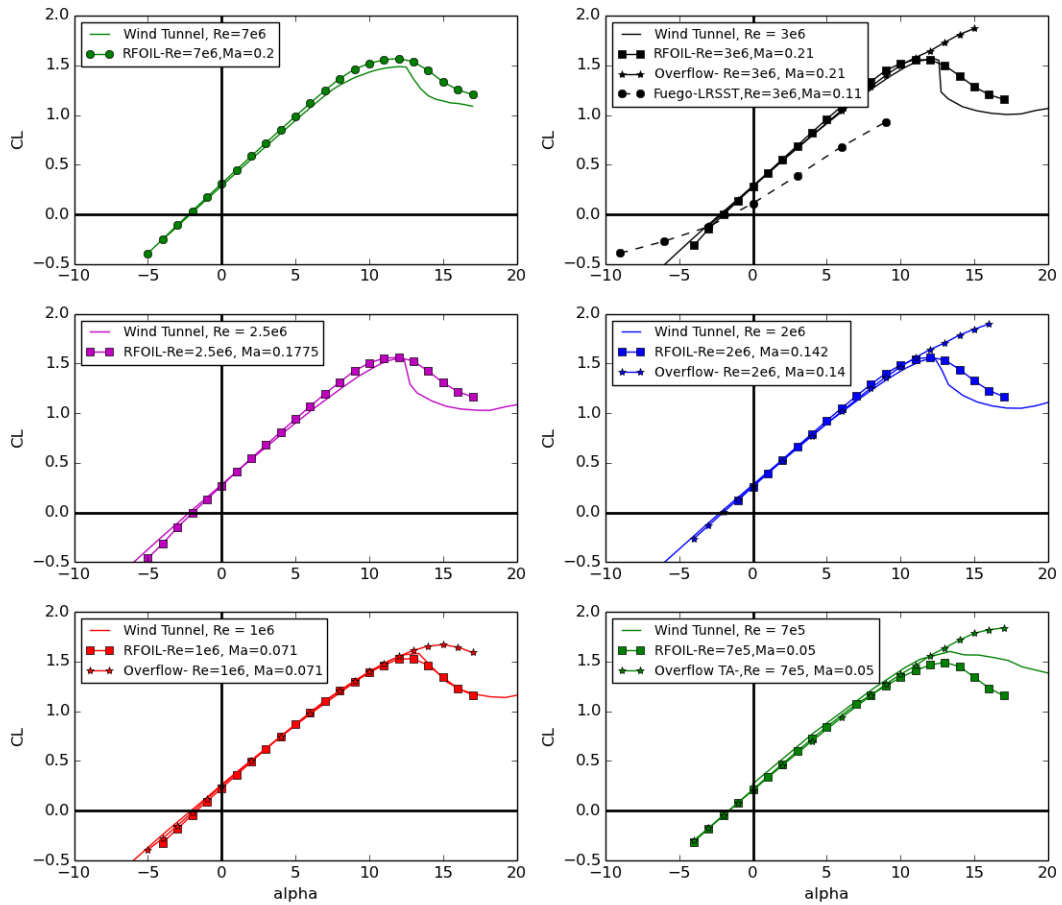


Figure 23. Comparison of the RFOIL, Overflow, and Fuego lift curves to the wind tunnel data for $Re = 7 \times 10^6$, 3×10^6 , 2.5×10^6 , 2×10^6 , 1×10^6 , and 0.7×10^6 for the DU 97-W-300Mod airfoil.

DU97-W-300Mod: Wind Tunnel,RFOIL,Fuego and Overflow Results

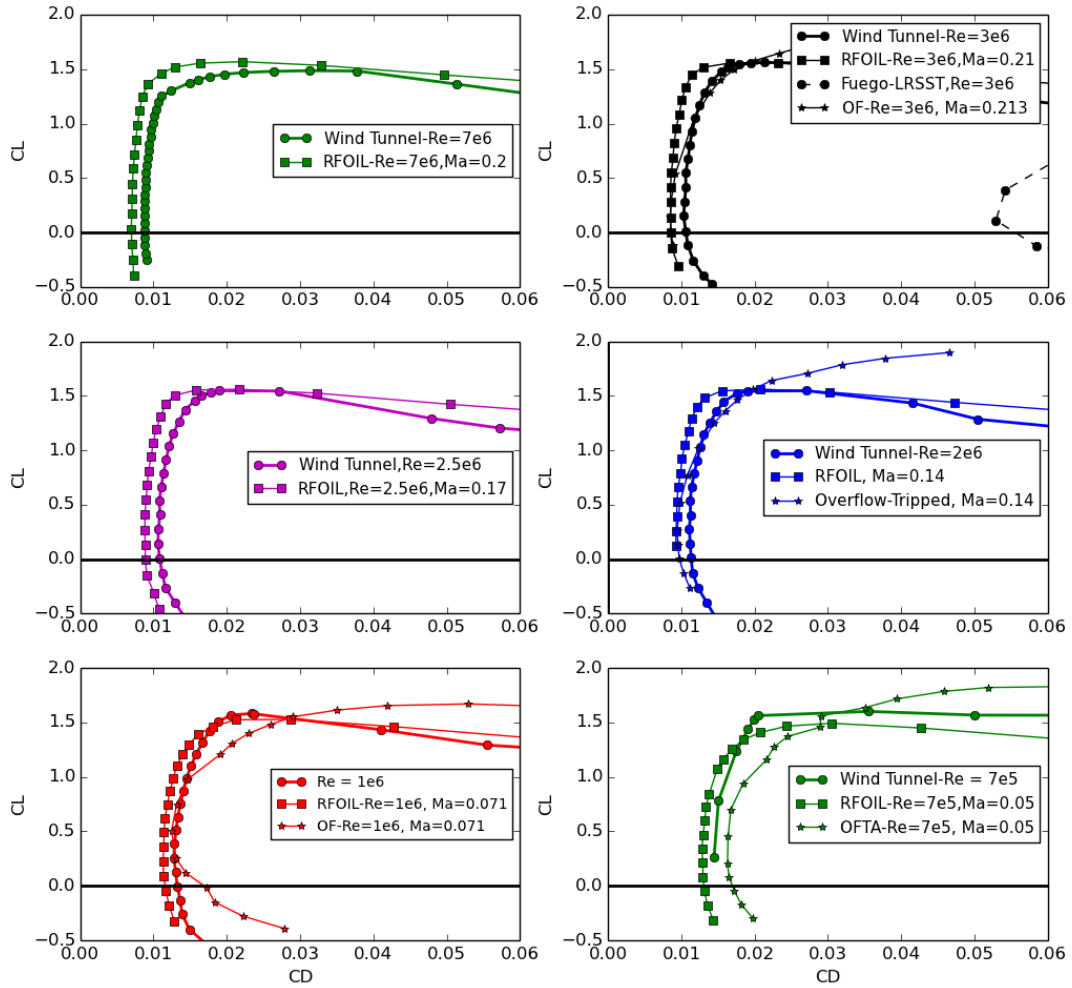


Figure 24. Comparison of the RFOIL, Fuego, and Overflow drag polars to the wind tunnel data for $Re = 7 \times 10^6, 3 \times 10^6, 2.5 \times 10^6, 2 \times 10^6, 1 \times 10^6$, and 0.7×10^6 for the DU 97-W-300Mod airfoil.

DU97-W2-300Mod: Wind Tunnel,RFOIL,Fuego and Overflow Results

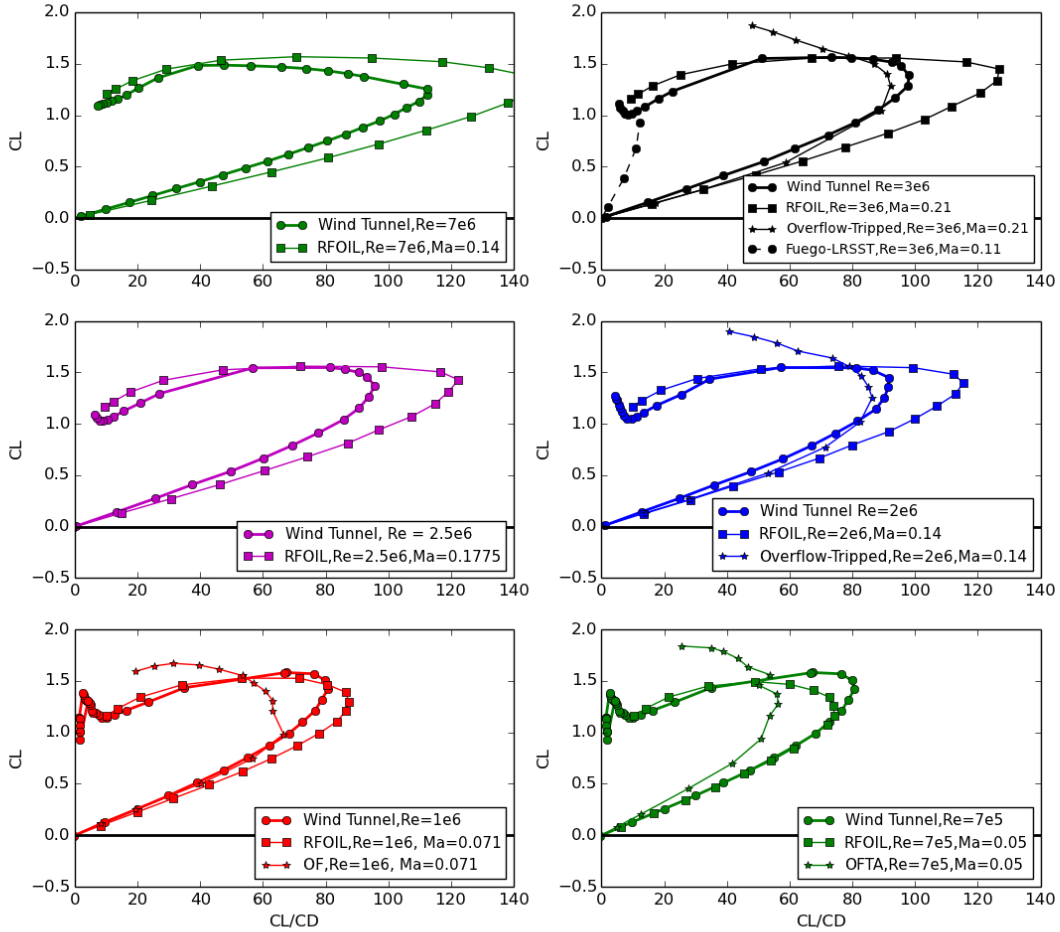


Figure 25. Comparison of the RFOIL, Fuego, and Overflow lift to drag ratios to the wind tunnel data for the DU 97-W-300Mod airfoil.

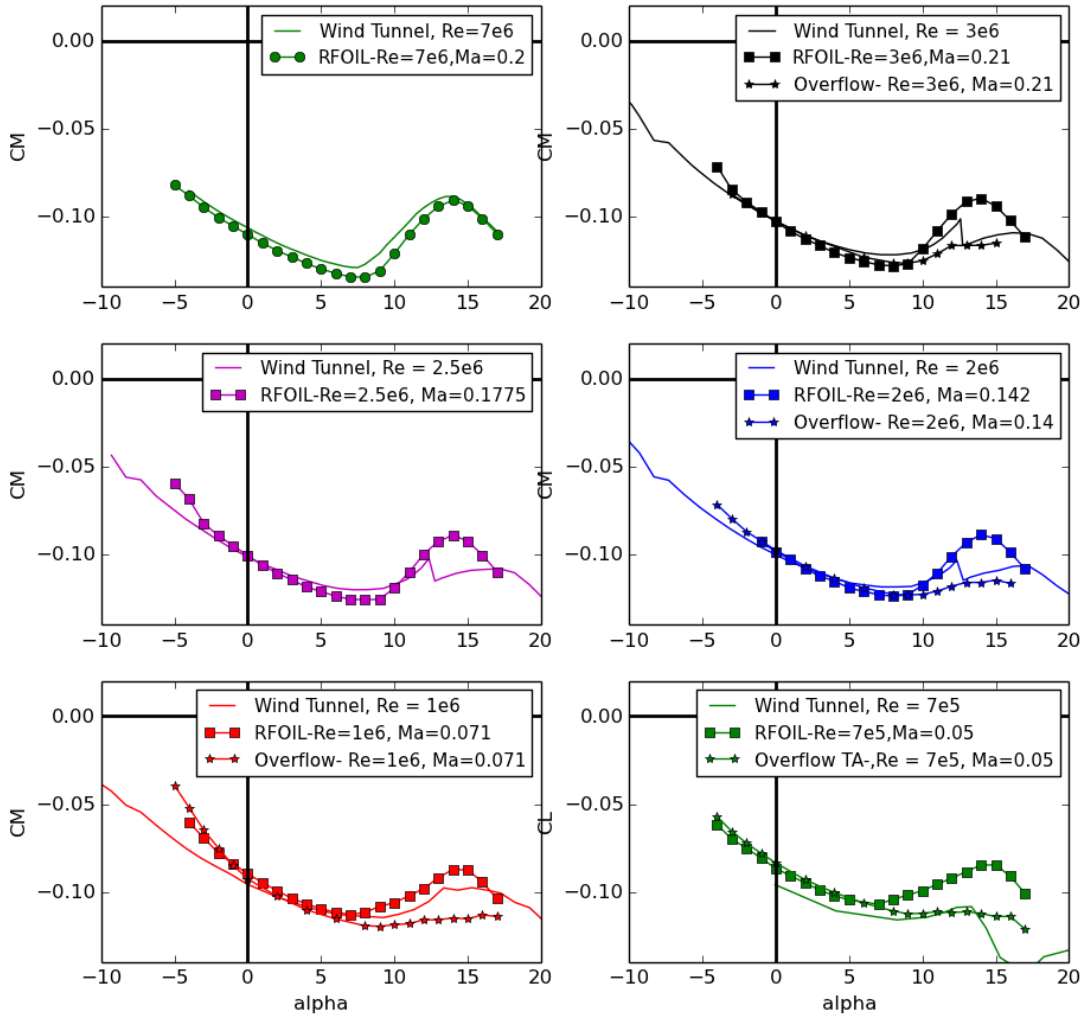


Figure 26. Comparison of Overflow and RFOIL pitching moment to experimental data [18] for DU 97-W-300Mod.

5.5 RFOIL and Overflow for low Reynolds Numbers

Figure 23 through Figure 26 compare the Overflow and RFOIL data to the experimental data for Reynolds numbers of 0.7, 1, 2, 2.5, 3, and 7 million. There is also Fuego data for the $Re = 3 \times 10^6$ case. For all Reynolds numbers, the results are fairly close, but the Overflow data does a slightly better job of matching the wind tunnel values, up until the airfoil reaches stall. Near and after stall, the RFOIL predictions for lift are more accurate. The Overflow drag results match fairly well until the stall region, as well. The operating range for the inboard section of the NRT blade will mostly be below stall, so these discrepancies should have a negligible negative effect on design parameters. The RFOIL drag results seem to capture the drag values and shape of the

curve quite well, however, for this airfoil Overflow does a better job at matching the experimental $C_L/C_{D_{max}}$. The Fuego drag results, however, are over predicted by a large amount. There is only Overflow and RFOIL data for pitching moment at $Re = 3 \times 10^6$, and both match the experimental values well (Figure 26)

The comparison of simulation results to experimental data show that the most suitable analysis approach is to use a combination of RFOIL and Overflow. Overflow is needed because the results for $C_L/C_{D_{max}}$ agree well and it can also be used in the next steps that will use its 3D capabilities. There are also other useful features such as the Langtry-Menter $\gamma-Re_\theta$ transition model [26] that will be tested so that the transition location from RFOIL will not have to be “hard coded” in to the calculations. Because Overflow does a somewhat better at predicting $C_L/C_{D_{max}}$, or at least not over predicting the value, it will be useful to use in conjunction with RFOIL for blade plan form design. Since Overflow does not capture $C_{L,max}$ well, it will be better to rely on RFOIL for that value.

This section compares the results for the RFOIL and Overflow for the Reynolds numbers of interest to the design of the scaled NRT blades. This will serve as a check to both methods.

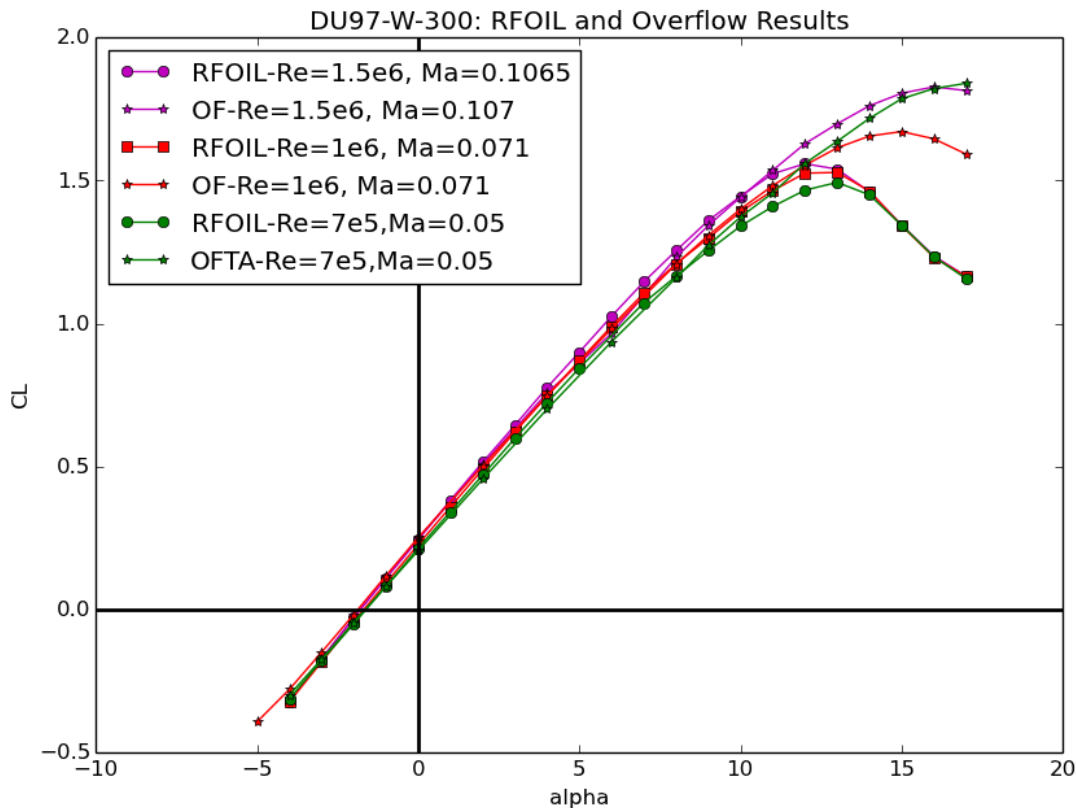


Figure 27. Comparison of RFOIL to Overflow lift curves for DU 97-W-300Mod airfoil at lower Reynolds numbers.

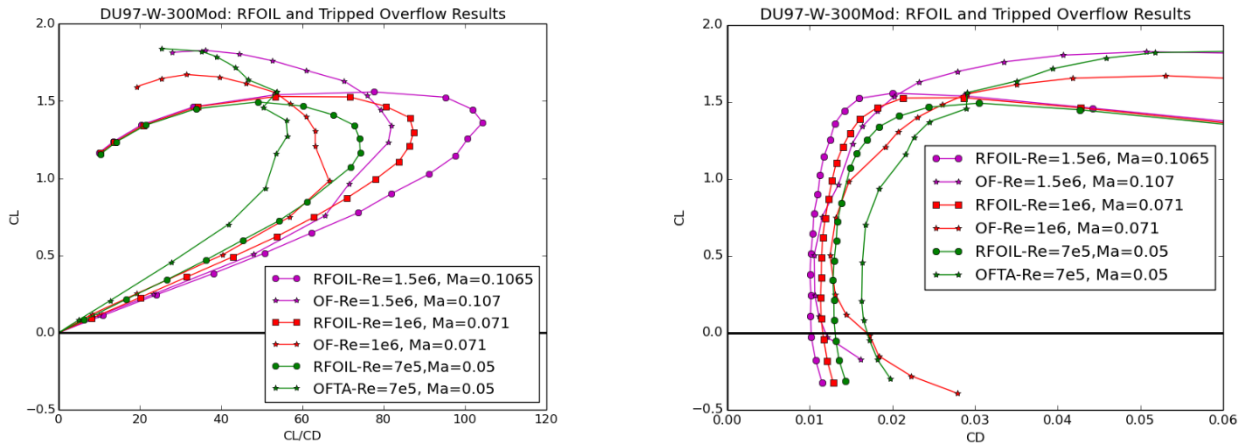


Figure 28. Comparison of RFOIL to Overflow lift to drag ratio and drag polar for DU 97-W-300Mod airfoil at lower Reynolds numbers.

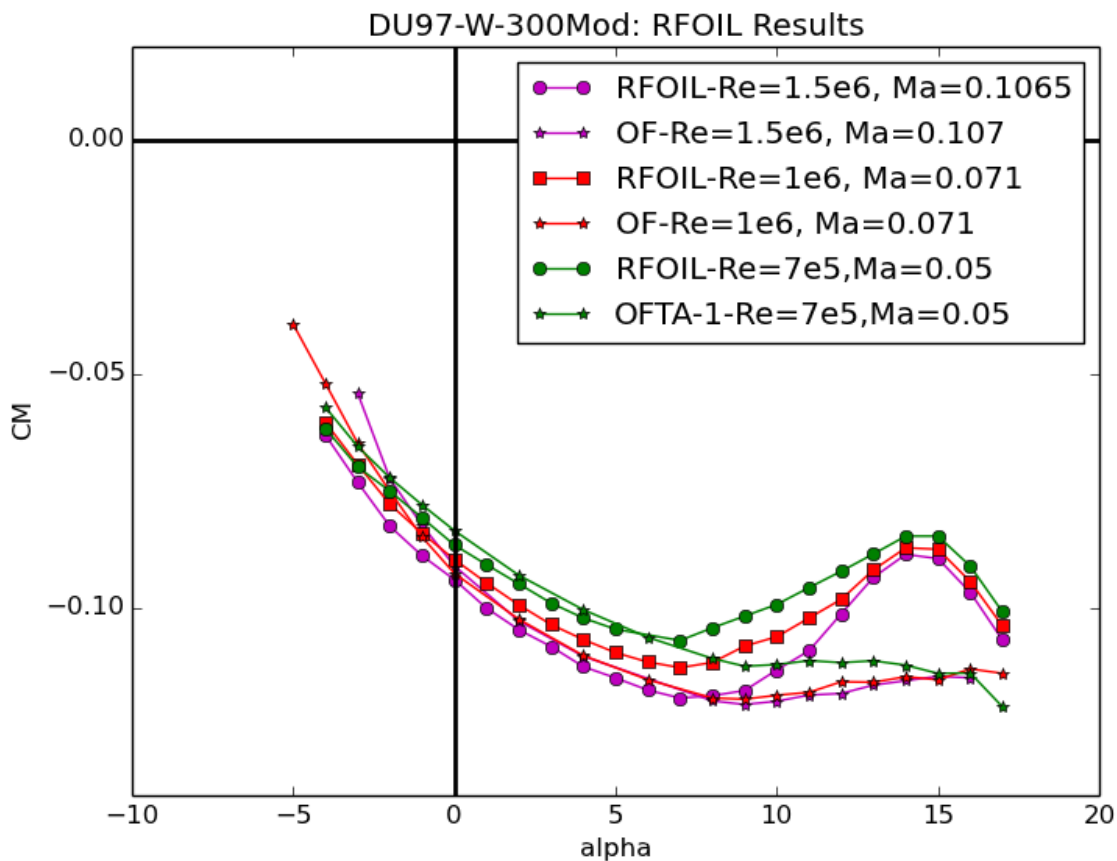


Figure 29. Comparison of RFOIL to Overflow pitching moments for DU 97-W-300Mod airfoil at lower Reynolds numbers.

6. SIMULATION RESULTS FOR 25% THICK AIRFOIL

The airfoil used for the simulations of the 25% thick airfoil is the DU 91-W2-250Mod, which will be considered in the design of the new NRT blade. Taking the lessons learned from the 30% thick airfoil, the Mach number is changed for each Reynolds number for the RFOIL and Overflow calculations. There were no Fuego calculations done for this airfoil.

6.1. RFOIL

The RFOIL calculations for the DU 91-W2-250Mod airfoil were run in a similar manner to what was done with the DU 97-W-300Mod airfoil. The default of $N_{crit} = 9$ was used, viscosity was turned on, and the Mach number was adjusted for each Reynolds number and are the same as what is used in Section 5.

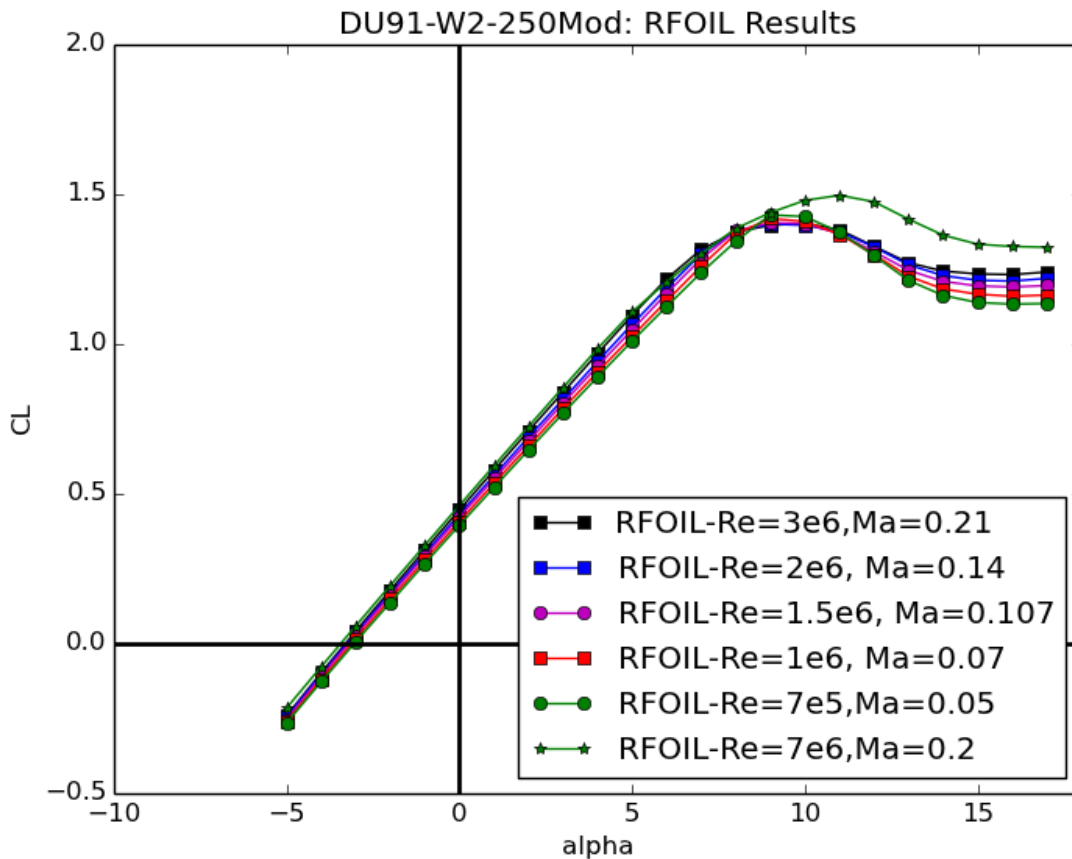


Figure 30. RFOIL DU 91-W2-250Mod lift curve for a wide range of Reynolds number values.

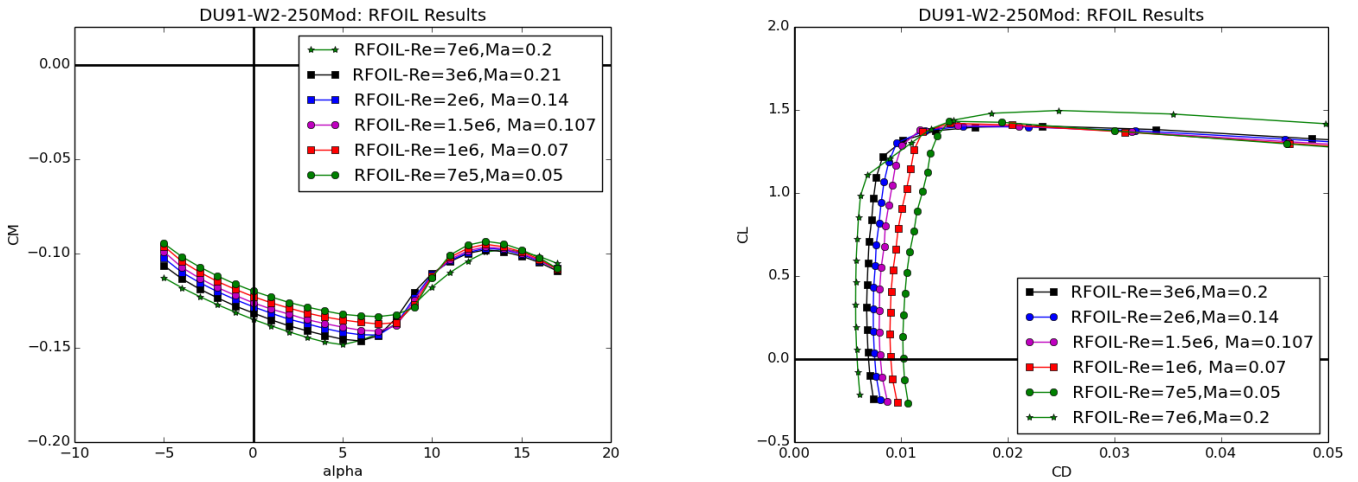


Figure 31. RFOIL DU 91-W2-250Mod pitching moment and drag for a wide range of Reynolds number values.

6.2. Overflow

The Overflow c-grid used for the DU 91-W2-250Mod airfoil is very similar to the DU 96-W-300Mod grid. It has 563 nodes around the airfoil and 96 nodes in the wake. There are 179 nodes perpendicular to the airfoil extending $30c$ away. Near the wall $y^+ \approx 1$. As with the DU 96-W-300Mod, the transition locations, which were predicted using RFOIL, were set for all of the Overflow simulations presented in this section. For the lower Reynolds numbers, $Re = 1$ and 0.7 million, the solution was not converging correctly so the “time accurate” mode with 12 Newton sub-iterations and a physical time step of $DTPHYS = 0.001$ was used. The simulations that are run using the time accurate mode are signified by “OFTA” in the figures. The iteration time step was also reduced to $DT = 0.001$. See Appendix A for more details on Overflow convergence.

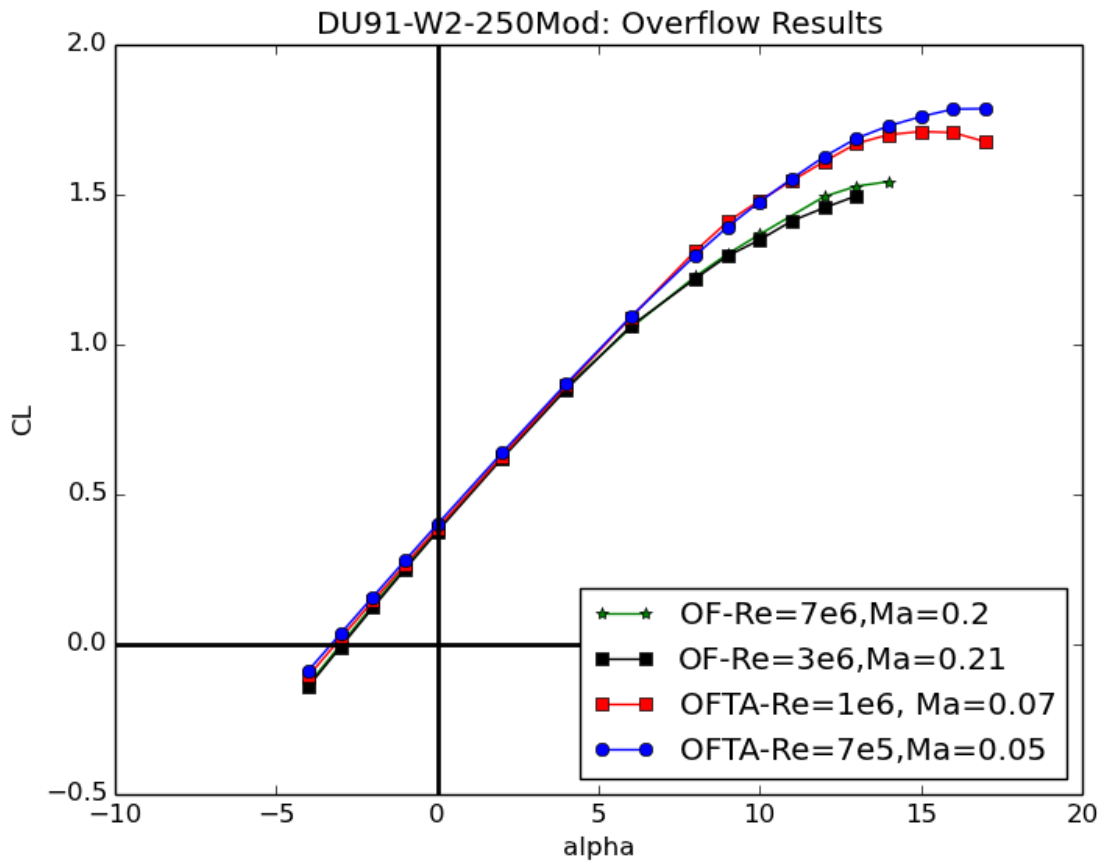


Figure 32. Overflow lift curve data for DU 91-W2-250Mod airfoil at Re ranging from 7 to 0.7 million. “OFTA” indicates that the time accurate mode was used.

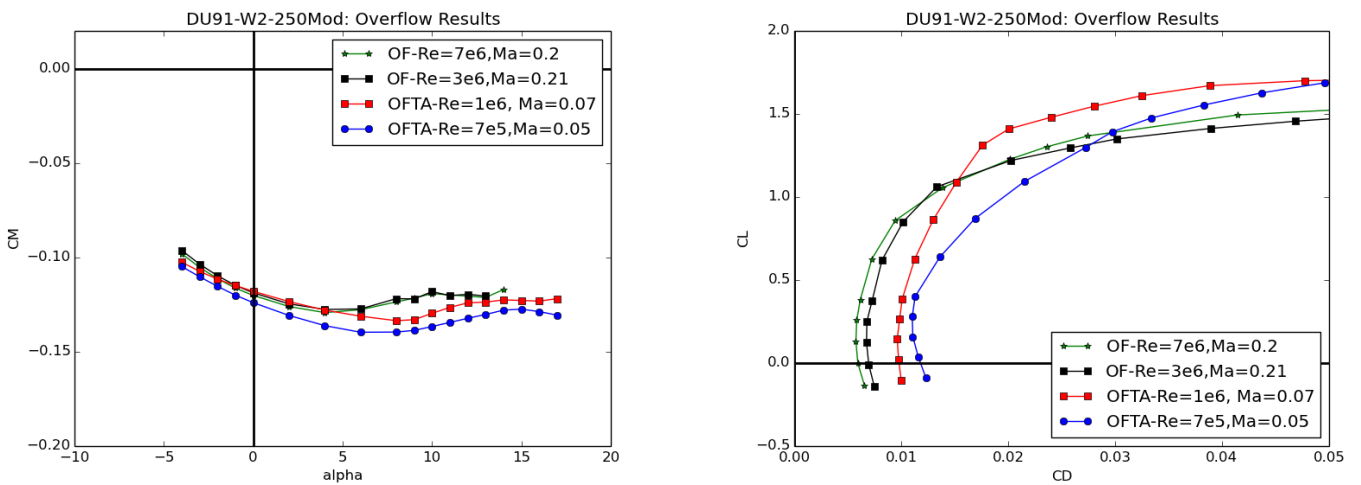


Figure 33. Overflow pitching moment and drag data for DU 91-W2-250Mod airfoil. “OFTA” indicates that the time accurate mode was used.

6.3. Compiled Results

This section shows the results from RFOIL and Overflow compared directly with the wind tunnel data. For this airfoil there are wind tunnel data available for $Re = 7 \times 10^6$ [18], 3×10^6 [20], 2×10^6 [20], 1.5×10^6 [21], 1×10^6 [16], and 7×10^5 [16].

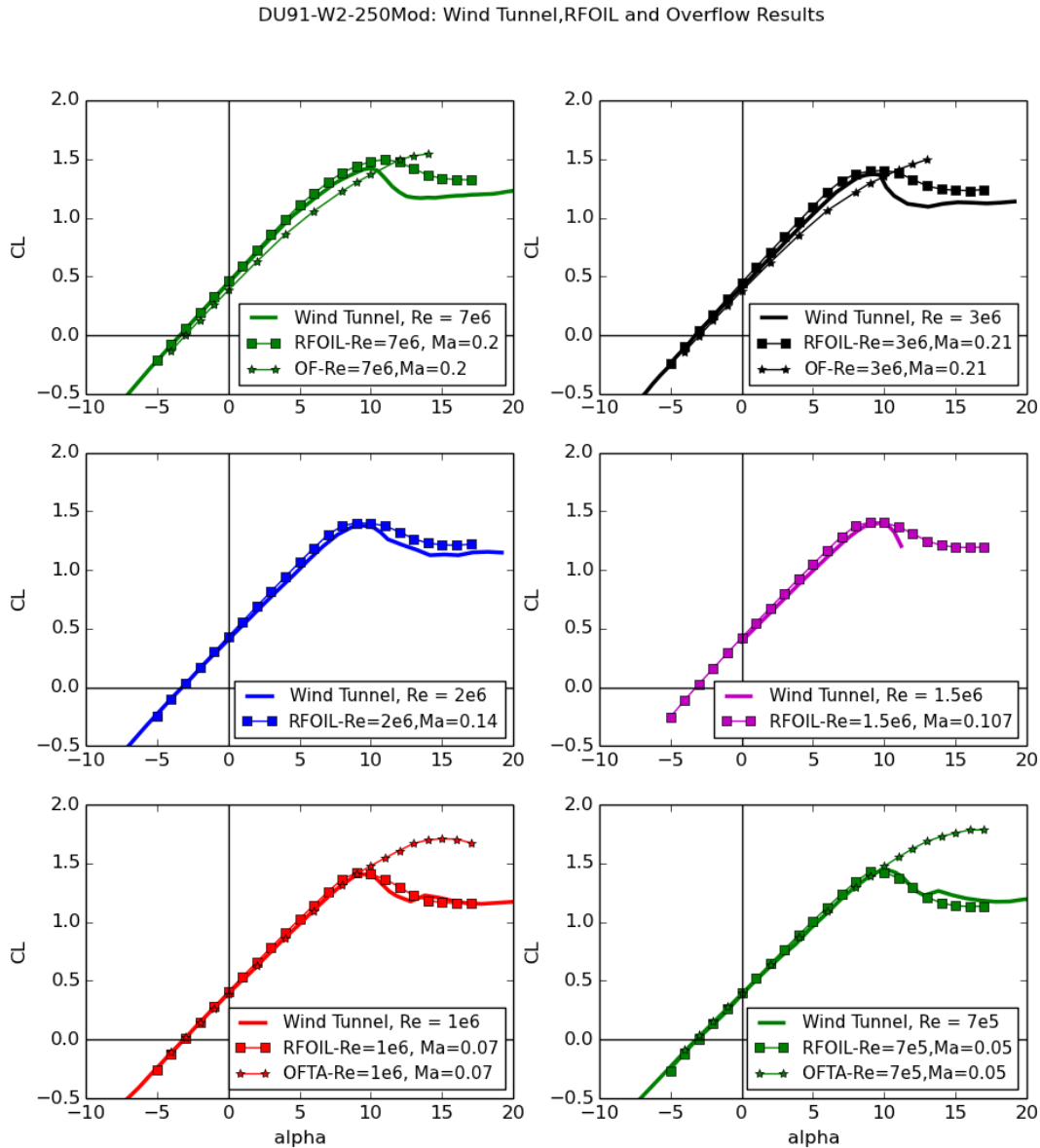


Figure 34. Comparison of RFOIL and Overflow lift curves to the wind tunnel data for the DU 91-W2-250Mod airfoil. “OFTA” indicates that the time accurate mode was used for the Overflow runs.

As was done with the DU97-W-300Mod airfoil in section 5.4, the RFOIL drag is corrected with a factor of 1.09. This is compared with RFOIL without the correction, Overflow, and wind tunnel data for both $Re = 3 \times 10^6$ and 1×10^6 . For this thinner airfoil, the correction factor does a much better job at bringing the RFOIL drag data into alignment with the experiment. For both Reynolds numbers, the corrected results match the wind tunnel data better than both the non-corrected RFOIL and the Overflow data.

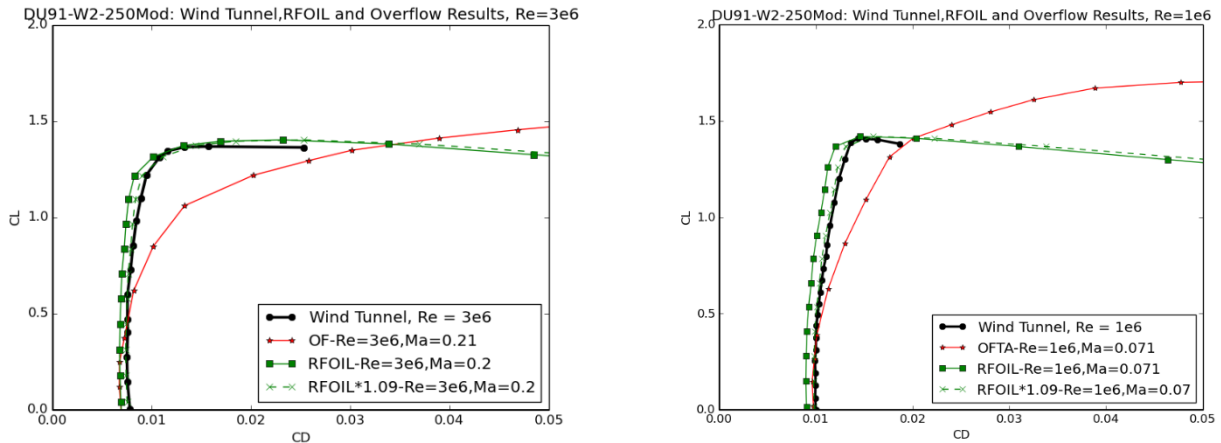


Figure 35. Left: For $Re = 3 \times 10^6$, RFOIL drag results with and without the correction factor of 1.09, and Overflow results are compared to wind tunnel data [20]. Right: the same for $Re = 1 \times 10^6$. “OFTA” indicates that the time accurate mode was used in Overflow.

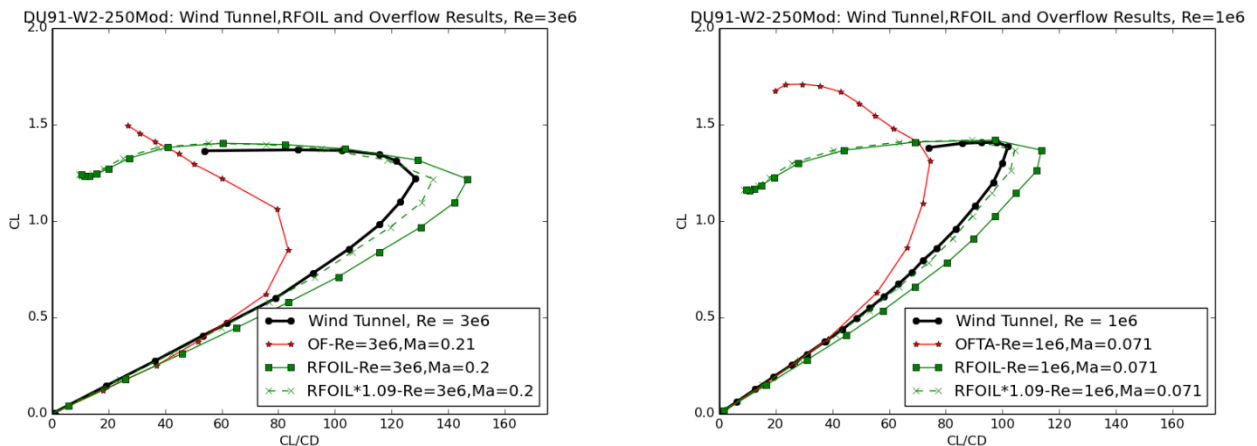


Figure 36. Left: For $Re = 3 \times 10^6$, RFOIL lift to drag results with and without the correction factor of 1.09, and Overflow results are compared to wind tunnel data [20]. Right: the same for $Re = 1 \times 10^6$. “OFTA” indicates that the time accurate mode was used in Overflow.

DU91-W2-250Mod: Wind Tunnel,RFOIL and Overflow Results

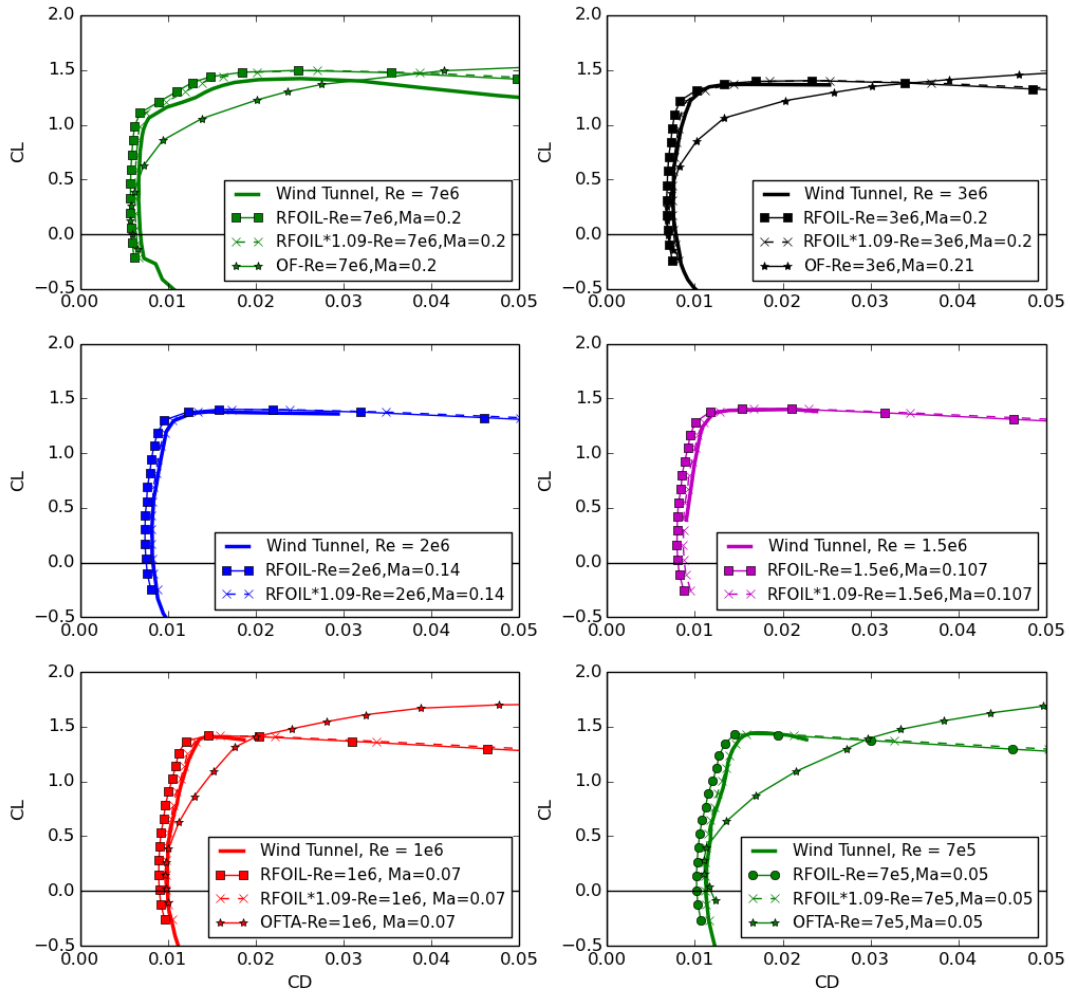


Figure 37. Comparison of RFOIL and Overflow drag polar data to the wind tunnel data for the DU 91-W2-250Mod airfoil. RFOIL results both with and without the 1.09 correction factor are shown. “OFTA” indicates that the time accurate mode was used for Overflow.

DU91-W2-250Mod: Wind Tunnel,RFOIL and Overflow Results

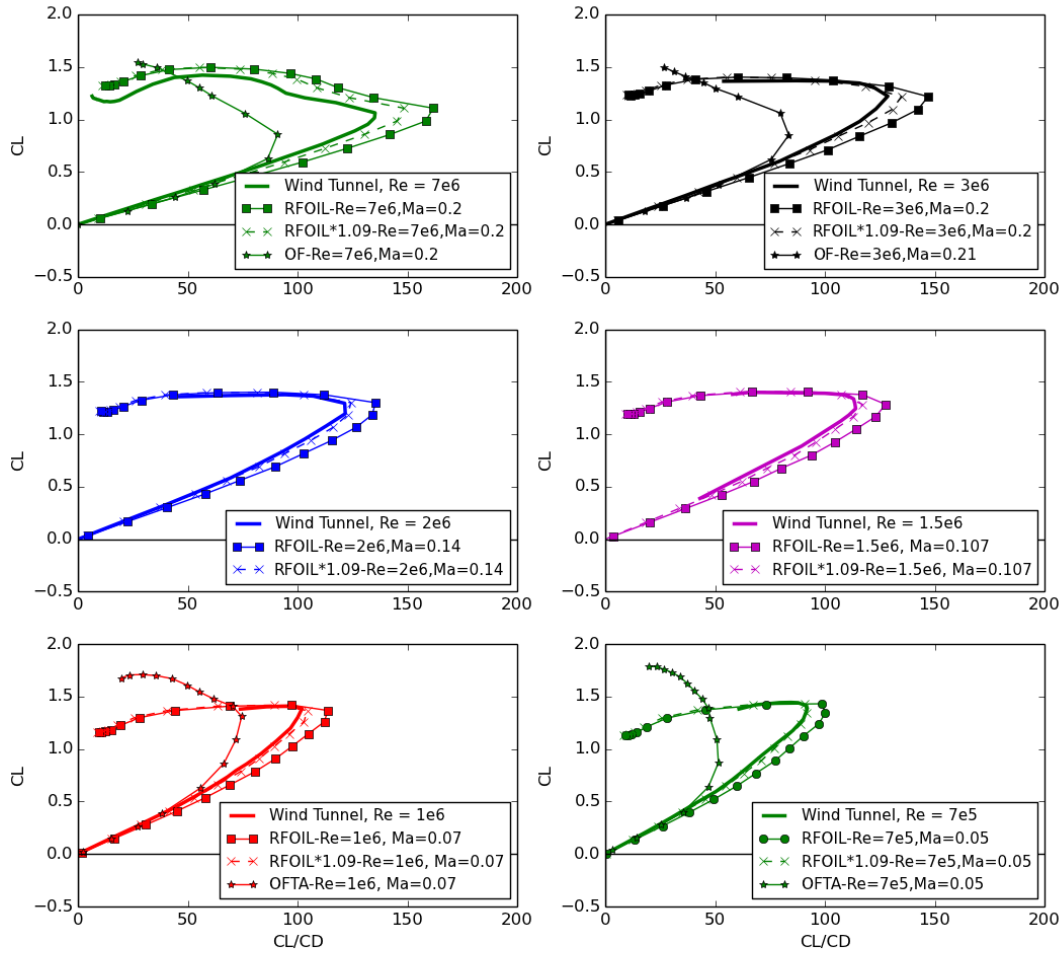


Figure 38. Comparison of RFOIL and Overflow lift to drag ratio to the wind tunnel data for the DU 91-W2-250Mod airfoil. RFOIL results both with and without the 1.09 correction factor are shown. “OFTA” indicates that the time accurate mode was used for Overflow.

DU91-W2-250Mod: Wind Tunnel, RFOIL and Overflow Results

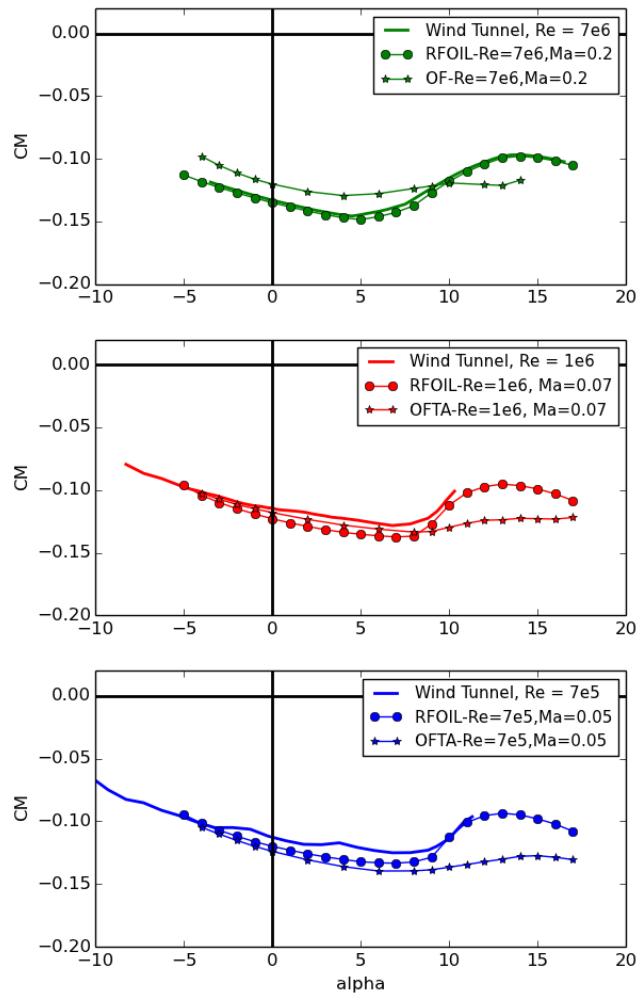


Figure 39. Comparison of RFOIL and Overflow pitching moment to the wind tunnel data for the DU 91-W2-250Mod airfoil. “OFTA” indicates that the time accurate mode was used for Overflow.

For this airfoil, RFOIL does a very good job fitting the wind tunnel data. It matches several key features of the various plots even better than Overflow. The match between the RFOIL drag results with the correction factor and the experimental data is even better than for the DU97-W-300Mod. Like with the DU97-W-300Mod airfoil, RFOIL captures the $C_{L,max}$ of the lift curve more closely (Figure 34). The upper left corner of the “drag bucket” in Figure 37 is matched very well by RFOIL with the correction factor, but is under predicted by Overflow. This can be seen again in Figure 38 which shows the lift to drag ratio. RFOIL slightly over predicts the $C_L/C_{D,max}$, while Overflow is under predicting it. However, the Overflow results are more conservative, even if they are farther off. Figure 39 shows that both match the pitching moment results fairly well, with RFOIL capturing the shape slightly more accurately.

7. SIMULATION RESULTS FOR 35% THICK AIRFOIL

For the 35% thick airfoil there is wind tunnel data at $Re = 7 \times 10^6$ for the DU 99-W3-350 airfoil and at $Re = 3 \times 10^6$ for the DU 99-W-350 airfoil. These two versions of this airfoil are sufficiently different that the simulations of one should not be compared to the wind tunnel experiments of the other. The NRT airfoil will use the DU 99-W3-350 [20, 21] version so the Overflow simulations are run with this airfoil.

7.1. RFOIL

Figure 40 shows the comparison of the RFOIL simulations to the wind tunnel data, and Figure 41 shows the RFOIL results for $Re = 7$ million to 0.7 million.

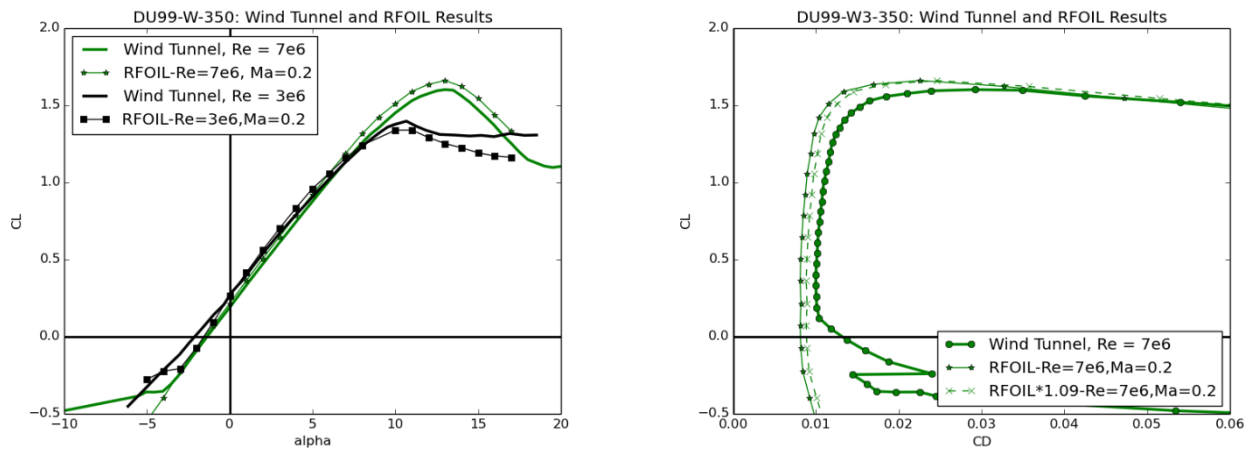


Figure 40. Left: Lift curve comparisons of RFOIL to wind tunnel results for the Adjusted DU99-W3-350lm airfoil at $Re = 3 \times 10^6$ [21] and the DU 99-W3-350 at $Re = 7 \times 10^6$ [18]. Right: Drag polar for $Re = 7 \times 10^6$ (DU 99-W3-350 [18]).

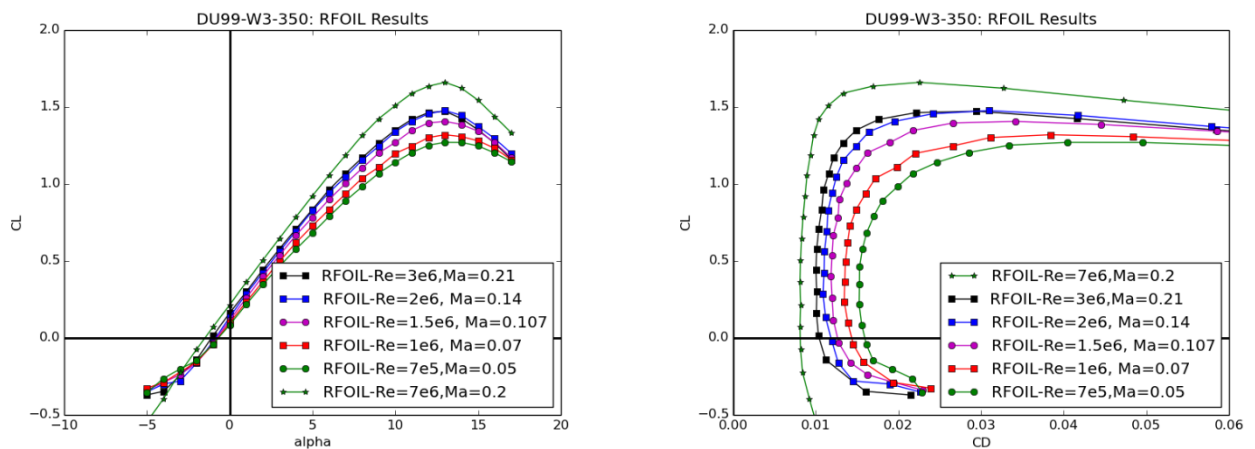


Figure 41. RFOIL DU 99-W3-350 lift curve for a wide range of Reynolds number values.

7.2. Overflow

Overflow calculations were made using the DU 99-W3-350 airfoil for $Re = 7$ and 1 million. These were both run in the time accurate mode, since it was expected that this thicker airfoil would have more trouble converging in the steady state mode due to shedding eddies. The mesh is a c-grid which has 560 nodes around the airfoil and 96 nodes in the wake. There are 204 nodes perpendicular to the airfoil extending $30c$ away. Near the wall $y^+ \approx 1$.

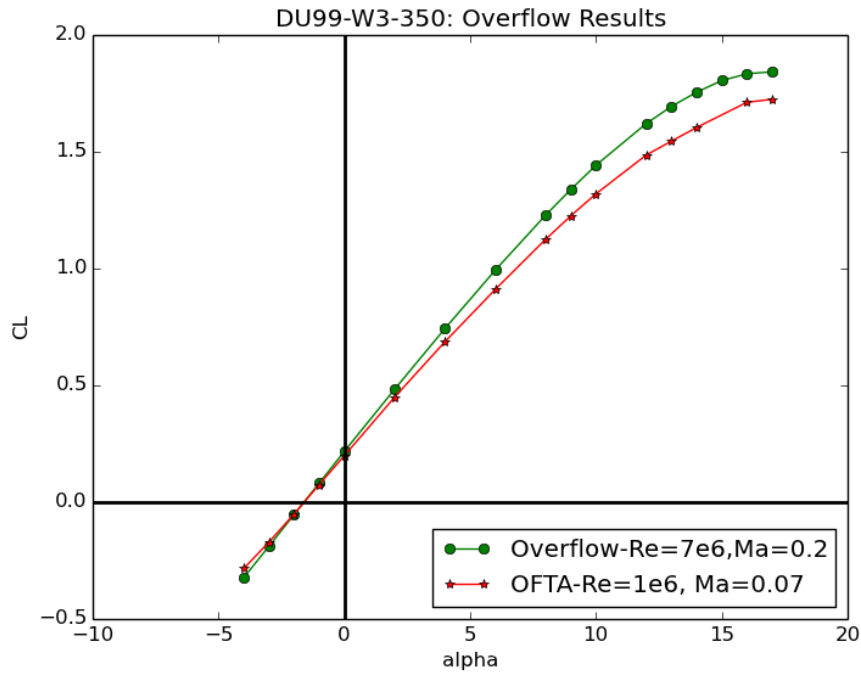


Figure 42. Lift curve for the DU 99-W3-350 airfoil at $Re = 7$ and 1 million. Both cases are run in the time accurate mode.

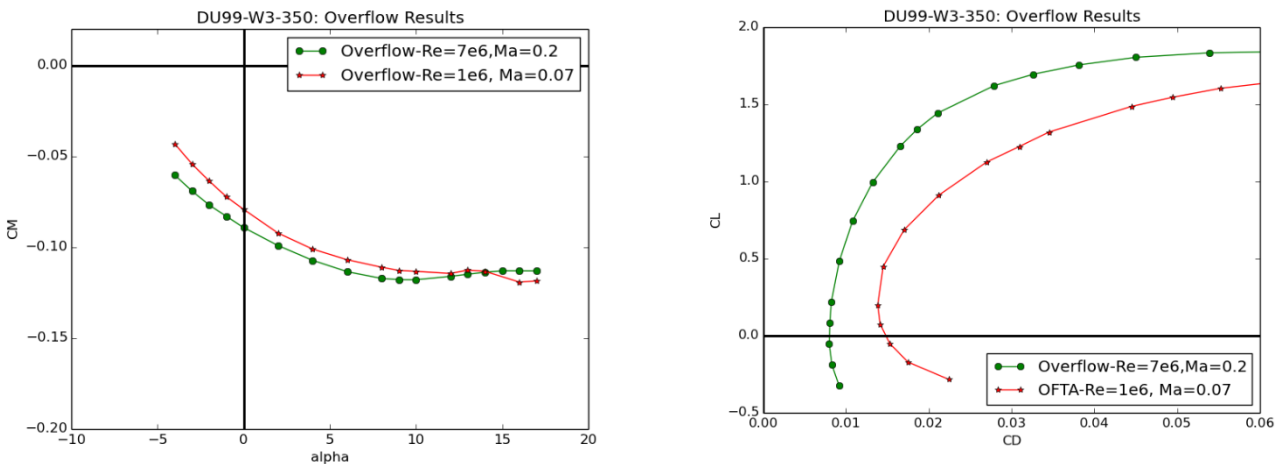


Figure 43. Pitching moment and drag polar for the DU 99-W3-350 airfoil.

7.3. Compiled Results

The RFOIL and Overflow results are compared to the wind tunnel data for DU 99-W3-350 at $Re = 7 \times 10^6$, and to each other at $Re = 3 \times 10^6$. RFOIL does a very good job at matching the experimental results for this airfoil, and is more accurate than Overflow for lift, drag, and pitching moment.

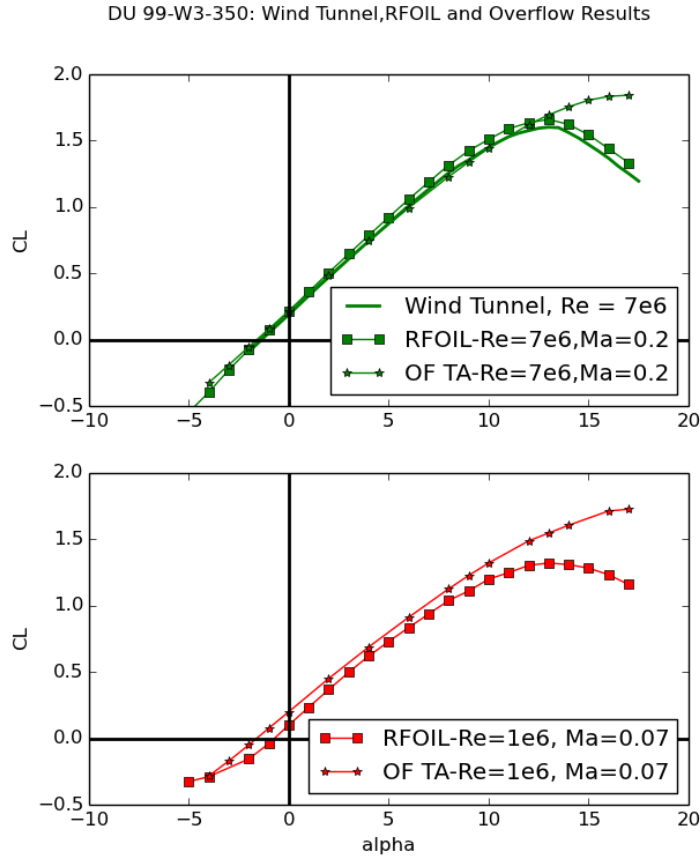


Figure 44. Comparison of RFOIL and Overflow lift curves to the wind tunnel data for the DU 99-W3-350 airfoil.

DU 99-W3-350: Wind Tunnel, RFOIL and Overflow Results

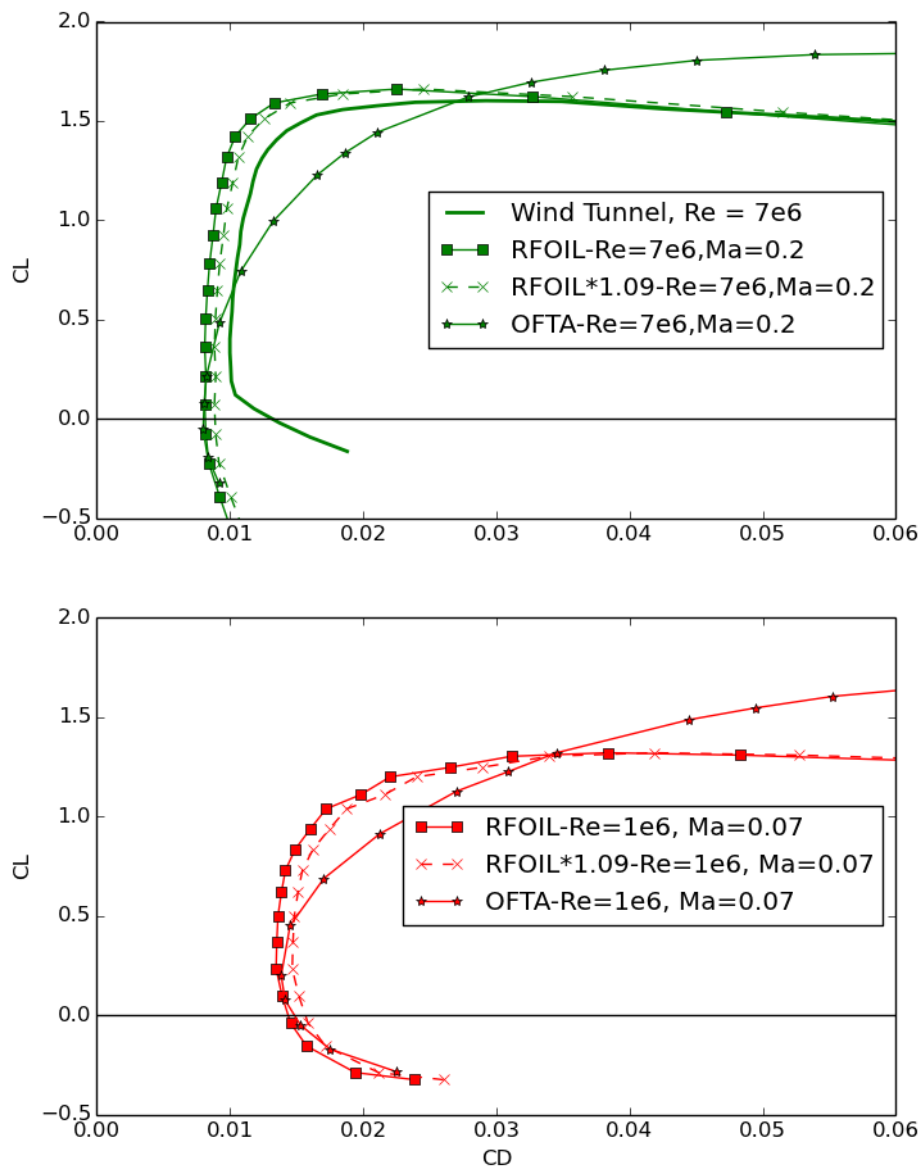


Figure 45. Comparison of RFOIL and Overflow drag polars to the wind tunnel data for the DU 99-W3-350 airfoil.

DU 99-W3-350: Wind Tunnel,RFOIL and Overflow Results

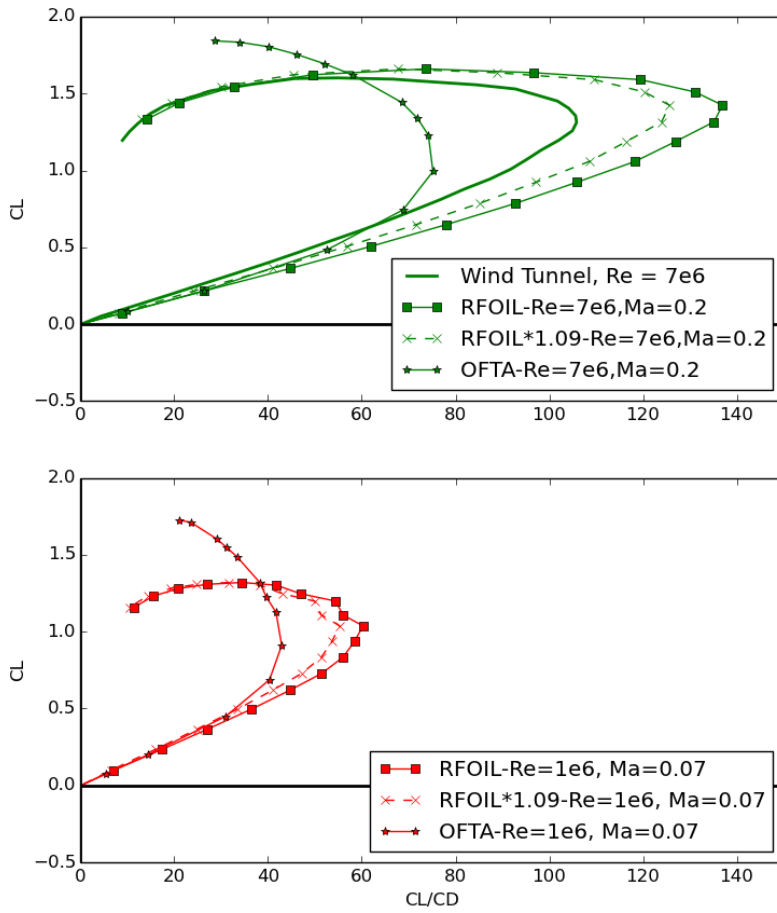


Figure 46. Comparison of RFOIL and Overflow lift to drag ratios to the wind tunnel data for the DU 99-W3-350 airfoil.

DU 99-W3-350: Wind Tunnel, RFOIL and Overflow Results

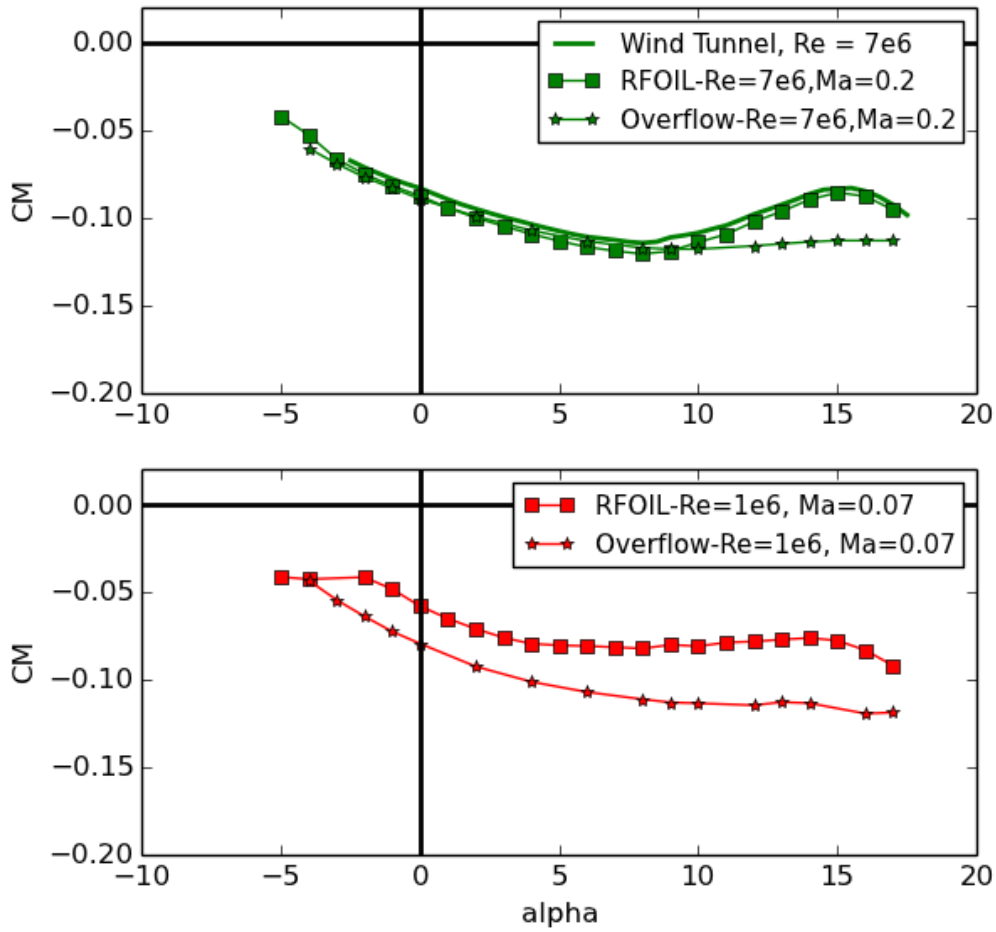


Figure 47. Comparison of RFOIL and Overflow pitching moments to the wind tunnel data for the DU 99-W3-350 airfoil.

8. SIMULATION RESULTS FOR 40% THICK AIRFOIL

Originally, a 40% thick airfoil was considered in the new NRT blade design. After this study had been started, it was decided to not use it due to its limited performance at lower Reynolds numbers. The data created before that point is presented here for completeness. Two 40% thick airfoils had available wind tunnel data. The DU 99-W3-405 has available wind tunnel data at $Re = 7 \times 10^6$ and the DU 00-W-401 has data at $Re = 3 \times 10^6$.

8.1. RFOIL

RFOIL results are compared to the wind tunnel data in Figure 48. Figure 49 shows the RFOIL lift and drag polars for $Re = 7$ million to $Re = 0.7$ million.

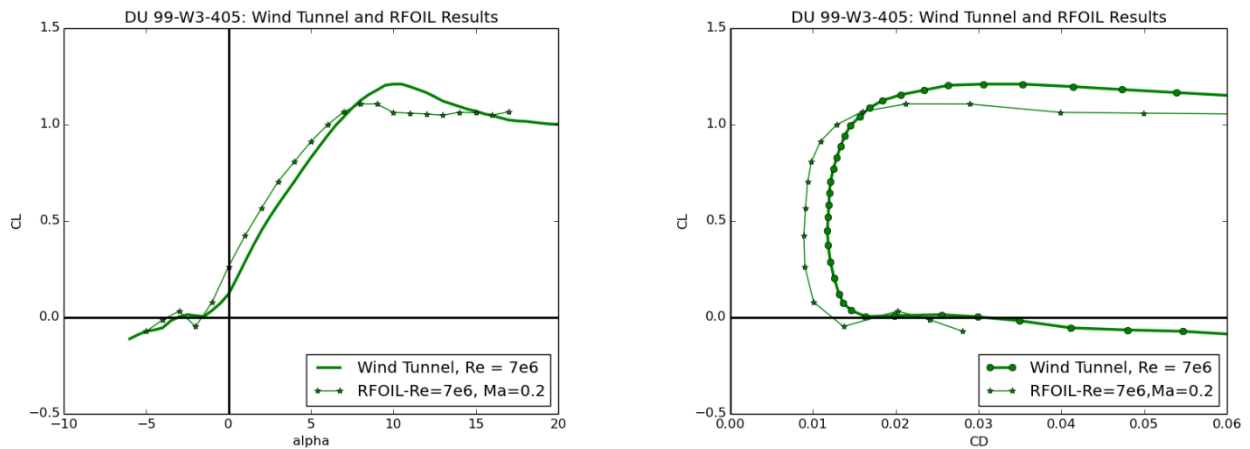


Figure 48. RFOIL data for DU 99-W3-405 compared with wind tunnel data at $Re = 7 \times 10^6$ [18] and $Re = 3 \times 10^6$ [21].

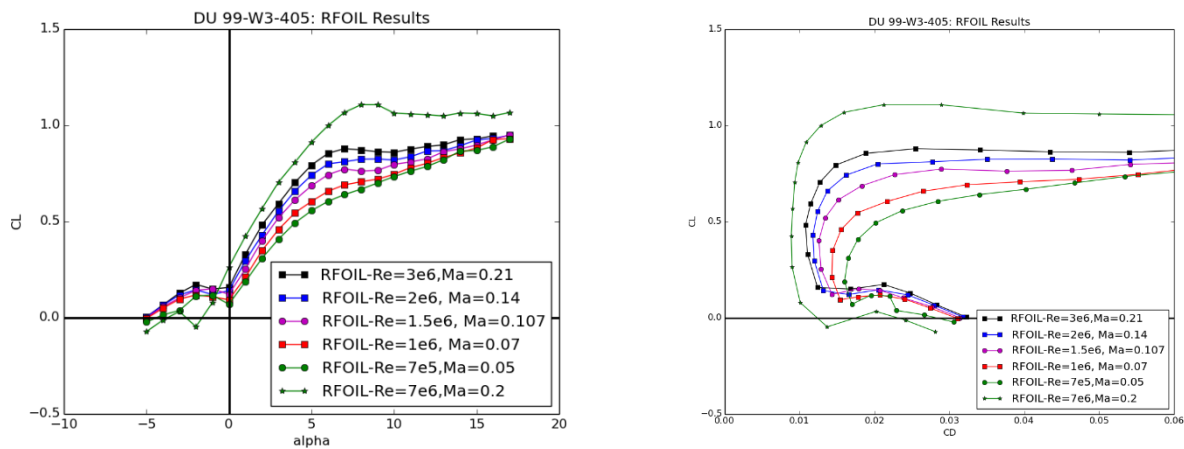


Figure 49. RFOIL DU 99-W3-405 lift curve for a wide range of Reynolds number values.

9. DISCUSSION

This study set out to explore the best way to model airfoils to insure that they will have the characteristics needed for the new NRT blade design. This includes being able to match circulation and dynamic loads of larger scale rotors while also having room for instrumentation.

There are several take away points from the study thus far. RFOIL has once again proven to be a very useful tool which gives accurate results and can be used for comparison to other codes for scenarios where experimental data are not available. Overflow, while it does miss the value of $C_{L,max}$, is fairly accurate otherwise and does have the option of expanding to 3D analysis. If that is needed it will be worthwhile to either explore methods that will increase the accuracy at $C_{L,max}$ or making sure that the angles of attack are within the range where Overflow works well.

The idea behind trying Sandia's low Mach Sierra code, Fuego, for this project was to expand the capabilities of the in-house codes to include more wind energy applications. Unfortunately, Fuego needs more features and lots of testing before it can be used successfully on thick airfoils. It also should be mentioned that it is not an open source code that can be shared with any future collaborators outside of SNL. There is a Sandia open source fluids code, Nalu, but it is primarily a Large Eddy Simulation code, so it is not necessarily suitable for the types of simulations performed for this study.

Overflow has been used extensively and successfully for CFD studies of airfoils (see work by van Dam, Chow, Blaylock, Baker, Sclanfani), including thick airfoils. Thick airfoils, especially at lower Reynolds numbers, can be tricky to simulate, but Overflow has several features that can be applied to help get an accurate model. These include transition models, Detached Eddy Simulation, and soiled leading edge functions. It also has 3D capabilities that can be used in the next step of blade design. While Overflow does a poor job at capturing correct stall lift and drag values, the operating range for the inboard section of the NRT blade will be mainly below stall. Overflow does an accurate job of predicting the forces on the blade in the angle of attacks of interest.

Simulations of thick airfoils at low Reynolds numbers are much more finicky than thin airfoils at high Reynolds numbers. Attention must be paid to convergence of these airfoils.

Further 2D airfoil studies for this project will include investigating other airfoil families, such as NREL's S-Series, and looking at the characteristics of transition airfoils at span locations between the standard airfoils. At the time of publication, the S-series seems to be the more likely choice for the airfoils used for the NRT. Lessons learned doing this study were applied to the analysis of those airfoils. Results for that family of airfoils will be presented in a different report.

10. CONCLUSIONS AND RECOMMENDATIONS

RFOIL does a very good job at capturing key design features such as $C_{L,max}$ and $C_L/C_{D,max}$. Drag accuracy is improved with the recommended 1.09 correction factor, especially for the DU 91-W2-250Mod airfoil.

Overflow accurately predicts the lift of thick airfoils at low Reynolds numbers better than Fuego so it will be used for any needed RANS analysis of the scaled NRT blade design.

Recommendations for moving forward into the next phase of the study are:

- Continue to explore the extra capabilities (e.g. transition model) in Overflow in 2D to perhaps get even more accurate predictions for the forces.
- Try DES in Overflow for a pseudo-3D blade section before moving into a 3D blade study.
- Conduct a parameter sweep study to see if another correction factor would better improve the accuracy of the RFOIL drag results for thicker airfoils.
- Calibrate the RANS models in Overflow using UQ methods.

11. REFERENCES

- [1] B. R. Resor and D. C. Maniaci, "Definition of the National Rotor Testbed: An Aeroelastically Relevant Research-Scale Wind Turbine Rotor," presented at the AIAA SciTech. 32nd ASME Wind Energy Symposium, National Harbor, Maryland, 2014.
- [2] D. M. Somers, "Theoretical Aerodynamic Analysis of Three DU Wind-Turbine Airfoils," Sandia National Laboratories July 2014 2014.
- [3] R. van Rooij, "Modification of the boundary layer calculation in RFOIL for improved airfoil stall prediction," Report IW-96087R, TU-Delft, the Netherlands.
- [4] M. Drela, "Two-Dimensional Transonic Aerodynamic Design and Analysis Using Euler Equations," Doctor Thesis, Massachusetts Institute of Technology, Boston, MA, USA, 1985.
- [5] C. D. Moen, G. H. Evans, S. P. Domino, and S. P. Burns, "A Multi-Mechanics Approach to Computational Heat Transfer," presented at the ASME 2002 International Mechanical Engineering Congress and Exposition, New Orleans, Louisiana, USA, 2002.
- [6] G. Schneider, "Elliptic systems: finite element method 1," in *Handbook of Numerical Heat Transfer*, W. Minkowycz, E. Sparrow, G. Schneider, and R. Pletcher, Eds., ed New York: J. Wiley and Sons, Inc, 1988.
- [7] F. R. Menter, "Two-equation eddy-viscosity turbulence models for engineering applications," *AIAA Journal*, vol. 32, pp. 1598-1605, 1994.
- [8] "SIERRA Low Mach Module: Fuego Theory Manual -- Version 4.28," Sandia National Laboratories 2014.
- [9] D. Jespersen, T. Pulliam, and P. Buning, "Recent Enhancements to OVERFLOW," in *35th AIAA Aerospace Sciences Meeting and Exhibit*, Reno, NV, 1997, pp. 1-17.
- [10] P. G. Buning, D. C. Jespersen, T. H. Pullian, W. M. Chan, J. P. Soltnick, S. E. Krist, *et al.*, "OVERFLOW User's Manual, Version 1.8ab," NASA Langley Research Center July 2003 2003.
- [11] R. L. Meakin, "Object X-Rays for Cutting Holes in Composite Overset Structured Grids," presented at the 15th AIAA Computational Fluid Dynamics Conference, Anaheim, CA, 2001.
- [12] W. M. Chan and P. G. Buning, *User's Manual for FOMOCO Utilities - Force and Moment Computation Tools for Overset Grids*. Ames Research Center: NASA, 1996.
- [13] W. M. Chan, "Overgrid Interface for Computational Simulations on Overset Grids," presented at the 40th AIAA Aerospace Sciences Meeting and Exhibit, Reno, NV, 2002
- [14] W. M. Chan, R. J. Gomez, S. E. Rogers, and P. G. and Buning, "Best Practices in Overset Grid Generation," presented at the 32nd AIAA Fluid Dynamics Conference and Exhibit St. Louis, MO, 2002
- [15] W. M. Chan, S. E. Rogers, S. M. Nash, P. G. Buning, and R. L. Meakin, "User's Manual for Chimera Grid Tools, Version 1.8," NASA Ames Research Center, Moffet Field, CA 2003
- [16] W. A. Timmer, "Sandia using DU airfoils results," M. Blaylock and D. C. Maniaci, Eds., ed, 2014.
- [17] J. Jonkman. (2005). *NREL 5MW Rotor Geometry: DOWEC-NREL 5MW airfoil data-v2.xls*. Available: <https://wind.nrel.gov/forum/wind/viewtopic.php?f=2&t=440>

- [18] H. J. T. Kooijman, C. Lindenburg, D. Winkelaar, and E. L. van der Hooft, "DOWEC 6MW Pre-Design: Aero-Elastic modelling of the DOWEC 6 MW pre-design in PHATAS," 2003.
- [19] W. A. Timmer and A. P. Schaffarczyk, "The effect of roughness at high Reynolds numbers on the performance of aerofoil DU 97-W-300Mod," *Wind Energy*, vol. 7, pp. 295–307.
- [20] W. A. Timmer and R. P. J. O. M. v. Rooij, "Summary of the Delft University Wind Turbine Dedicated Airfoils," *Journal of Solar Energy Engineering*, vol. 125, pp. 488-496, 2003.
- [21] R. P. J. O. M. van Rooij and W. A. Timmer, "Roughness Sensitivity Considerations for Thick Rotor Blade Airfoils," *ASME*, vol. 125, pp. 468-478, 2003.
- [22] S. Arunajatesan, M. Blaylock, Ed., Email correspondence. ed, 2013.
- [23] N. Gregory and C. L. O'Reilly, "Low-Speed Aerodynamic Characteristics of NACA 0012 Aerofoil Sections, including the Effects of Upper-Surface Roughness Simulation Hoar Frost," NASA R&M 3726Jan 1970 1970.
- [24] M. F. Barone and D. Berg, "Aerodynamic and Aeroacoustic Properties of a Flatback Airfoil: An Update," presented at the 47th AIAA Aerospace Sciences Meeting Including The New Horizons Forum and Aerospace Exposition, Orlando, Florida, 2009.
- [25] W. A. Timmer, "An overview of NACA 6-digit airfoil series characteristics with reference to airfoils for large wind turbine blades," in *47th AIAA Aerospace Sciences Meeting Including The New Horizons Forum and Aerospace Exposition*, Orlando, FL, 2009.
- [26] A. Sclafani, J. Slotnick, J. Vassberg, and T. Pulliam, "Extended OVERFLOW Analysis of the NASA Trap Wing Wind Tunnel Model," presented at the 30th AIAA Applied Aerodynamics Conference, New Orleans, Louisiana, 2012.

APPENDIX A: CONVERGENCE TEST FOR OVERFLOW

As discussed in Section 4 (Figure 16), the higher Reynolds number curves ($Re = 3 \times 10^6$, 2×10^6 , and 1.5×10^6) behave well and match the experimental data well up to stall. The lower Reynolds number cases ($Re = 1 \times 10^6$ and 7×10^5) are not as believable, especially at lower angles of attack. The time evolution of the lift, drag, and pitching moment as well as the L2 residual was examined to check for convergence. The “worst case”, which is for $\alpha = -4^\circ$, $Re = 7 \times 10^5$, will be presented here.

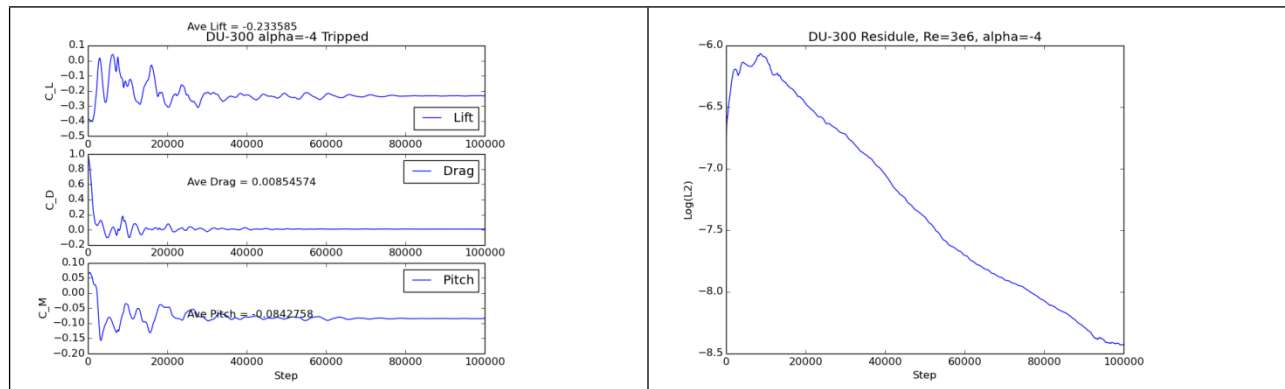


Figure 50. $Re = 3 \times 10^6$, $Ma = 0.11$, Low Mach Preconditioning on: example of good convergence

Figure 50 shows an example of good convergence. This is for the $Re = 3 \times 10^6$ case at $\alpha = -4^\circ$. The force measurements have stopped changing (left) and the L2 residual has dropped more than two orders of magnitude (right).

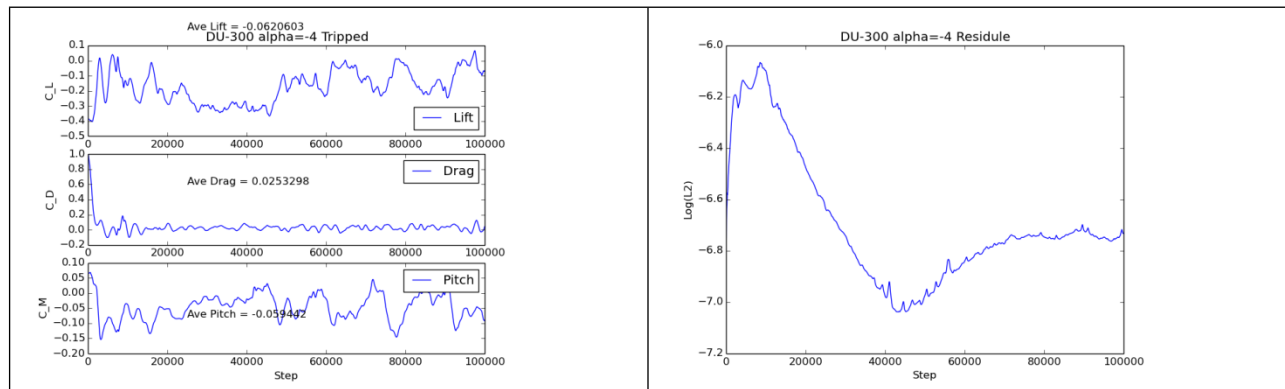


Figure 51. $Re = 7 \times 10^5$, $Ma = 0.11$, Low Mach Preconditioning on: example of poor convergence

Figure 51 shows the case for $Re = 7 \times 10^5$ at $\alpha = -4^\circ$ (as seen in Figure 16). The lift, drag, and pitching moment are not constant, and the L2 residual is actually increasing. To try to get convergence, several tactics were tried and are described below.

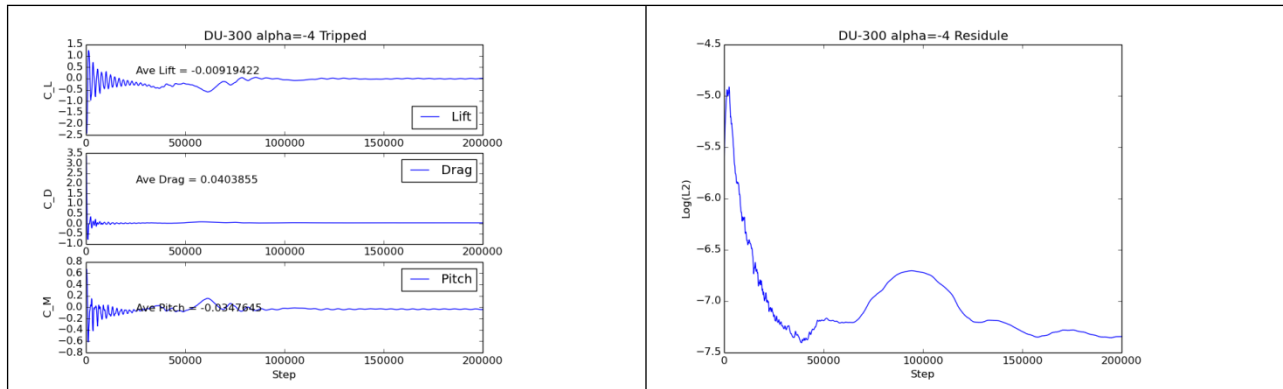


Figure 52. $Re = 7 \times 10^5$, $Ma = 0.11$, Low Mach Preconditioning off

First, the parameters were kept the same but the Low Mach Number Preconditioning was turned off. This feature scales the eigenvalues of the Navier-Stokes equation to help remove the stiffness that occurs at low speeds. While this is still in the low Mach regime and might converge faster with this feature turned on, it has been found that turning this off greatly increased accuracy for cases done involving thick airfoils with circulation control. This case is shown in Figure 52. While this is much steadier, it converges to a lift value that is higher than expected, $C_L \approx 0.0$.

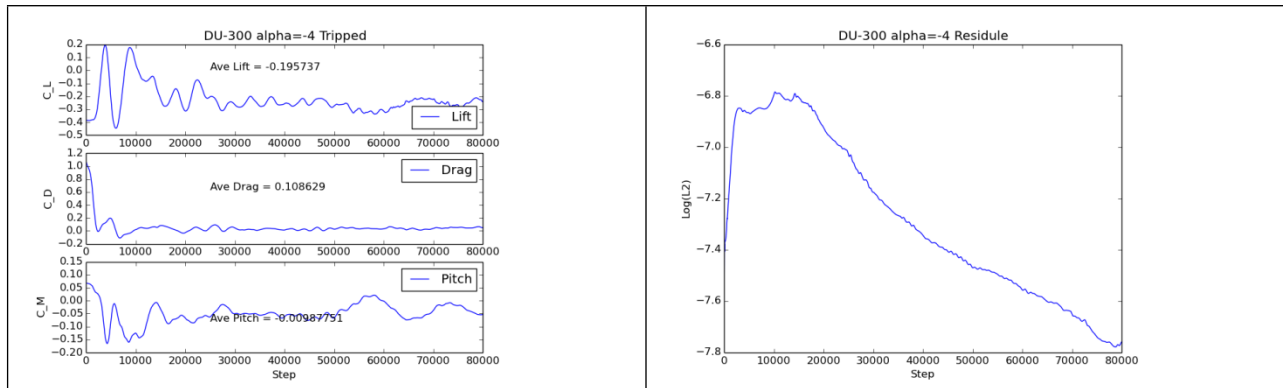


Figure 53. $Re = 7 \times 10^5$, $Ma = 0.05$, $DT = 0.05$

Next, the time step is lowered the $DT = 0.05$, it is run in steady state mode, and the low Mach preconditioning is on. The Mach number was also lowered to $Ma = 0.05$. For all the Reynolds numbers shown in Figure 16, the Mach number and the chord length were kept constant. This means effectively that the viscosity and/or density is changing. A quick calculation showed that if the change is solely in the density, that it would have to drop to $\rho = 0.34 \text{ m}^2/\text{s}$ (from $\rho = 1.47 \text{ m}^2/\text{s}$ at $Re = 3 \times 10^6$). This is probably not realistic. To keep the density and viscosity constant, the Mach needs to be lowered to $Ma = 0.05$. The results for this are shown in Figure 53. The residual shows convergence and the force values have become steady. The lift value of $C_L = -0.2$ is also what would be expected on the lift curve graph. The RFOIL study shows that the Mach number has little effect on the lift curves, so lowering it for the Overflow runs should not affect the results negatively. Therefore, going forward with work in Overflow, the Mach number will

be changed for each Reynolds number. This would also be more consistent with how the data was taken in the wind tunnel.

Below are three images showing the Mach number in the flow field. The left side of Figure 54 corresponds to turning off the low Mach preconditioning (same run as Figure 52). The right side of Figure 54 shows the results of lowering the Mach number to $Ma = 0.05$. Both show a large separation region on the pressure side of the airfoil. There seems like there might be shedding of eddies near the start of the separation region. Figure 55 shows the $Re = 2 \times 10^6$ case at $\alpha = -4^\circ$ for comparison.

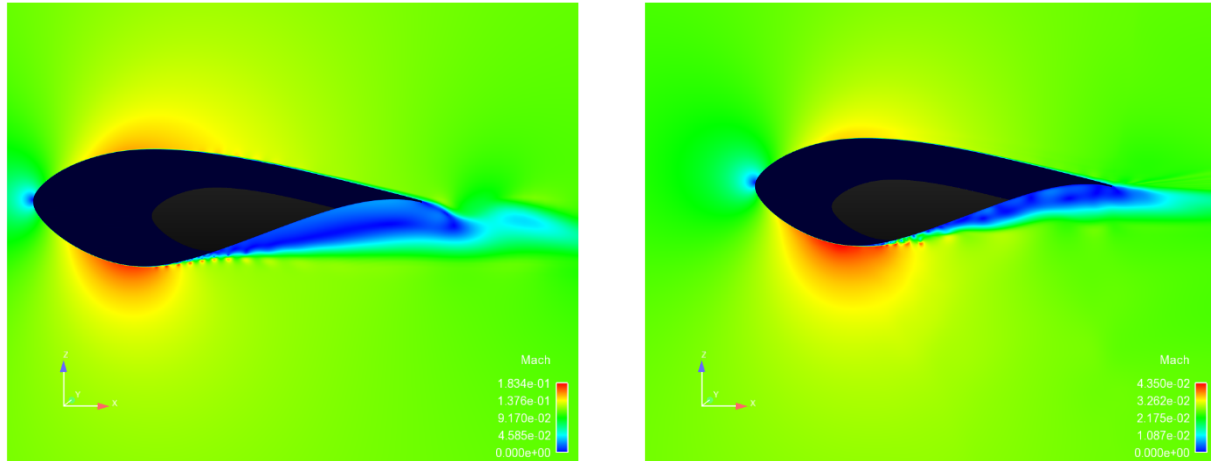


Figure 54. Left: $Re = 7 \times 10^5$, $Ma = 0.11$, $DT = 0.1$, no low Mach preconditioning, no sub-iterations (Corresponding to Figure 51) Right: $Re = 7 \times 10^5$, $Ma = 0.05$, $DT = 0.05$ (Corresponding to Figure 53)

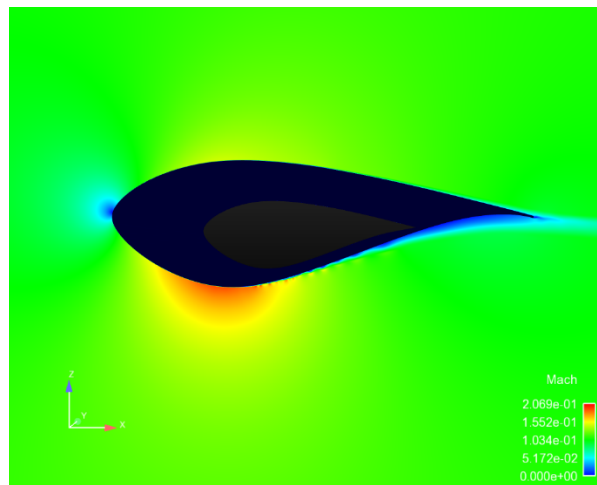


Figure 55. $Re = 2 \times 10^6$, $Ma = 0.11$, $DT = 0.1$, low Mach preconditioning turned on, no sub-iterations

Since there are some indications that the flow has eddies and other time accurate features, the cases for the lower Reynolds numbers were also run with the time accurate option. The residual drop and the force values both seem reasonable with this method. It is used for several cases: DU

91-W2-250Mod at $Re = 1 \times 10^6$ and 7×10^5 ; DU 97-W-300Mod at $Re = 7 \times 10^5$; and DU99 W3-350 at $Re = 7 \times 10^6$ and 1×10^6 .

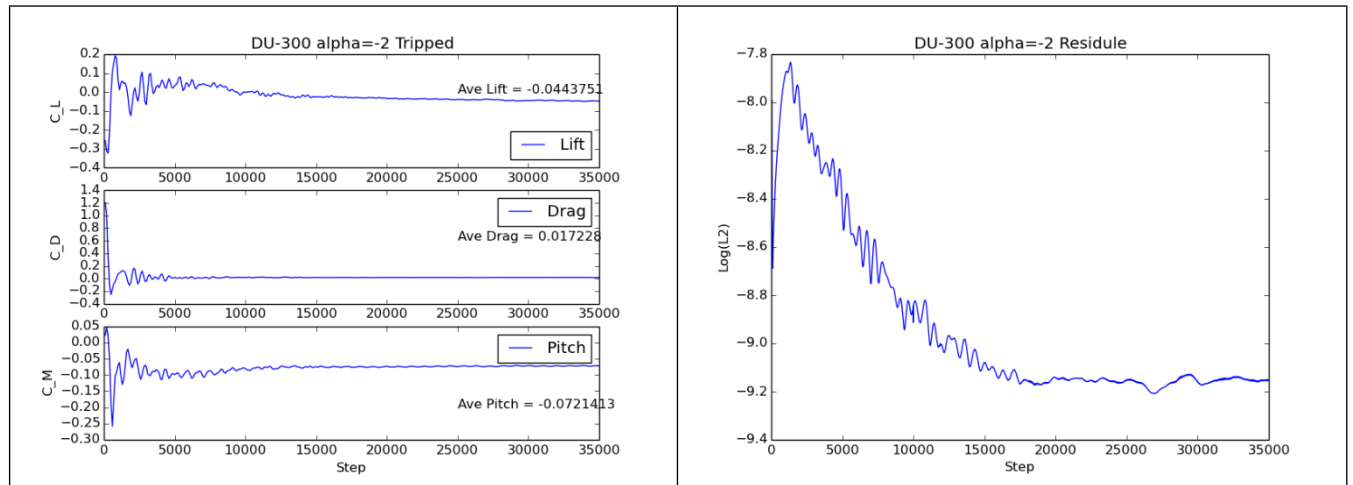


Figure 56. $Re = 7 \times 10^5$, $Ma = 0.026$, Low Mach Preconditioning on, Time accurate with DTPHYS = 0.001, $DT = 0.001$, 18 Newton Sub-iterations

APPENDIX B: RFOIL RESULTS

Presented here are the outputs from the RFOIL runs for the three airfoils being considered for the new NRT blade design: DU 91-W2-250Mod, DU 97-W-300Mod, and DU 99-W3-350. The calculations were made over a range of Reynolds numbers. The values of S_xtr and P_xtr are the suction and pressure side x-location of separation which are then used in Overflow calculations.

DU 91-W2-250Mod

RFOIL Version 1.1

Calculated polar for: du250lm

1 Reynolds number fixed

xtrf = 1.000 (suction) 1.000 (pressure)
 Rot. Parameters: f0 = 1.000 c/r = 0.000
 Mach = 0.050 Re = 0.700 e 6 Ncrit = 9.000

alpha	CL	CD	Re(CL)	CM	S_xtr	P_xtr	CDp
-5.000	-0.2643	0.01068	0.70000	-0.0948	0.6019	0.4252	0.00517
-4.500	-0.1938	0.01046	0.70000	-0.0988	0.5900	0.4327	0.00480
-4.000	-0.1270	0.01034	0.70000	-0.1017	0.5788	0.4395	0.00465
-3.500	-0.0581	0.01021	0.70000	-0.1051	0.5681	0.4471	0.00442
-3.000	0.0063	0.01021	0.70000	-0.1072	0.5584	0.4530	0.00438
-2.500	0.0740	0.01014	0.70000	-0.1101	0.5484	0.4601	0.00424
-2.000	0.1377	0.01018	0.70000	-0.1120	0.5398	0.4663	0.00425
-1.500	0.2033	0.01016	0.70000	-0.1142	0.5317	0.4722	0.00422
-1.000	0.2676	0.01026	0.70000	-0.1163	0.5241	0.4787	0.00421
-0.500	0.3315	0.01027	0.70000	-0.1181	0.5170	0.4837	0.00429
0.000	0.3957	0.01038	0.70000	-0.1200	0.5100	0.4898	0.00432
0.500	0.4586	0.01046	0.70000	-0.1216	0.5034	0.4951	0.00442
1.000	0.5214	0.01055	0.70000	-0.1231	0.4971	0.5001	0.00455
1.500	0.5840	0.01077	0.70000	-0.1246	0.4914	0.5055	0.00466
2.000	0.6463	0.01083	0.70000	-0.1260	0.4855	0.5104	0.00481
2.500	0.7079	0.01098	0.70000	-0.1272	0.4804	0.5150	0.00501
3.000	0.7690	0.01122	0.70000	-0.1284	0.4751	0.5199	0.00520
3.500	0.8304	0.01137	0.70000	-0.1296	0.4696	0.5251	0.00540
4.000	0.8907	0.01151	0.70000	-0.1305	0.4646	0.5290	0.00564
4.500	0.9504	0.01176	0.70000	-0.1314	0.4598	0.5334	0.00589
5.000	1.0105	0.01204	0.70000	-0.1323	0.4540	0.5382	0.00616
5.500	1.0691	0.01214	0.70000	-0.1329	0.4480	0.5426	0.00641
6.000	1.1258	0.01248	0.70000	-0.1331	0.4407	0.5464	0.00673
6.500	1.1830	0.01255	0.70000	-0.1334	0.4294	0.5511	0.00691
7.000	1.2389	0.01276	0.70000	-0.1335	0.4168	0.5556	0.00715
7.500	1.2918	0.01307	0.70000	-0.1331	0.4060	0.5597	0.00753
8.000	1.3433	0.01342	0.70000	-0.1324	0.3919	0.5635	0.00792
8.500	1.3939	0.01379	0.70000	-0.1316	0.3701	0.5679	0.00832
9.000	1.4318	0.01451	0.70000	-0.1287	0.3372	0.5725	0.00896
9.500	1.4400	0.01617	0.70000	-0.1214	0.2896	0.5758	0.01043

10.000	1.4256	0.01947	0.70000	-0.1128	0.2318	0.5790	0.01349
10.500	1.4040	0.02393	0.70000	-0.1059	0.1920	0.5827	0.01785
11.000	1.3741	0.03003	0.70000	-0.1009	0.1627	0.5860	0.02393
11.500	1.3372	0.03763	0.70000	-0.0977	0.1413	0.5891	0.03164
12.000	1.2957	0.04612	0.70000	-0.0956	0.1250	0.5917	0.04029
12.500	1.2521	0.05499	0.70000	-0.0941	0.1120	0.5937	0.04932
13.000	1.2128	0.06394	0.70000	-0.0936	0.0998	0.5958	0.05841
13.500	1.1831	0.07252	0.70000	-0.0940	0.0874	0.5982	0.06709
14.000	1.1626	0.08052	0.70000	-0.0949	0.0757	0.6008	0.07515
14.500	1.1481	0.08826	0.70000	-0.0962	0.0657	0.6033	0.08294
15.000	1.1389	0.09569	0.70000	-0.0981	0.0572	0.6067	0.09047
15.500	1.1330	0.10290	0.70000	-0.1001	0.0500	0.6092	0.09776
16.000	1.1336	0.10942	0.70000	-0.1023	0.0444	0.6118	0.10438
16.500	1.1335	0.11617	0.70000	-0.1049	0.0396	0.6147	0.11122
17.000	1.1356	0.12282	0.70000	-0.1080	0.0359	0.6178	0.11795

Calculated polar for: du250lm

1 Reynolds number fixed

xtrf = 1.000 (suction) 1.000 (pressure)
 Rot. Parameters: f0 = 1.000 c/r = 0.000
 Mach = 0.071 Re = 1.000 e 6 Ncrit = 9.000

alpha	CL	CD	Re(CL)	CM	S_xtr	P_xtr	CDp
-5.000	-0.2608	0.00965	1.00000	-0.0962	0.5814	0.4128	0.00452
-4.000	-0.1188	0.00921	1.00000	-0.1042	0.5594	0.4283	0.00391
-3.000	0.0164	0.00903	1.00000	-0.1100	0.5401	0.4422	0.00363
-2.000	0.1488	0.00897	1.00000	-0.1149	0.5227	0.4554	0.00350
-1.000	0.2791	0.00901	1.00000	-0.1191	0.5081	0.4684	0.00348
0.000	0.4082	0.00908	1.00000	-0.1229	0.4950	0.4799	0.00352
1.000	0.5354	0.00926	1.00000	-0.1262	0.4830	0.4906	0.00368
2.000	0.6600	0.00953	1.00000	-0.1290	0.4719	0.5010	0.00397
3.000	0.7848	0.00974	1.00000	-0.1316	0.4623	0.5112	0.00424
4.000	0.9070	0.01010	1.00000	-0.1337	0.4518	0.5203	0.00464
5.000	1.0263	0.01053	1.00000	-0.1353	0.4413	0.5290	0.00511
6.000	1.1442	0.01092	1.00000	-0.1365	0.4240	0.5375	0.00553
7.000	1.2605	0.01124	1.00000	-0.1374	0.3976	0.5463	0.00599
8.000	1.3679	0.01203	1.00000	-0.1367	0.3625	0.5543	0.00670
9.000	1.4193	0.01458	1.00000	-0.1271	0.2599	0.5623	0.00883
10.000	1.4095	0.02038	1.00000	-0.1120	0.1676	0.5694	0.01424
11.000	1.3671	0.03097	1.00000	-0.1021	0.1166	0.5763	0.02490
12.000	1.2993	0.04635	1.00000	-0.0973	0.0898	0.5813	0.04054
13.000	1.2265	0.06325	1.00000	-0.0952	0.0725	0.5861	0.05772
14.000	1.1843	0.07914	1.00000	-0.0965	0.0565	0.5915	0.07386
15.000	1.1666	0.09352	1.00000	-0.0991	0.0439	0.5965	0.08842
16.000	1.1599	0.10744	1.00000	-0.1031	0.0345	0.6023	0.10249
17.000	1.1638	0.12079	1.00000	-0.1084	0.0287	0.6085	0.11605

Calculated polar for: du250lm

1 Reynolds number fixed

xtrf = 1.000 (suction) 1.000 (pressure)
 Rot. Parameters: f0 = 1.000 c/r = 0.000
 Mach = 0.106 Re = 1.500 e 6 Ncrit = 9.000

alpha	CL	CD	Re(CL)	CM	S_xtr	P_xtr	CDp
-5.000	-0.2528	0.00873	1.50000	-0.0991	0.5593	0.3994	0.00395
-4.000	-0.1087	0.00824	1.50000	-0.1074	0.5388	0.4144	0.00334
-3.000	0.0277	0.00804	1.50000	-0.1132	0.5203	0.4287	0.00305
-2.000	0.1611	0.00796	1.50000	-0.1181	0.5049	0.4431	0.00292
-1.000	0.2923	0.00799	1.50000	-0.1223	0.4906	0.4561	0.00289
0.000	0.4225	0.00801	1.50000	-0.1262	0.4794	0.4685	0.00292
1.000	0.5505	0.00815	1.50000	-0.1295	0.4682	0.4800	0.00305
2.000	0.6760	0.00843	1.50000	-0.1322	0.4567	0.4904	0.00328
3.000	0.8030	0.00854	1.50000	-0.1351	0.4484	0.5008	0.00350
4.000	0.9262	0.00886	1.50000	-0.1372	0.4381	0.5100	0.00383
5.000	1.0481	0.00919	1.50000	-0.1391	0.4263	0.5189	0.00420
6.000	1.1692	0.00950	1.50000	-0.1407	0.4016	0.5280	0.00454
7.000	1.2848	0.01007	1.50000	-0.1412	0.3726	0.5362	0.00508
8.000	1.3777	0.01177	1.50000	-0.1383	0.2864	0.5444	0.00639
9.000	1.4057	0.01530	1.50000	-0.1250	0.1780	0.5515	0.00938
10.000	1.4027	0.02106	1.50000	-0.1118	0.1124	0.5591	0.01496
11.000	1.3683	0.03159	1.50000	-0.1032	0.0758	0.5649	0.02559
12.000	1.3089	0.04628	1.50000	-0.0986	0.0600	0.5700	0.04054
13.000	1.2466	0.06222	1.50000	-0.0966	0.0494	0.5756	0.05684
14.000	1.2095	0.07757	1.50000	-0.0975	0.0399	0.5807	0.07245
15.000	1.1943	0.09173	1.50000	-0.1000	0.0323	0.5856	0.08680
16.000	1.1907	0.10542	1.50000	-0.1037	0.0266	0.5922	0.10069
17.000	1.1955	0.11853	1.50000	-0.1084	0.0228	0.5978	0.11399

RFOIL Version 1.1

Calculated polar for: du250lm

1 Reynolds number fixed

xtrf = 1.000 (suction) 1.000 (pressure)
 Rot. Parameters: f0 = 1.000 c/r = 0.000
 Mach = 0.142 Re = 2.000 e 6 Ncrit = 9.000

alpha	CL	CD	Re(CL)	CM	S_xtr	P_xtr	CDp
-5.000	-0.2444	0.00807	2.00000	-0.1025	0.5443	0.3905	0.00352
-4.000	-0.1017	0.00768	2.00000	-0.1100	0.5247	0.4052	0.00301
-3.000	0.0347	0.00751	2.00000	-0.1155	0.5070	0.4194	0.00275
-2.000	0.1687	0.00742	2.00000	-0.1203	0.4932	0.4332	0.00262
-1.000	0.3010	0.00741	2.00000	-0.1245	0.4802	0.4471	0.00258
0.000	0.4319	0.00745	2.00000	-0.1283	0.4683	0.4598	0.00262
1.000	0.5609	0.00760	2.00000	-0.1317	0.4567	0.4720	0.00275
2.000	0.6899	0.00769	2.00000	-0.1349	0.4483	0.4832	0.00289
3.000	0.8157	0.00795	2.00000	-0.1373	0.4384	0.4923	0.00313
4.000	0.9418	0.00815	2.00000	-0.1398	0.4292	0.5026	0.00340
5.000	1.0661	0.00842	2.00000	-0.1418	0.4163	0.5121	0.00372
6.000	1.1867	0.00886	2.00000	-0.1431	0.3880	0.5201	0.00411
7.000	1.3012	0.00961	2.00000	-0.1433	0.3439	0.5291	0.00473
8.000	1.3766	0.01229	2.00000	-0.1374	0.2218	0.5366	0.00676
9.000	1.4010	0.01579	2.00000	-0.1236	0.1334	0.5446	0.00987
10.000	1.3968	0.02195	2.00000	-0.1111	0.0808	0.5508	0.01592
11.000	1.3755	0.03192	2.00000	-0.1039	0.0576	0.5575	0.02605
12.000	1.3245	0.04595	2.00000	-0.0995	0.0462	0.5634	0.04040
13.000	1.2650	0.06151	2.00000	-0.0973	0.0388	0.5678	0.05628
14.000	1.2286	0.07678	2.00000	-0.0980	0.0321	0.5731	0.07179
15.000	1.2133	0.09113	2.00000	-0.1005	0.0265	0.5787	0.08638
16.000	1.2103	0.10472	2.00000	-0.1040	0.0225	0.5839	0.10015
17.000	1.2196	0.11714	2.00000	-0.1081	0.0194	0.5904	0.11274

Calculated polar for: du250lm

1 Reynolds number fixed

xtrf = 1.000 (suction) 1.000 (pressure)
 Rot. Parameters: f0 = 1.000 c/r = 0.000
 Mach = 0.210 Re = 3.000 e 6 Ncrit = 9.000

alpha	CL	CD	Re(CL)	CM	S_xtr	P_xtr	CDp
-5.000	-0.2406	0.00743	3.00000	-0.1065	0.5229	0.3759	0.00314
-4.000	-0.0970	0.00709	3.00000	-0.1134	0.5048	0.3905	0.00271
-3.000	0.0419	0.00692	3.00000	-0.1189	0.4896	0.4055	0.00247
-2.000	0.1783	0.00683	3.00000	-0.1236	0.4762	0.4195	0.00234
-1.000	0.3133	0.00679	3.00000	-0.1279	0.4649	0.4333	0.00230
0.000	0.4464	0.00684	3.00000	-0.1316	0.4537	0.4461	0.00233
1.000	0.5788	0.00692	3.00000	-0.1352	0.4437	0.4592	0.00241
2.000	0.7104	0.00702	3.00000	-0.1384	0.4347	0.4712	0.00255
3.000	0.8394	0.00726	3.00000	-0.1410	0.4245	0.4821	0.00278
4.000	0.9685	0.00743	3.00000	-0.1434	0.4162	0.4913	0.00300
5.000	1.0961	0.00770	3.00000	-0.1455	0.3998	0.5012	0.00329
6.000	1.2177	0.00829	3.00000	-0.1464	0.3620	0.5100	0.00375
7.000	1.3160	0.01019	3.00000	-0.1436	0.2560	0.5187	0.00516
8.000	1.3747	0.01326	3.00000	-0.1343	0.1398	0.5258	0.00763
9.000	1.3965	0.01693	3.00000	-0.1206	0.0835	0.5335	0.01113
10.000	1.4033	0.02325	3.00000	-0.1106	0.0545	0.5396	0.01748
11.000	1.3819	0.03388	3.00000	-0.1044	0.0401	0.5470	0.02834
12.000	1.3265	0.04844	3.00000	-0.1000	0.0333	0.5517	0.04323
13.000	1.2716	0.06390	3.00000	-0.0981	0.0287	0.5564	0.05897
14.000	1.2438	0.07865	3.00000	-0.0991	0.0242	0.5621	0.07399
15.000	1.2344	0.09249	3.00000	-0.1014	0.0203	0.5676	0.08802
16.000	1.2321	0.10622	3.00000	-0.1048	0.0175	0.5724	0.10193
17.000	1.2407	0.11933	3.00000	-0.1093	0.0155	0.5795	0.11524

Calculated polar for: du250lm

1 Reynolds number fixed

xtrf = 1.000 (suction) 1.000 (pressure)
 Rot. Parameters: f0 = 1.000 c/r = 0.000
 Mach = 0.200 Re = 7.000 e 6 Ncrit = 9.000

alpha	CL	CD	Re(CL)	CM	S_xtr	P_xtr	CDp
-5.000	-0.2143	0.00224	7.00000	-0.1108	0.4886	0.3502	-0.00157
-4.000	-0.0774	0.00223	7.00000	-0.1161	0.4748	0.3659	-0.00163
-3.000	0.0576	0.00221	7.00000	-0.1207	0.4619	0.3798	-0.00167
-2.000	0.1914	0.00219	7.00000	-0.1250	0.4509	0.3936	-0.00170
-1.000	0.3241	0.00217	7.00000	-0.1290	0.4389	0.4084	-0.00174
0.000	0.4559	0.00215	7.00000	-0.1326	0.4301	0.4224	-0.00176
1.000	0.5869	0.00213	7.00000	-0.1359	0.4218	0.4361	-0.00177
2.000	0.7165	0.00211	7.00000	-0.1389	0.4127	0.4488	-0.00179
3.000	0.8456	0.00208	7.00000	-0.1416	0.4034	0.4606	-0.00179
4.000	0.9729	0.00205	7.00000	-0.1439	0.3891	0.4722	-0.00181
5.000	1.0904	0.00206	7.00000	-0.1444	0.3279	0.4814	-0.00205
6.000	1.1823	0.00213	7.00000	-0.1405	0.1985	0.4901	-0.00256
7.000	1.2621	0.00223	7.00000	-0.1345	0.1077	0.4991	-0.00285
8.000	1.3090	0.00231	7.00000	-0.1226	0.0637	0.5057	-0.00290
9.000	1.3143	0.00295	7.00000	-0.1072	0.0423	0.5132	-0.00215
10.000	1.2523	0.00840	7.00000	-0.0905	0.0337	0.5181	0.00363
11.000	1.4968	0.02478	7.00000	-0.1102	0.0207	0.5304	0.01945
12.000	1.4754	0.03545	7.00000	-0.1041	0.0178	0.5358	0.03037
13.000	1.4172	0.04973	7.00000	-0.0993	0.0162	0.5406	0.04496
14.000	1.3639	0.06533	7.00000	-0.0979	0.0150	0.5459	0.06086
15.000	1.3337	0.08052	7.00000	-0.0992	0.0134	0.5512	0.07629
16.000	1.3259	0.09423	7.00000	-0.1016	0.0122	0.5562	0.09018
17.000	1.3233	0.10819	7.00000	-0.1053	0.0111	0.5624	0.10433

DU 97-W-300Mod

RFOIL Version 1.1

Calculated polar for: du300

1 Reynolds number fixed

xtrf = 1.000 (suction) 1.000 (pressure)
Rot. Parameters: f0 = 1.000 c/r = 0.000
Mach = 0.050 Re = 0.700 e 6 Ncrit = 9.000

alpha	CL	CD	Re(CL)	CM	S_xtr	P_xtr	CDp
-4.000	-0.3127	0.01436	0.70000	-0.0616	0.5465	0.3631	0.00820
-3.000	-0.1783	0.01356	0.70000	-0.0698	0.5160	0.3674	0.00717
-2.000	-0.0501	0.01317	0.70000	-0.0750	0.4897	0.3713	0.00675
-1.000	0.0818	0.01295	0.70000	-0.0807	0.4662	0.3753	0.00643
0.000	0.2149	0.01293	0.70000	-0.0865	0.4442	0.3793	0.00621
1.000	0.3422	0.01282	0.70000	-0.0907	0.4255	0.3848	0.00615
2.000	0.4704	0.01296	0.70000	-0.0948	0.4084	0.3894	0.00627
3.000	0.5987	0.01321	0.70000	-0.0989	0.3943	0.3941	0.00646
4.000	0.7232	0.01335	0.70000	-0.1021	0.3810	0.4007	0.00676
5.000	0.8439	0.01380	0.70000	-0.1045	0.3690	0.4065	0.00725
7.000	1.0723	0.01490	0.70000	-0.1069	0.3474	0.4197	0.00854
8.000	1.1652	0.01569	0.70000	-0.1042	0.3365	0.4271	0.00944
9.000	1.2550	0.01695	0.70000	-0.1017	0.3252	0.4346	0.01080
10.000	1.3405	0.01840	0.70000	-0.0992	0.3126	0.4428	0.01243
11.000	1.4090	0.02083	0.70000	-0.0956	0.2953	0.4516	0.01506
12.000	1.4662	0.02436	0.70000	-0.0921	0.2775	0.4608	0.01880
13.000	1.4932	0.03044	0.70000	-0.0884	0.2528	0.4694	0.02511
14.000	1.4496	0.04272	0.70000	-0.0846	0.2210	0.4770	0.03758
15.000	1.3433	0.06257	0.70000	-0.0846	0.1930	0.4814	0.05777
16.000	1.2331	0.08728	0.70000	-0.0910	0.1664	0.4851	0.08278
17.000	1.1566	0.11120	0.70000	-0.1008	0.1407	0.4899	0.10690

Calculated polar for: du300

1 Reynolds number fixed

xtrf = 1.000 (suction) 1.000 (pressure)
 Rot. Parameters: f0 = 1.000 c/r = 0.000
 Mach = 0.071 Re = 1.000 e 6 Ncrit = 9.000

alpha	CL	CD	Re(CL)	CM	S_xtr	P_xtr	CDp
-4.000	-0.3227	0.01285	1.00000	-0.0603	0.5249	0.3574	0.00722
-3.000	-0.1834	0.01214	1.00000	-0.0693	0.4956	0.3612	0.00632
-2.000	-0.0417	0.01170	1.00000	-0.0778	0.4705	0.3646	0.00571
-1.000	0.0929	0.01139	1.00000	-0.0840	0.4482	0.3694	0.00534
0.000	0.2271	0.01132	1.00000	-0.0896	0.4272	0.3735	0.00520
1.000	0.3593	0.01140	1.00000	-0.0946	0.4095	0.3779	0.00520
2.000	0.4908	0.01144	1.00000	-0.0993	0.3936	0.3831	0.00523
3.000	0.6209	0.01158	1.00000	-0.1035	0.3803	0.3881	0.00542
4.000	0.7469	0.01189	1.00000	-0.1067	0.3679	0.3930	0.00573
5.000	0.8702	0.01227	1.00000	-0.1095	0.3564	0.3998	0.00616
6.000	0.9904	0.01271	1.00000	-0.1115	0.3456	0.4056	0.00666
7.000	1.1064	0.01322	1.00000	-0.1127	0.3354	0.4122	0.00726
8.000	1.2088	0.01399	1.00000	-0.1116	0.3244	0.4194	0.00812
9.000	1.2983	0.01486	1.00000	-0.1081	0.3129	0.4259	0.00908
10.000	1.3909	0.01609	1.00000	-0.1061	0.2973	0.4346	0.01046
11.000	1.4645	0.01818	1.00000	-0.1021	0.2789	0.4429	0.01263
12.000	1.5257	0.02128	1.00000	-0.0981	0.2551	0.4519	0.01590
13.000	1.5280	0.02867	1.00000	-0.0918	0.2196	0.4593	0.02333
14.000	1.4627	0.04275	1.00000	-0.0871	0.1886	0.4654	0.03765
15.000	1.3420	0.06448	1.00000	-0.0874	0.1663	0.4689	0.05975
16.000	1.2312	0.08999	1.00000	-0.0943	0.1444	0.4721	0.08558
17.000	1.1642	0.11310	1.00000	-0.1038	0.1218	0.4780	0.10891

Calculated polar for: du300

1 Reynolds number fixed

xtrf = 1.000 (suction) 1.000 (pressure)
 Rot. Parameters: f0 = 1.000 c/r = 0.000
 Mach = 0.106 Re = 1.500 e 6 Ncrit = 9.000

alpha	CL	CD	Re(CL)	CM	S_xtr	P_xtr	CDp
-4.000	-0.3205	0.01148	1.50000	-0.0630	0.4996	0.3505	0.00625
-3.000	-0.1745	0.01071	1.50000	-0.0731	0.4733	0.3547	0.00534
-2.000	-0.0274	0.01020	1.50000	-0.0825	0.4498	0.3588	0.00472
-1.000	0.1101	0.01010	1.50000	-0.0888	0.4275	0.3624	0.00450
0.000	0.2443	0.01015	1.50000	-0.0939	0.4086	0.3653	0.00444
1.000	0.3823	0.01004	1.50000	-0.1000	0.3922	0.3713	0.00432
2.000	0.5152	0.01015	1.50000	-0.1046	0.3778	0.3758	0.00442
3.000	0.6445	0.01037	1.50000	-0.1082	0.3651	0.3795	0.00462
4.000	0.7763	0.01052	1.50000	-0.1125	0.3540	0.3863	0.00483
5.000	0.8999	0.01098	1.50000	-0.1149	0.3422	0.3917	0.00526
6.000	1.0256	0.01125	1.50000	-0.1175	0.3327	0.3978	0.00561
7.000	1.1456	0.01172	1.50000	-0.1192	0.3220	0.4043	0.00616
8.000	1.2548	0.01246	1.50000	-0.1187	0.3105	0.4101	0.00690
9.000	1.3598	0.01303	1.50000	-0.1176	0.2968	0.4185	0.00759
10.000	1.4447	0.01418	1.50000	-0.1132	0.2791	0.4247	0.00876
11.000	1.5235	0.01599	1.50000	-0.1091	0.2522	0.4342	0.01062
12.000	1.5586	0.02008	1.50000	-0.1012	0.2147	0.4406	0.01466
13.000	1.5392	0.02887	1.50000	-0.0934	0.1780	0.4483	0.02353
14.000	1.4605	0.04421	1.50000	-0.0885	0.1535	0.4530	0.03914
15.000	1.3445	0.06601	1.50000	-0.0894	0.1363	0.4560	0.06132
16.000	1.2359	0.09181	1.50000	-0.0966	0.1194	0.4590	0.08747
17.000	1.1650	0.11615	1.50000	-0.1068	0.0994	0.4641	0.11208

Calculated polar for: du300

1 Reynolds number fixed

xtrf = 1.000 (suction) 1.000 (pressure)
 Rot. Parameters: f0 = 1.000 c/r = 0.000
 Mach = 0.142 Re = 2.000 e 6 Ncrit = 9.000

alpha	CL	CD	Re(CL)	CM	S_xtr	P_xtr	CDp
-1.000	0.1247	0.00928	2.00000	-0.0929	0.4143	0.3582	0.00397
0.000	0.2619	0.00926	2.00000	-0.0984	0.3967	0.3619	0.00389
1.000	0.3955	0.00939	2.00000	-0.1029	0.3807	0.3651	0.00394
2.000	0.5326	0.00940	2.00000	-0.1082	0.3673	0.3712	0.00396
3.000	0.6651	0.00958	2.00000	-0.1123	0.3549	0.3758	0.00413
4.000	0.7927	0.00992	2.00000	-0.1152	0.3437	0.3795	0.00443
5.000	0.9245	0.01008	2.00000	-0.1190	0.3341	0.3869	0.00468
6.000	1.0490	0.01049	2.00000	-0.1211	0.3233	0.3922	0.00511
7.000	1.1710	0.01095	2.00000	-0.1228	0.3128	0.3986	0.00560
8.000	1.2904	0.01142	2.00000	-0.1238	0.3010	0.4053	0.00614
9.000	1.3995	0.01213	2.00000	-0.1229	0.2848	0.4121	0.00687
10.000	1.4822	0.01321	2.00000	-0.1176	0.2619	0.4198	0.00797
11.000	1.5455	0.01554	2.00000	-0.1107	0.2257	0.4255	0.01019
12.000	1.5617	0.02069	2.00000	-0.1011	0.1836	0.4341	0.01530
13.000	1.5349	0.03021	2.00000	-0.0932	0.1515	0.4395	0.02492
14.000	1.4403	0.04721	2.00000	-0.0888	0.1293	0.4434	0.04220
15.000	1.3259	0.06980	2.00000	-0.0910	0.1154	0.4471	0.06521
16.000	1.2271	0.09524	2.00000	-0.0988	0.1011	0.4504	0.09102
17.000	1.1664	0.11809	2.00000	-0.1083	0.0851	0.4547	0.11408

Calculated polar for: du300

1 Reynolds number fixed

xtrf = 1.000 (suction) 1.000 (pressure)
 Rot. Parameters: f0 = 1.000 c/r = 0.000
 Mach = 0.213 Re = 3.000 e 6 Ncrit = 9.000

alpha	CL	CD	Re(CL)	CM	S_xtr	P_xtr	CDp
-4.000	-0.3122	0.00962	3.00000	-0.0713	0.4589	0.3385	0.00497
-3.000	-0.1475	0.00873	3.00000	-0.0845	0.4356	0.3440	0.00394
-2.000	-0.0028	0.00855	3.00000	-0.0916	0.4136	0.3477	0.00366
-1.000	0.1375	0.00854	3.00000	-0.0972	0.3951	0.3506	0.00356
0.000	0.2778	0.00854	3.00000	-0.1027	0.3792	0.3542	0.00349
1.000	0.4189	0.00852	3.00000	-0.1083	0.3646	0.3593	0.00345
2.000	0.5556	0.00865	3.00000	-0.1126	0.3526	0.3636	0.00356
3.000	0.6901	0.00887	3.00000	-0.1164	0.3408	0.3674	0.00374
4.000	0.8261	0.00903	3.00000	-0.1204	0.3308	0.3735	0.00393
5.000	0.9579	0.00930	3.00000	-0.1232	0.3212	0.3782	0.00423
6.000	1.0864	0.00972	3.00000	-0.1254	0.3099	0.3846	0.00465
7.000	1.2149	0.01006	3.00000	-0.1274	0.3007	0.3907	0.00505
8.000	1.3366	0.01059	3.00000	-0.1279	0.2876	0.3961	0.00560
9.000	1.4485	0.01142	3.00000	-0.1268	0.2653	0.4043	0.00641
10.000	1.5174	0.01304	3.00000	-0.1184	0.2266	0.4092	0.00790
11.000	1.5557	0.01657	3.00000	-0.1083	0.1814	0.4168	0.01132
12.000	1.5557	0.02321	3.00000	-0.0984	0.1457	0.4223	0.01797
13.000	1.4981	0.03598	3.00000	-0.0914	0.1188	0.4266	0.03091
14.000	1.3940	0.05514	3.00000	-0.0895	0.1051	0.4307	0.05044
15.000	1.2849	0.07881	3.00000	-0.0939	0.0934	0.4336	0.07450
16.000	1.2040	0.10293	3.00000	-0.1022	0.0806	0.4369	0.09892
17.000	1.1572	0.12447	3.00000	-0.1117	0.0671	0.4406	0.12065

Calculated polar for: du300

1 Reynolds number fixed

xtrf = 1.000 (suction) 1.000 (pressure)
 Rot. Parameters: f0 = 1.000 c/r = 0.000
 Mach = 0.200 Re = 7.000 e 6 Ncrit = 9.000

alpha	CL	CD	Re(CL)	CM	S_xtr	P_xtr	CDp
-5.000	-0.3916	0.00730	7.00000	-0.0820	0.4405	0.3279	0.00320
-4.000	-0.2502	0.00720	7.00000	-0.0881	0.4198	0.3299	0.00299
-3.000	-0.1069	0.00704	7.00000	-0.0947	0.3989	0.3347	0.00275
-2.000	0.0338	0.00699	7.00000	-0.1004	0.3819	0.3379	0.00264
-1.000	0.1722	0.00703	7.00000	-0.1054	0.3671	0.3406	0.00262
0.000	0.3099	0.00710	7.00000	-0.1101	0.3529	0.3437	0.00262
1.000	0.4484	0.00715	7.00000	-0.1150	0.3402	0.3487	0.00265
2.000	0.5850	0.00725	7.00000	-0.1192	0.3311	0.3526	0.00273
3.000	0.7195	0.00742	7.00000	-0.1229	0.3208	0.3553	0.00288
4.000	0.8541	0.00762	7.00000	-0.1265	0.3093	0.3615	0.00306
5.000	0.9877	0.00781	7.00000	-0.1297	0.3012	0.3667	0.00327
6.000	1.1185	0.00810	7.00000	-0.1322	0.2905	0.3714	0.00356
7.000	1.2474	0.00847	7.00000	-0.1342	0.2776	0.3779	0.00393
8.000	1.3661	0.00928	7.00000	-0.1344	0.2437	0.3829	0.00459
9.000	1.4601	0.01105	7.00000	-0.1307	0.1805	0.3901	0.00605
10.000	1.5197	0.01297	7.00000	-0.1210	0.1398	0.3955	0.00781
11.000	1.5554	0.01642	7.00000	-0.1102	0.1031	0.4005	0.01115
12.000	1.5686	0.02219	7.00000	-0.1011	0.0798	0.4073	0.01697
13.000	1.5345	0.03288	7.00000	-0.0941	0.0656	0.4115	0.02785
14.000	1.4473	0.04962	7.00000	-0.0906	0.0583	0.4142	0.04493
15.000	1.3339	0.07281	7.00000	-0.0937	0.0535	0.4171	0.06852
16.000	1.2526	0.09629	7.00000	-0.1010	0.0478	0.4213	0.09233
17.000	1.2062	0.11749	7.00000	-0.1097	0.0410	0.4251	0.11377

DU 99-W3-350

RFOIL Version 1.1

Calculated polar for: du350

1 Reynolds number fixed

xtrf = 1.000 (suction) 1.000 (pressure)
Rot. Parameters: f0 = 1.000 c/r = 0.000
Mach = 0.050 Re = 0.700 e 6 Ncrit = 9.000

alpha	CL	CD	Re(CL)	CM	S_xtr	P_xtr	CDp
-5.000	-0.3544	0.02288	0.70000	-0.0422	0.5115	0.3515	0.01677
-4.000	-0.2633	0.02169	0.70000	-0.0434	0.4792	0.3548	0.01550
-3.000	-0.2015	0.01922	0.70000	-0.0437	0.4510	0.3587	0.01292
-2.000	-0.1480	0.01696	0.70000	-0.0439	0.4282	0.3627	0.01041
-1.000	-0.0395	0.01612	0.70000	-0.0477	0.4071	0.3671	0.00950
0.000	0.0853	0.01557	0.70000	-0.0540	0.3891	0.3707	0.00890
1.000	0.2180	0.01526	0.70000	-0.0611	0.3748	0.3747	0.00852
2.000	0.3464	0.01530	0.70000	-0.0667	0.3621	0.3787	0.00843
3.000	0.4652	0.01532	0.70000	-0.0697	0.3522	0.3838	0.00855
4.000	0.5772	0.01565	0.70000	-0.0715	0.3430	0.3881	0.00891
5.000	0.6818	0.01616	0.70000	-0.0721	0.3348	0.3924	0.00941
6.000	0.7891	0.01701	0.70000	-0.0736	0.3266	0.3986	0.01038
7.000	0.8922	0.01805	0.70000	-0.0747	0.3193	0.4037	0.01156
8.000	0.9820	0.01989	0.70000	-0.0743	0.3110	0.4084	0.01333
9.000	1.0703	0.02175	0.70000	-0.0748	0.3043	0.4155	0.01552
10.000	1.1417	0.02472	0.70000	-0.0739	0.2960	0.4216	0.01853
11.000	1.2048	0.02852	0.70000	-0.0736	0.2885	0.4281	0.02259
12.000	1.2519	0.03337	0.70000	-0.0726	0.2795	0.4348	0.02757
13.000	1.2706	0.04044	0.70000	-0.0718	0.2699	0.4406	0.03497
14.000	1.2700	0.04953	0.70000	-0.0719	0.2580	0.4472	0.04434
15.000	1.2474	0.06202	0.70000	-0.0740	0.2438	0.4526	0.05711
16.000	1.2020	0.07892	0.70000	-0.0792	0.2270	0.4575	0.07427
17.000	1.1459	0.09898	0.70000	-0.0874	0.2068	0.4626	0.09451

Calculated polar for: du350

1 Reynolds number fixed

xtrf = 1.000 (suction) 1.000 (pressure)
 Rot. Parameters: f0 = 1.000 c/r = 0.000
 Mach = 0.071 Re = 1.000 e 6 Ncrit = 9.000

alpha	CL	CD	Re(CL)	CM	S_xtr	P_xtr	CDp
-5.000	-0.3256	0.02387	1.00000	-0.0412	0.4859	0.3452	0.01835
-4.000	-0.2891	0.01939	1.00000	-0.0424	0.4586	0.3493	0.01359
-2.000	-0.1559	0.01575	1.00000	-0.0413	0.4095	0.3573	0.00979
-1.000	-0.0408	0.01455	1.00000	-0.0481	0.3903	0.3609	0.00844
0.000	0.0991	0.01390	1.00000	-0.0578	0.3739	0.3636	0.00761
1.000	0.2338	0.01346	1.00000	-0.0649	0.3611	0.3692	0.00721
2.000	0.3662	0.01351	1.00000	-0.0708	0.3496	0.3732	0.00720
3.000	0.4973	0.01360	1.00000	-0.0758	0.3407	0.3770	0.00728
4.000	0.6190	0.01386	1.00000	-0.0793	0.3321	0.3824	0.00755
5.000	0.7287	0.01416	1.00000	-0.0802	0.3243	0.3869	0.00795
6.000	0.8339	0.01489	1.00000	-0.0806	0.3174	0.3916	0.00871
7.000	0.9364	0.01602	1.00000	-0.0813	0.3096	0.3976	0.00992
8.000	1.0377	0.01722	1.00000	-0.0820	0.3032	0.4029	0.01128
9.000	1.1093	0.01982	1.00000	-0.0799	0.2945	0.4077	0.01388
10.000	1.1987	0.02202	1.00000	-0.0807	0.2879	0.4152	0.01634
11.000	1.2471	0.02657	1.00000	-0.0786	0.2791	0.4207	0.02097
12.000	1.3023	0.03114	1.00000	-0.0780	0.2709	0.4265	0.02577
13.000	1.3201	0.03839	1.00000	-0.0769	0.2603	0.4335	0.03327
14.000	1.3081	0.04835	1.00000	-0.0760	0.2478	0.4386	0.04343
15.000	1.2810	0.06123	1.00000	-0.0775	0.2333	0.4428	0.05655
16.000	1.2322	0.07904	1.00000	-0.0830	0.2154	0.4489	0.07466
17.000	1.1579	0.10166	1.00000	-0.0918	0.1953	0.4527	0.09748

Calculated polar for: du350

1 Reynolds number fixed

xtrf = 1.000 (suction) 1.000 (pressure)
 Rot. Parameters: f0 = 1.000 c/r = 0.000
 Mach = 0.106 Re = 1.500 e 6 Ncrit = 9.000

alpha	CL	CD	Re(CL)	CM	S_xtr	P_xtr	CDp
-5.000	-0.3388	0.02295	1.50000	-0.0399	0.4599	0.3396	0.01782
-4.000	-0.2893	0.01947	1.50000	-0.0406	0.4323	0.3438	0.01423
-3.000	-0.2379	0.01626	1.50000	-0.0405	0.4092	0.3473	0.01086
-2.000	-0.1622	0.01423	1.50000	-0.0426	0.3897	0.3498	0.00864
-1.000	-0.0320	0.01279	1.50000	-0.0523	0.3730	0.3553	0.00715
0.000	0.1160	0.01214	1.50000	-0.0627	0.3587	0.3588	0.00641
1.000	0.2597	0.01199	1.50000	-0.0710	0.3462	0.3622	0.00615
2.000	0.4010	0.01185	1.50000	-0.0780	0.3374	0.3667	0.00601
3.000	0.5361	0.01198	1.50000	-0.0837	0.3280	0.3713	0.00614
4.000	0.6678	0.01213	1.50000	-0.0881	0.3208	0.3754	0.00631
5.000	0.7834	0.01270	1.50000	-0.0896	0.3124	0.3792	0.00683
6.000	0.8999	0.01286	1.50000	-0.0913	0.3065	0.3854	0.00714
7.000	1.0033	0.01370	1.50000	-0.0909	0.2999	0.3903	0.00800
8.000	1.1019	0.01490	1.50000	-0.0903	0.2927	0.3954	0.00927
9.000	1.2016	0.01622	1.50000	-0.0905	0.2855	0.4018	0.01073
10.000	1.2703	0.01900	1.50000	-0.0878	0.2778	0.4071	0.01359
11.000	1.3485	0.02182	1.50000	-0.0871	0.2694	0.4139	0.01657
12.000	1.3968	0.02665	1.50000	-0.0852	0.2595	0.4198	0.02158
13.000	1.4069	0.03414	1.50000	-0.0822	0.2479	0.4246	0.02921
14.000	1.3866	0.04456	1.50000	-0.0804	0.2349	0.4308	0.03987
15.000	1.3436	0.05854	1.50000	-0.0810	0.2201	0.4354	0.05412
16.000	1.2719	0.07825	1.50000	-0.0857	0.2014	0.4390	0.07410
17.000	1.1706	0.10470	1.50000	-0.0956	0.1823	0.4412	0.10079

Calculated polar for: du350

1 Reynolds number fixed

xtrf = 1.000 (suction) 1.000 (pressure)
 Rot. Parameters: f0 = 1.000 c/r = 0.000
 Mach = 0.142 Re = 2.000 e 6 Ncrit = 9.000

alpha	CL	CD	Re(CL)	CM	S_xtr	P_xtr	CDp
-5.000	-0.3502	0.02260	2.00000	-0.0392	0.4397	0.3353	0.01776
-4.000	-0.2998	0.01900	2.00000	-0.0400	0.4150	0.3389	0.01400
-3.000	-0.2798	0.01454	2.00000	-0.0383	0.3955	0.3438	0.00942
-2.000	-0.1638	0.01275	2.00000	-0.0462	0.3768	0.3471	0.00750
-1.000	-0.0234	0.01197	2.00000	-0.0553	0.3608	0.3495	0.00657
0.000	0.1357	0.01119	2.00000	-0.0682	0.3471	0.3546	0.00568
1.000	0.2867	0.01088	2.00000	-0.0773	0.3383	0.3584	0.00536
2.000	0.4236	0.01101	2.00000	-0.0828	0.3280	0.3620	0.00544
3.000	0.5615	0.01106	2.00000	-0.0882	0.3215	0.3657	0.00549
4.000	0.6945	0.01135	2.00000	-0.0930	0.3114	0.3712	0.00576
5.000	0.8267	0.01150	2.00000	-0.0968	0.3064	0.3754	0.00598
6.000	0.9448	0.01200	2.00000	-0.0982	0.2994	0.3793	0.00647
7.000	1.0467	0.01251	2.00000	-0.0970	0.2927	0.3860	0.00708
8.000	1.1556	0.01334	2.00000	-0.0972	0.2859	0.3908	0.00797
9.000	1.2457	0.01487	2.00000	-0.0952	0.2778	0.3961	0.00956
10.000	1.3405	0.01646	2.00000	-0.0946	0.2706	0.4026	0.01128
11.000	1.4069	0.01952	2.00000	-0.0916	0.2613	0.4078	0.01444
12.000	1.4562	0.02415	2.00000	-0.0890	0.2505	0.4146	0.01919
13.000	1.4772	0.03093	2.00000	-0.0860	0.2377	0.4206	0.02615
14.000	1.4459	0.04169	2.00000	-0.0825	0.2244	0.4243	0.03711
15.000	1.3735	0.05791	2.00000	-0.0824	0.2072	0.4282	0.05359
16.000	1.2951	0.07843	2.00000	-0.0872	0.1909	0.4325	0.07441
17.000	1.2004	0.10429	2.00000	-0.0967	0.1739	0.4354	0.10056

Calculated polar for: du350

1 Reynolds number fixed

xtrf = 1.000 (suction) 1.000 (pressure)
 Rot. Parameters: f0 = 1.000 c/r = 0.000
 Mach = 0.000 Re = 3.000 e 6 Ncrit = 9.000

alpha	CL	CD	Re(CL)	CM	S_xtr	P_xtr	CDp
-5.000	-0.3705	0.02145	3.00000	-0.0372	0.4150	0.3301	0.01689
-4.000	-0.3467	0.01602	3.00000	-0.0376	0.3941	0.3340	0.01128
-2.000	-0.1412	0.01120	3.00000	-0.0527	0.3599	0.3410	0.00616
-1.000	0.0156	0.01034	3.00000	-0.0655	0.3457	0.3449	0.00518
0.000	0.1631	0.01009	3.00000	-0.0744	0.3350	0.3479	0.00485
1.000	0.2996	0.01013	3.00000	-0.0801	0.3256	0.3499	0.00485
2.000	0.4430	0.01002	3.00000	-0.0876	0.3177	0.3557	0.00472
3.000	0.5785	0.01013	3.00000	-0.0929	0.3094	0.3600	0.00483
4.000	0.7082	0.01037	3.00000	-0.0968	0.3034	0.3631	0.00507
5.000	0.8356	0.01073	3.00000	-0.1005	0.2945	0.3686	0.00541
6.000	0.9630	0.01095	3.00000	-0.1039	0.2894	0.3737	0.00570
7.000	1.0698	0.01158	3.00000	-0.1036	0.2814	0.3775	0.00630
8.000	1.1701	0.01216	3.00000	-0.1023	0.2751	0.3842	0.00697
9.000	1.2666	0.01331	3.00000	-0.1011	0.2679	0.3896	0.00817
10.000	1.3511	0.01493	3.00000	-0.0987	0.2583	0.3936	0.00985
11.000	1.4203	0.01765	3.00000	-0.0960	0.2471	0.4015	0.01266
12.000	1.4640	0.02216	3.00000	-0.0922	0.2335	0.4066	0.01725
13.000	1.4730	0.02946	3.00000	-0.0881	0.2201	0.4117	0.02469
14.000	1.4246	0.04166	3.00000	-0.0841	0.2040	0.4166	0.03714
15.000	1.3517	0.05842	3.00000	-0.0839	0.1897	0.4200	0.05417
16.000	1.2656	0.08047	3.00000	-0.0887	0.1753	0.4228	0.07654
17.000	1.1608	0.10889	3.00000	-0.0988	0.1586	0.4244	0.10524

Calculated polar for: du350

1 Reynolds number fixed

xtrf = 1.000 (suction) 1.000 (pressure)
 Rot. Parameters: f0 = 1.000 c/r = 0.000
 Mach = 0.200 Re = 7.000 e 6 Ncrit = 9.000

alpha	CL	CD	Re(CL)	CM	S_xtr	P_xtr	CDp
-5.000	-0.5465	0.01003	7.00000	-0.0420	0.3800	0.3235	0.00585
-4.000	-0.3946	0.00924	7.00000	-0.0527	0.3611	0.3251	0.00492
-3.000	-0.2261	0.00842	7.00000	-0.0664	0.3458	0.3299	0.00399
-2.000	-0.0740	0.00818	7.00000	-0.0750	0.3348	0.3329	0.00369
-1.000	0.0729	0.00810	7.00000	-0.0818	0.3246	0.3354	0.00357
0.000	0.2152	0.00819	7.00000	-0.0875	0.3151	0.3369	0.00358
1.000	0.3629	0.00810	7.00000	-0.0943	0.3084	0.3419	0.00349
2.000	0.5063	0.00817	7.00000	-0.1000	0.3003	0.3458	0.00354
3.000	0.6471	0.00830	7.00000	-0.1048	0.2936	0.3490	0.00366
4.000	0.7862	0.00847	7.00000	-0.1093	0.2875	0.3530	0.00382
5.000	0.9235	0.00872	7.00000	-0.1133	0.2798	0.3582	0.00406
6.000	1.0588	0.00895	7.00000	-0.1167	0.2729	0.3624	0.00432
7.000	1.1881	0.00936	7.00000	-0.1189	0.2657	0.3666	0.00471
8.000	1.3159	0.00974	7.00000	-0.1207	0.2577	0.3725	0.00513
9.000	1.4241	0.01040	7.00000	-0.1190	0.2455	0.3774	0.00578
10.000	1.5101	0.01152	7.00000	-0.1140	0.2313	0.3832	0.00689
11.000	1.5903	0.01331	7.00000	-0.1094	0.2173	0.3890	0.00871
12.000	1.6357	0.01691	7.00000	-0.1023	0.1987	0.3928	0.01231
13.000	1.6605	0.02252	7.00000	-0.0963	0.1849	0.3998	0.01803
14.000	1.6225	0.03273	7.00000	-0.0896	0.1690	0.4039	0.02841
15.000	1.5445	0.04724	7.00000	-0.0856	0.1566	0.4074	0.04316
16.000	1.4397	0.06827	7.00000	-0.0877	0.1464	0.4089	0.06449
17.000	1.3335	0.09393	7.00000	-0.0955	0.1355	0.4119	0.09046

APPENDIX C: AIRFOIL COORDINATES

The following are the coordinates of the airfoils used in the simulations.

Table 3. Airfoil Coordinates

DU 91-W2-250Mod		DU 97-W-300Mod		DU 99-W3-350		DU 99-W3-405	
x/c	y/c	x/c	y/c	x/c	y/c	x/c	y/c
1	0.002131	1	0.00246	1.00000	0.00283	1.00000	0.00347
0.9966	0.003137	0.9966	0.003402	0.99660	0.00378	0.99660	0.00455
0.99314	0.004139	0.99314	0.004371	0.99314	0.00477	0.99314	0.00565
0.98961	0.005151	0.98961	0.005364	0.98961	0.00578	0.98961	0.00678
0.98601	0.006171	0.98601	0.006376	0.98601	0.00683	0.98601	0.00795
0.98235	0.007196	0.98235	0.007398	0.98235	0.00789	0.98235	0.00914
0.97863	0.008224	0.97863	0.008426	0.97863	0.00897	0.97863	0.01035
0.97484	0.009259	0.97484	0.009465	0.97484	0.01006	0.97484	0.01158
0.97098	0.010301	0.97098	0.010513	0.97098	0.01116	0.97098	0.01283
0.96706	0.011348	0.96706	0.01157	0.96706	0.01228	0.96706	0.01410
0.963069	0.012403	0.96307	0.012637	0.96307	0.01342	0.96307	0.01539
0.95902	0.013465	0.95902	0.01371	0.95902	0.01456	0.95902	0.01670
0.954901	0.014539	0.9549	0.014793	0.95490	0.01571	0.95490	0.01803
0.95072	0.015622	0.95072	0.015883	0.95072	0.01688	0.95072	0.01937
0.94647	0.016719	0.94647	0.016984	0.94647	0.01806	0.94647	0.02074
0.94216	0.017829	0.94216	0.018095	0.94216	0.01926	0.94216	0.02212
0.93778	0.018954	0.93778	0.01922	0.93778	0.02046	0.93778	0.02352
0.93333	0.020093	0.93333	0.020358	0.93333	0.02169	0.93333	0.02495
0.92882	0.021245	0.92882	0.02151	0.92882	0.02292	0.92882	0.02639
0.92425	0.02241	0.92425	0.022675	0.92425	0.02419	0.92425	0.02786
0.91961	0.02359	0.91961	0.023856	0.91961	0.02547	0.91961	0.02936
0.9149	0.024787	0.9149	0.025053	0.91490	0.02675	0.91490	0.03087
0.91013	0.025997	0.91013	0.026263	0.91013	0.02807	0.91013	0.03242
0.90529	0.027224	0.90529	0.027489	0.90529	0.02941	0.90529	0.03400
0.90039	0.028464	0.90039	0.028729	0.90039	0.03077	0.90039	0.03560
0.89542	0.029719	0.89542	0.029987	0.89542	0.03214	0.89542	0.03723
0.89039	0.030989	0.89039	0.031259	0.89039	0.03353	0.89039	0.03887
0.88529	0.032274	0.88529	0.032546	0.88529	0.03495	0.88529	0.04056
0.88013	0.033572	0.88013	0.033846	0.88013	0.03638	0.88013	0.04226
0.8749	0.034887	0.8749	0.035163	0.87490	0.03782	0.87490	0.04399
0.86961	0.036215	0.86961	0.036494	0.86961	0.03929	0.86961	0.04575
0.86425	0.037558	0.86425	0.037841	0.86425	0.04079	0.86425	0.04754
0.85882	0.038915	0.85882	0.039205	0.85882	0.04230	0.85882	0.04935
0.85333	0.040285	0.85333	0.040581	0.85333	0.04383	0.85333	0.05119
0.84778	0.041666	0.84778	0.041969	0.84778	0.04538	0.84778	0.05305
0.84216	0.04306	0.84216	0.043373	0.84216	0.04694	0.84216	0.05493

0.83647	0.044467	0.83647	0.044792	0.83647	0.04853	0.83647	0.05685
0.83072	0.045886	0.83072	0.046224	0.83072	0.05013	0.83072	0.05878
0.8249	0.047319	0.8249	0.047669	0.82490	0.05176	0.82490	0.06076
0.81902	0.048765	0.81902	0.049125	0.81902	0.05340	0.81902	0.06275
0.81307	0.050226	0.81307	0.050596	0.81307	0.05506	0.81307	0.06476
0.80706	0.051699	0.80706	0.052078	0.80706	0.05673	0.80706	0.06680
0.80098	0.053185	0.80098	0.053572	0.80098	0.05842	0.80098	0.06886
0.79484	0.054682	0.79484	0.055075	0.79484	0.06013	0.79484	0.07094
0.78863	0.056193	0.78863	0.05659	0.78863	0.06184	0.78863	0.07304
0.78235	0.057714	0.78235	0.058118	0.78235	0.06358	0.78235	0.07517
0.77601	0.059245	0.77601	0.059653	0.77601	0.06531	0.77601	0.07730
0.76961	0.060782	0.76961	0.061198	0.76961	0.06708	0.76961	0.07947
0.76314	0.062328	0.76314	0.062754	0.76314	0.06885	0.76314	0.08165
0.7566	0.063883	0.7566	0.06432	0.75660	0.07064	0.75660	0.08386
0.75	0.065444	0.75	0.065892	0.75000	0.07244	0.75000	0.08608
0.74333	0.067014	0.74333	0.067472	0.74333	0.07426	0.74333	0.08832
0.73667	0.068573	0.73667	0.069044	0.73667	0.07606	0.73667	0.09056
0.73	0.070128	0.73	0.070609	0.73000	0.07786	0.73000	0.09279
0.72333	0.071676	0.72333	0.072166	0.72333	0.07966	0.72333	0.09502
0.71667	0.073216	0.71667	0.073711	0.71667	0.08144	0.71667	0.09724
0.71	0.074751	0.71	0.075251	0.71000	0.08322	0.71000	0.09946
0.70333	0.076276	0.70333	0.076781	0.70333	0.08498	0.70333	0.10166
0.69667	0.077791	0.69667	0.078301	0.69667	0.08674	0.69667	0.10386
0.69	0.079299	0.69	0.079812	0.69000	0.08849	0.69000	0.10605
0.68333	0.080795	0.68333	0.081313	0.68333	0.09022	0.68333	0.10822
0.67667	0.082279	0.67667	0.082801	0.67667	0.09196	0.67667	0.11040
0.67	0.083754	0.67	0.084279	0.67000	0.09368	0.67000	0.11256
0.66333	0.085217	0.66333	0.085748	0.66333	0.09539	0.66333	0.11471
0.65667	0.086666	0.65667	0.087201	0.65667	0.09708	0.65667	0.11685
0.65	0.088103	0.65	0.088644	0.65000	0.09876	0.65000	0.11897
0.64333	0.089527	0.64333	0.090076	0.64333	0.10044	0.64333	0.12109
0.63667	0.090934	0.63667	0.091493	0.63667	0.10210	0.63667	0.12318
0.63	0.092328	0.63	0.092898	0.63000	0.10375	0.63000	0.12527
0.62333	0.093708	0.62333	0.094288	0.62333	0.10538	0.62333	0.12733
0.61667	0.095071	0.61667	0.095662	0.61667	0.10699	0.61667	0.12938
0.61	0.096418	0.61	0.097025	0.61000	0.10859	0.61000	0.13142
0.60333	0.097748	0.60333	0.098372	0.60333	0.11017	0.60333	0.13343
0.59667	0.099058	0.59667	0.099703	0.59667	0.11174	0.59667	0.13543
0.59	0.100353	0.59	0.101019	0.59000	0.11330	0.59000	0.13742
0.58333	0.101632	0.58333	0.102317	0.58333	0.11483	0.58333	0.13938
0.57667	0.10289	0.57667	0.103597	0.57667	0.11634	0.57667	0.14131
0.57	0.10413	0.57	0.104864	0.57000	0.11784	0.57000	0.14323
0.56333	0.105351	0.56333	0.106113	0.56333	0.11931	0.56333	0.14512

0.55667	0.106549	0.55667	0.107342	0.55667	0.12077	0.55667	0.14698
0.55	0.107728	0.55	0.108553	0.55000	0.12220	0.55000	0.14882
0.54333	0.108883	0.54333	0.109746	0.54333	0.12363	0.54333	0.15064
0.53667	0.110014	0.53667	0.110918	0.53667	0.12502	0.53667	0.15242
0.53	0.111124	0.529999	0.112072	0.53000	0.12639	0.53000	0.15417
0.52333	0.112209	0.52333	0.113205	0.52333	0.12775	0.52333	0.15591
0.51667	0.113266	0.51667	0.114316	0.51667	0.12907	0.51667	0.15759
0.51	0.114297	0.51	0.115406	0.51000	0.13037	0.51000	0.15925
0.50333	0.115302	0.50333	0.116476	0.50333	0.13165	0.50333	0.16088
0.49667	0.116279	0.49667	0.11752	0.49667	0.13289	0.49667	0.16246
0.49	0.117228	0.49	0.118543	0.49000	0.13411	0.49000	0.16401
0.48333	0.118151	0.48333	0.119541	0.48333	0.13531	0.48333	0.16553
0.47667	0.119044	0.47667	0.120514	0.47667	0.13648	0.47667	0.16701
0.47	0.119909	0.47	0.121462	0.47000	0.13761	0.47000	0.16844
0.46333	0.120742	0.46333	0.122386	0.46333	0.13873	0.46333	0.16985
0.45667	0.12154	0.45667	0.123282	0.45667	0.13980	0.45667	0.17120
0.45	0.122304	0.45	0.124153	0.45000	0.14086	0.45000	0.17253
0.44333	0.12303	0.44333	0.124996	0.44333	0.14189	0.44333	0.17381
0.43667	0.123717	0.43667	0.125808	0.43667	0.14288	0.43667	0.17504
0.43	0.124364	0.43	0.126591	0.43000	0.14384	0.43000	0.17624
0.42333	0.124971	0.42333	0.127342	0.42333	0.14477	0.42333	0.17739
0.41667	0.125536	0.41667	0.12806	0.41667	0.14566	0.41667	0.17849
0.409999	0.126062	0.41	0.128746	0.41000	0.14653	0.41000	0.17957
0.40333	0.126545	0.40333	0.129398	0.40333	0.14736	0.40333	0.18058
0.39667	0.126985	0.39667	0.130013	0.39667	0.14814	0.39667	0.18154
0.39	0.127382	0.389999	0.130592	0.39000	0.14889	0.39000	0.18246
0.38333	0.127732	0.38333	0.131134	0.38333	0.14960	0.38333	0.18333
0.37667	0.128032	0.37667	0.131635	0.37667	0.15028	0.37667	0.18415
0.37	0.128276	0.37	0.132098	0.37000	0.15091	0.37000	0.18491
0.36333	0.128462	0.36333	0.132519	0.36333	0.15151	0.36333	0.18563
0.35667	0.128582	0.35667	0.132897	0.35667	0.15207	0.35667	0.18629
0.35	0.128635	0.35	0.133232	0.35000	0.15258	0.35000	0.18690
0.34333	0.128618	0.34333	0.133522	0.34333	0.15306	0.34333	0.18746
0.33667	0.128532	0.33667	0.133766	0.33667	0.15351	0.33667	0.18797
0.33	0.128374	0.33	0.133961	0.33000	0.15391	0.33000	0.18842
0.32333	0.128147	0.32333	0.134107	0.32333	0.15426	0.32333	0.18881
0.31667	0.12785	0.31667	0.1342	0.31667	0.15457	0.31667	0.18914
0.31	0.127486	0.31	0.13424	0.31000	0.15482	0.31000	0.18940
0.30333	0.127054	0.30333	0.134223	0.30333	0.15502	0.30333	0.18961
0.29667	0.12656	0.29667	0.134147	0.29667	0.15516	0.29667	0.18973
0.29	0.126	0.29	0.134011	0.29000	0.15524	0.29000	0.18979
0.28333	0.125376	0.283329	0.133811	0.28333	0.15525	0.28333	0.18977
0.27667	0.124688	0.27667	0.133545	0.27667	0.15520	0.27667	0.18968

0.27	0.123936	0.27	0.133207	0.27000	0.15507	0.27000	0.18950
0.26333	0.12312	0.26333	0.132796	0.26333	0.15486	0.26333	0.18924
0.25667	0.122242	0.25667	0.132308	0.25667	0.15457	0.25667	0.18890
0.25	0.121298	0.25	0.131737	0.25000	0.15419	0.25000	0.18845
0.24342	0.120303	0.24342	0.131086	0.24342	0.15372	0.24342	0.18791
0.23693	0.119261	0.23693	0.130356	0.23693	0.15316	0.23693	0.18729
0.23053	0.118173	0.23053	0.129548	0.23053	0.15250	0.23053	0.18657
0.22421	0.117039	0.22421	0.128664	0.22421	0.15175	0.22421	0.18575
0.21798	0.115863	0.21798	0.127707	0.21798	0.15094	0.21798	0.18487
0.21184	0.114648	0.21184	0.126684	0.21184	0.15002	0.21184	0.18388
0.20579	0.113395	0.20579	0.125594	0.20579	0.14904	0.20579	0.18282
0.19982	0.112103	0.19982	0.124443	0.19982	0.14798	0.19982	0.18167
0.19395	0.110779	0.19395	0.123236	0.19395	0.14686	0.19395	0.18046
0.18816	0.109419	0.18816	0.121974	0.18816	0.14566	0.18816	0.17916
0.18245	0.108025	0.18245	0.12066	0.18245	0.14439	0.18245	0.17778
0.17684	0.106604	0.17684	0.1193	0.17684	0.14308	0.17684	0.17634
0.17131	0.105151	0.17131	0.117892	0.17131	0.14169	0.17131	0.17482
0.16587	0.103672	0.16587	0.11644	0.16587	0.14025	0.16587	0.17323
0.16052	0.102168	0.16052	0.114948	0.16052	0.13875	0.16052	0.17158
0.15526	0.100639	0.15526	0.113417	0.15526	0.13721	0.15526	0.16987
0.15008	0.099085	0.15008	0.111846	0.15008	0.13561	0.15008	0.16809
0.14499	0.097509	0.14499	0.11024	0.14499	0.13396	0.14499	0.16625
0.13999	0.095913	0.13999	0.108599	0.13999	0.13226	0.13999	0.16436
0.13508	0.094297	0.13508	0.106925	0.13508	0.13052	0.13508	0.16240
0.13026	0.092663	0.13026	0.105221	0.13026	0.12873	0.13026	0.16038
0.12552	0.091008	0.12552	0.103484	0.12552	0.12689	0.12552	0.15831
0.12087	0.089336	0.12087	0.101719	0.12087	0.12502	0.12087	0.15619
0.11631	0.087651	0.11631	0.099929	0.11631	0.12311	0.11631	0.15402
0.11183	0.085948	0.11183	0.09811	0.11183	0.12115	0.11183	0.15179
0.10745	0.084235	0.10745	0.096271	0.10745	0.11917	0.10745	0.14953
0.10315	0.082507	0.10315	0.094406	0.10315	0.11715	0.10315	0.14722
0.09893	0.080764	0.09893	0.092517	0.09893	0.11509	0.09893	0.14485
0.09481	0.079015	0.09481	0.090612	0.09481	0.11299	0.09481	0.14243
0.09077	0.077252	0.09077	0.088685	0.09077	0.11087	0.09077	0.13998
0.08683	0.075487	0.08683	0.086745	0.08683	0.10871	0.08683	0.13748
0.08297	0.07371	0.08297	0.084783	0.08297	0.10652	0.08297	0.13493
0.07919	0.071922	0.07919	0.082803	0.07919	0.10430	0.07919	0.13234
0.07551	0.070134	0.07551	0.080817	0.07551	0.10207	0.07551	0.12972
0.07191	0.068338	0.07191	0.078813	0.07191	0.09979	0.07191	0.12705
0.0684	0.066539	0.0684	0.076798	0.06840	0.09750	0.06840	0.12435
0.06498	0.064738	0.06498	0.074774	0.06498	0.09517	0.06498	0.12161
0.06164	0.062932	0.06164	0.072737	0.06164	0.09284	0.06164	0.11884
0.0584	0.061132	0.0584	0.0707	0.05840	0.09048	0.05840	0.11603

0.05524	0.059329	0.05524	0.068651	0.05524	0.08809	0.05524	0.11319
0.05217	0.057528	0.05217	0.066598	0.05217	0.08569	0.05217	0.11031
0.04918	0.055726	0.04918	0.064535	0.04918	0.08327	0.04918	0.10740
0.04629	0.053932	0.04629	0.062478	0.04629	0.08084	0.04629	0.10447
0.04348	0.052137	0.04348	0.060415	0.04348	0.07839	0.04348	0.10150
0.04076	0.050349	0.04076	0.058352	0.04076	0.07592	0.04076	0.09851
0.03812	0.048561	0.03812	0.056286	0.03812	0.07345	0.03812	0.09549
0.03558	0.046787	0.03558	0.05423	0.03558	0.07096	0.03558	0.09246
0.03312	0.045017	0.03312	0.052173	0.03312	0.06847	0.03312	0.08940
0.03075	0.043257	0.03075	0.050123	0.03075	0.06597	0.03075	0.08632
0.02847	0.041508	0.02847	0.048081	0.02847	0.06348	0.02847	0.08324
0.02627	0.039764	0.02627	0.046039	0.02627	0.06097	0.02627	0.08013
0.02417	0.03804	0.02417	0.044018	0.02417	0.05847	0.02417	0.07701
0.02215	0.036323	0.02215	0.041998	0.02215	0.05596	0.02215	0.07387
0.02022	0.034622	0.02022	0.039992	0.02022	0.05344	0.02022	0.07070
0.01837	0.032929	0.01837	0.037991	0.01837	0.05091	0.01837	0.06751
0.01662	0.031264	0.01662	0.036018	0.01662	0.04841	0.01662	0.06433
0.01495	0.029608	0.01495	0.034051	0.01495	0.04589	0.01495	0.06111
0.01337	0.027973	0.01337	0.032107	0.01337	0.04339	0.01337	0.05790
0.01187	0.026346	0.01187	0.03017	0.01187	0.04088	0.01187	0.05468
0.01047	0.024753	0.01047	0.028266	0.01047	0.03840	0.01047	0.05148
0.00915	0.023169	0.00915	0.026373	0.00915	0.03591	0.00915	0.04826
0.00792	0.021609	0.00792	0.024503	0.00792	0.03343	0.00792	0.04505
0.00678	0.020072	0.00678	0.022664	0.00678	0.03096	0.00678	0.04181
0.00572	0.018547	0.00572	0.02083	0.00572	0.02845	0.00572	0.03847
0.00476	0.017056	0.00476	0.019041	0.00476	0.02592	0.00476	0.03502
0.00388	0.015569	0.00388	0.017251	0.00388	0.02329	0.00388	0.03133
0.00309	0.014094	0.00309	0.01548	0.00309	0.02056	0.00309	0.02736
0.00238	0.012606	0.00238	0.0137	0.00238	0.01774	0.00238	0.02318
0.00177	0.011096	0.00177	0.011937	0.00177	0.01503	0.00177	0.01920
0.00124	0.009445	0.00124	0.010102	0.00124	0.01240	0.00124	0.01552
0.0008	0.007656	0.0008	0.008201	0.00080	0.00990	0.00080	0.01217
0.00044	0.005684	0.00044	0.006121	0.00044	0.00733	0.00044	0.00892
0.00018	0.003633	0.00018	0.003902	0.00018	0.00465	0.00018	0.00563
0	0	0	0	0.00000	0.00000	0.00000	0.00000
0.00018	-0.0036	0.00018	-0.00382	0.00018	-0.00461	0.00018	-0.00567
0.00044	-0.00572	0.00044	-0.00601	0.00044	-0.00726	0.00044	-0.00905
0.0008	-0.00778	0.0008	-0.00815	0.00080	-0.00990	0.00080	-0.01247
0.00124	-0.00974	0.00124	-0.01017	0.00124	-0.01246	0.00124	-0.01591
0.00177	-0.01169	0.00177	-0.01216	0.00177	-0.01509	0.00177	-0.01956
0.00238	-0.01359	0.00238	-0.01412	0.00238	-0.01776	0.00238	-0.02333
0.00309	-0.01549	0.00309	-0.01611	0.00309	-0.02049	0.00309	-0.02716
0.00388	-0.01736	0.00388	-0.01811	0.00388	-0.02317	0.00388	-0.03085

0.00476	-0.01921	0.00476	-0.02014	0.00476	-0.02585	0.00476	-0.03442
0.00572	-0.02104	0.00572	-0.02217	0.00572	-0.02848	0.00572	-0.03783
0.00678	-0.02288	0.00678	-0.02423	0.00678	-0.03112	0.00678	-0.04120
0.00792	-0.0247	0.00792	-0.0263	0.00792	-0.03376	0.00792	-0.04453
0.00915	-0.02652	0.00915	-0.0284	0.00915	-0.03642	0.00915	-0.04785
0.01047	-0.02835	0.01047	-0.03053	0.01047	-0.03911	0.01047	-0.05117
0.01187	-0.03019	0.01187	-0.03267	0.01187	-0.04178	0.01187	-0.05447
0.01337	-0.03205	0.01337	-0.03485	0.01337	-0.04450	0.01337	-0.05781
0.01495	-0.03392	0.01495	-0.03705	0.01495	-0.04721	0.01495	-0.06113
0.01662	-0.03581	0.01662	-0.03929	0.01662	-0.04995	0.01662	-0.06446
0.01837	-0.0377	0.01837	-0.04154	0.01837	-0.05269	0.01837	-0.06775
0.02022	-0.03961	0.02022	-0.04385	0.02022	-0.05547	0.02022	-0.07107
0.02215	-0.04153	0.02215	-0.04617	0.02215	-0.05825	0.02215	-0.07437
0.02417	-0.04345	0.02417	-0.04852	0.02417	-0.06105	0.02417	-0.07766
0.02627	-0.04537	0.02627	-0.05088	0.02627	-0.06386	0.02627	-0.08092
0.02847	-0.0473	0.02847	-0.05328	0.02847	-0.06670	0.02847	-0.08421
0.03075	-0.04921	0.03075	-0.05569	0.03075	-0.06955	0.03075	-0.08748
0.03312	-0.05112	0.03312	-0.05813	0.03312	-0.07244	0.03312	-0.09076
0.03558	-0.05302	0.03558	-0.0606	0.03558	-0.07536	0.03558	-0.09406
0.03812	-0.05491	0.03812	-0.06308	0.03812	-0.07828	0.03812	-0.09733
0.04076	-0.05679	0.04076	-0.06559	0.04076	-0.08125	0.04076	-0.10064
0.04348	-0.05865	0.04348	-0.06811	0.04348	-0.08422	0.04348	-0.10392
0.04629	-0.06051	0.04629	-0.07064	0.04629	-0.08720	0.04629	-0.10720
0.04918	-0.06234	0.04918	-0.07318	0.04918	-0.09020	0.04918	-0.11047
0.05217	-0.06418	0.05217	-0.07574	0.05217	-0.09321	0.05217	-0.11374
0.05524	-0.066	0.05524	-0.07831	0.05524	-0.09622	0.05524	-0.11698
0.0584	-0.0678	0.0584	-0.08088	0.05840	-0.09925	0.05840	-0.12023
0.06164	-0.0696	0.06164	-0.08345	0.06164	-0.10225	0.06164	-0.12344
0.06498	-0.07139	0.06498	-0.08604	0.06498	-0.10528	0.06498	-0.12665
0.0684	-0.07316	0.0684	-0.08862	0.06840	-0.10829	0.06840	-0.12982
0.07191	-0.07492	0.07191	-0.09121	0.07191	-0.11131	0.07191	-0.13299
0.07551	-0.07668	0.07551	-0.09379	0.07551	-0.11431	0.07551	-0.13612
0.07919	-0.07842	0.07919	-0.09637	0.07919	-0.11730	0.07919	-0.13922
0.08297	-0.08015	0.08297	-0.09895	0.08297	-0.12028	0.08297	-0.14230
0.08683	-0.08186	0.08683	-0.10152	0.08683	-0.12325	0.08683	-0.14535
0.09077	-0.08356	0.09077	-0.10408	0.09077	-0.12619	0.09077	-0.14835
0.09481	-0.08525	0.09481	-0.10665	0.09481	-0.12914	0.09481	-0.15135
0.09893	-0.08692	0.09893	-0.10919	0.09893	-0.13205	0.09893	-0.15429
0.10315	-0.08858	0.10315	-0.11173	0.10315	-0.13494	0.10315	-0.15720
0.10745	-0.09022	0.10745	-0.11425	0.10745	-0.13780	0.10745	-0.16006
0.11183	-0.09182	0.11183	-0.11675	0.11183	-0.14065	0.11183	-0.16289
0.11631	-0.09342	0.11631	-0.11923	0.11631	-0.14345	0.11631	-0.16567
0.12087	-0.09498	0.12087	-0.12169	0.12087	-0.14624	0.12087	-0.16842

0.12552	-0.09652	0.12552	-0.12412	0.12552	-0.14898	0.12552	-0.17111
0.13026	-0.09803	0.13026	-0.12652	0.13026	-0.15169	0.13026	-0.17376
0.13508	-0.09951	0.13508	-0.12888	0.13508	-0.15435	0.13508	-0.17635
0.13999	-0.10095	0.13999	-0.13121	0.13999	-0.15697	0.13999	-0.17890
0.14499	-0.10237	0.14499	-0.1335	0.14499	-0.15954	0.14499	-0.18137
0.15008	-0.10376	0.15008	-0.13576	0.15008	-0.16207	0.15008	-0.18380
0.155259	-0.10511	0.15526	-0.13797	0.15526	-0.16454	0.15526	-0.18616
0.16052	-0.10642	0.16052	-0.14014	0.16052	-0.16696	0.16052	-0.18847
0.16587	-0.10769	0.16587	-0.14225	0.16587	-0.16932	0.16587	-0.19070
0.17131	-0.10892	0.17131	-0.14432	0.17131	-0.17163	0.17131	-0.19287
0.17684	-0.11011	0.17684	-0.14633	0.17684	-0.17387	0.17684	-0.19496
0.18245	-0.11126	0.18245	-0.14828	0.18245	-0.17603	0.18245	-0.19698
0.18816	-0.11236	0.18816	-0.15017	0.18816	-0.17814	0.18816	-0.19894
0.19395	-0.11341	0.19395	-0.15198	0.19395	-0.18015	0.19395	-0.20080
0.19982	-0.11441	0.19982	-0.15371	0.19982	-0.18207	0.19982	-0.20257
0.20579	-0.11536	0.20579	-0.15537	0.20579	-0.18391	0.20579	-0.20425
0.21184	-0.11626	0.21184	-0.15693	0.21184	-0.18564	0.21184	-0.20584
0.21798	-0.1171	0.217981	-0.1584	0.21798	-0.18727	0.21798	-0.20733
0.22421	-0.11789	0.22421	-0.15976	0.22421	-0.18877	0.22421	-0.20870
0.23053	-0.11862	0.23053	-0.16101	0.23053	-0.19015	0.23053	-0.20996
0.23693	-0.11929	0.23693	-0.16214	0.23693	-0.19140	0.23693	-0.21110
0.24342	-0.1199	0.24342	-0.16314	0.24342	-0.19250	0.24342	-0.21210
0.25	-0.12045	0.25	-0.16399	0.25000	-0.19343	0.25000	-0.21297
0.25667	-0.12094	0.25667	-0.1647	0.25667	-0.19420	0.25667	-0.21370
0.26333	-0.12135	0.26333	-0.16526	0.26333	-0.19481	0.26333	-0.21429
0.27	-0.12168	0.27	-0.16567	0.27000	-0.19525	0.27000	-0.21472
0.27667	-0.12195	0.27667	-0.16592	0.27667	-0.19552	0.27667	-0.21501
0.28333	-0.12214	0.28333	-0.16602	0.28333	-0.19562	0.28333	-0.21515
0.29	-0.12227	0.29	-0.16598	0.29000	-0.19556	0.29000	-0.21516
0.29667	-0.12232	0.29667	-0.1658	0.29667	-0.19535	0.29667	-0.21502
0.30333	-0.12231	0.30333	-0.16548	0.30333	-0.19498	0.30333	-0.21476
0.31	-0.12222	0.31	-0.16503	0.31000	-0.19448	0.31000	-0.21437
0.31667	-0.12207	0.31667	-0.16445	0.31667	-0.19383	0.31667	-0.21384
0.32333	-0.12186	0.32333	-0.16374	0.32333	-0.19303	0.32333	-0.21320
0.33	-0.12157	0.33	-0.16291	0.33000	-0.19211	0.33000	-0.21243
0.33667	-0.12123	0.33667	-0.16198	0.33667	-0.19107	0.33667	-0.21155
0.34333	-0.12082	0.34333	-0.16094	0.34333	-0.18991	0.34333	-0.21057
0.35	-0.12034	0.35	-0.1598	0.35000	-0.18864	0.35000	-0.20948
0.35667	-0.11981	0.35667	-0.15855	0.35667	-0.18725	0.35667	-0.20827
0.36333	-0.11922	0.36333	-0.15722	0.36333	-0.18577	0.36333	-0.20697
0.37	-0.11857	0.37	-0.1558	0.37000	-0.18418	0.37000	-0.20556
0.37667	-0.11785	0.37667	-0.15429	0.37667	-0.18251	0.37667	-0.20407
0.38333	-0.11708	0.38333	-0.1527	0.38333	-0.18074	0.38333	-0.20248

0.39	-0.11625	0.39	-0.15104	0.39000	-0.17889	0.39000	-0.20081
0.39667	-0.11537	0.39667	-0.14931	0.39667	-0.17695	0.39667	-0.19904
0.40333	-0.11442	0.40333	-0.14752	0.40333	-0.17496	0.40333	-0.19720
0.410001	-0.11342	0.41	-0.14566	0.41000	-0.17288	0.41000	-0.19527
0.41667	-0.11236	0.41667	-0.14374	0.41667	-0.17074	0.41667	-0.19327
0.42333	-0.11124	0.42333	-0.14178	0.42333	-0.16855	0.42333	-0.19119
0.43	-0.11006	0.43	-0.13977	0.43000	-0.16631	0.43000	-0.18905
0.43667	-0.10881	0.43667	-0.13772	0.43667	-0.16402	0.43667	-0.18683
0.44333	-0.10752	0.44333	-0.13562	0.44333	-0.16167	0.44333	-0.18454
0.45	-0.10615	0.45	-0.13348	0.45000	-0.15929	0.45000	-0.18219
0.45667	-0.10474	0.45667	-0.1313	0.45667	-0.15684	0.45667	-0.17976
0.46333	-0.10326	0.46333	-0.12908	0.46333	-0.15436	0.46333	-0.17727
0.47	-0.10173	0.47	-0.12683	0.47000	-0.15185	0.47000	-0.17473
0.47667	-0.10015	0.47667	-0.12456	0.47667	-0.14930	0.47667	-0.17212
0.48333	-0.09851	0.483331	-0.12225	0.48333	-0.14671	0.48333	-0.16945
0.49	-0.09682	0.49	-0.11992	0.49000	-0.14410	0.49000	-0.16673
0.49667	-0.09508	0.49667	-0.11757	0.49667	-0.14147	0.49667	-0.16397
0.50333	-0.09329	0.50333	-0.1152	0.50333	-0.13881	0.50333	-0.16115
0.51	-0.09145	0.51	-0.11281	0.51000	-0.13613	0.51000	-0.15828
0.51667	-0.08956	0.51667	-0.1104	0.51667	-0.13342	0.51667	-0.15537
0.523329	-0.08764	0.52333	-0.10799	0.52333	-0.13071	0.52333	-0.15242
0.53	-0.08567	0.53	-0.10555	0.53000	-0.12797	0.53000	-0.14942
0.53667	-0.08366	0.53667	-0.1031	0.53667	-0.12522	0.53667	-0.14639
0.54333	-0.08162	0.54333	-0.10065	0.54333	-0.12247	0.54333	-0.14333
0.55	-0.07953	0.55	-0.09818	0.55000	-0.11970	0.55000	-0.14024
0.55667	-0.07742	0.55667	-0.0957	0.55667	-0.11692	0.55667	-0.13713
0.56333	-0.07527	0.56333	-0.09321	0.56333	-0.11413	0.56333	-0.13399
0.57	-0.07309	0.57	-0.09071	0.57000	-0.11133	0.57000	-0.13083
0.57667	-0.07088	0.57667	-0.08821	0.57667	-0.10853	0.57667	-0.12765
0.58333	-0.06865	0.58333	-0.08571	0.58333	-0.10573	0.58333	-0.12446
0.589999	-0.06639	0.59	-0.0832	0.59000	-0.10293	0.59000	-0.12125
0.59667	-0.0641	0.59667	-0.0807	0.59667	-0.10014	0.59667	-0.11804
0.60333	-0.0618	0.60333	-0.07819	0.60333	-0.09734	0.60333	-0.11482
0.61	-0.05948	0.61	-0.07569	0.61000	-0.09456	0.61000	-0.11160
0.61667	-0.05713	0.61667	-0.07319	0.61667	-0.09178	0.61667	-0.10838
0.62333	-0.05478	0.62333	-0.0707	0.62333	-0.08901	0.62333	-0.10515
0.63	-0.05242	0.63	-0.0682	0.63000	-0.08624	0.63000	-0.10192
0.63667	-0.05005	0.63667	-0.06572	0.63667	-0.08348	0.63667	-0.09870
0.64333	-0.04767	0.64333	-0.06325	0.64333	-0.08074	0.64333	-0.09549
0.65	-0.0453	0.65	-0.06079	0.65000	-0.07801	0.65000	-0.09228
0.65667	-0.04293	0.65667	-0.05834	0.65667	-0.07529	0.65667	-0.08909
0.66333	-0.04057	0.66333	-0.0559	0.66333	-0.07257	0.66333	-0.08590
0.67	-0.03822	0.67	-0.05347	0.67000	-0.06987	0.67000	-0.08274

0.67667	-0.03588	0.67667	-0.05106	0.67667	-0.06719	0.67667	-0.07958
0.68333	-0.03357	0.68333	-0.04867	0.68333	-0.06452	0.68333	-0.07645
0.69	-0.03127	0.69	-0.04629	0.69000	-0.06186	0.69000	-0.07333
0.69667	-0.029	0.69667	-0.04394	0.69667	-0.05922	0.69667	-0.07024
0.70333	-0.02676	0.70333	-0.04161	0.70333	-0.05661	0.70333	-0.06717
0.71	-0.02456	0.71	-0.03931	0.71000	-0.05401	0.71000	-0.06413
0.71667	-0.02238	0.71667	-0.03703	0.71667	-0.05144	0.71667	-0.06112
0.72333	-0.02026	0.72333	-0.03478	0.72333	-0.04889	0.72333	-0.05814
0.73	-0.01817	0.73	-0.03256	0.73000	-0.04637	0.73000	-0.05519
0.73667	-0.01614	0.73667	-0.03037	0.73667	-0.04386	0.73667	-0.05228
0.74333	-0.01416	0.74333	-0.02822	0.74333	-0.04140	0.74333	-0.04941
0.75	-0.01223	0.75	-0.0261	0.75000	-0.03896	0.75000	-0.04658
0.75667	-0.01038	0.75667	-0.02405	0.75667	-0.03658	0.75667	-0.04382
0.76333	-0.00861	0.76333	-0.02205	0.76333	-0.03425	0.76333	-0.04114
0.76967	-0.00692	0.76967	-0.02013	0.76967	-0.03199	0.76967	-0.03853
0.77601	-0.00532	0.77601	-0.01827	0.77601	-0.02979	0.77601	-0.03600
0.78235	-0.00381	0.78235	-0.01647	0.78235	-0.02765	0.78235	-0.03354
0.78863	-0.00238	0.78863	-0.01474	0.78863	-0.02557	0.78863	-0.03116
0.79484	-0.00103	0.79484	-0.01309	0.79484	-0.02357	0.79484	-0.02887
0.80098	0.000232	0.80098	-0.0115	0.80098	-0.02162	0.80098	-0.02665
0.80706	0.001409	0.80706	-0.00998	0.80706	-0.01974	0.80706	-0.02452
0.81307	0.002501	0.81307	-0.00854	0.81307	-0.01794	0.81307	-0.02247
0.819019	0.00351	0.81902	-0.00717	0.81902	-0.01621	0.81902	-0.02050
0.8249	0.004437	0.8249	-0.00586	0.82490	-0.01454	0.82490	-0.01862
0.83072	0.005286	0.83072	-0.00462	0.83072	-0.01294	0.83072	-0.01681
0.83647	0.006056	0.83647	-0.00346	0.83647	-0.01142	0.83647	-0.01510
0.84216	0.00675	0.84216	-0.00236	0.84216	-0.00996	0.84216	-0.01346
0.84778	0.007368	0.84778	-0.00133	0.84778	-0.00858	0.84778	-0.01191
0.85333	0.007912	0.85333	-0.00037	0.85333	-0.00727	0.85333	-0.01045
0.85882	0.008387	0.85882	0.000521	0.85882	-0.00604	0.85882	-0.00907
0.86425	0.008792	0.86425	0.001342	0.86425	-0.00487	0.86425	-0.00776
0.86961	0.009128	0.86961	0.002095	0.86961	-0.00377	0.86961	-0.00653
0.8749	0.009399	0.8749	0.002779	0.87490	-0.00276	0.87490	-0.00539
0.88013	0.009606	0.88013	0.0034	0.88013	-0.00182	0.88013	-0.00434
0.88529	0.009749	0.88529	0.003954	0.88529	-0.00095	0.88529	-0.00335
0.89039	0.009831	0.89039	0.004444	0.89039	-0.00014	0.89039	-0.00245
0.89542	0.009853	0.89542	0.004872	0.89542	0.00061	0.89542	-0.00160
0.90039	0.009816	0.90039	0.005241	0.90039	0.00128	0.90039	-0.00085
0.90529	0.00972	0.90529	0.005552	0.90529	0.00189	0.90529	-0.00015
0.91013	0.00957	0.91013	0.005804	0.91013	0.00243	0.91013	0.00046
0.9149	0.009364	0.9149	0.005999	0.91490	0.00293	0.91490	0.00103
0.91961	0.009104	0.91961	0.006137	0.91961	0.00335	0.91961	0.00151
0.92425	0.008796	0.92425	0.006221	0.92425	0.00370	0.92425	0.00193

0.92882	0.00844	0.92882	0.00625	0.92882	0.00401	0.92882	0.00229
0.93333	0.008039	0.93333	0.006226	0.93333	0.00425	0.93333	0.00258
0.93778	0.007596	0.93778	0.006149	0.93778	0.00441	0.93778	0.00279
0.94216	0.007115	0.94216	0.006016	0.94216	0.00452	0.94216	0.00295
0.94647	0.006602	0.94647	0.005828	0.94647	0.00455	0.94647	0.00303
0.95072	0.006059	0.95072	0.005582	0.95072	0.00451	0.95072	0.00303
0.9549	0.005491	0.9549	0.005282	0.95490	0.00439	0.95490	0.00296
0.95902	0.0049	0.95902	0.004928	0.95902	0.00420	0.95902	0.00282
0.96307	0.004291	0.96307	0.004517	0.96307	0.00394	0.96307	0.00261
0.96706	0.003666	0.96706	0.004046	0.96706	0.00358	0.96706	0.00232
0.97098	0.00303	0.97098	0.003521	0.97098	0.00315	0.97098	0.00194
0.97484	0.002384	0.97484	0.002942	0.97484	0.00264	0.97484	0.00149
0.97863	0.001734	0.97863	0.002312	0.97863	0.00206	0.97863	0.00098
0.98235	0.001083	0.98235	0.001634	0.98235	0.00141	0.98235	0.00040
0.98601	0.000432	0.98601	0.000904	0.98601	0.00069	0.98601	-0.00025
0.98961	-0.00022	0.98961	0.000121	0.98961	-0.00011	0.98961	-0.00097
0.99314	-0.00086	0.99314	-0.00071	0.99314	-0.00097	0.99314	-0.00176
0.9966	-0.00149	0.9966	-0.00158	0.99660	-0.00190	0.99660	-0.00261
1	-0.00213	1	-0.00246	1	-0.00283	1	-0.00347

Distribution

1	MS0825	Mathew Barone	Org. 1515 (electronic copy)
1	MS0836	Stefan Domino	Org. 1541 (electronic copy)
1	MS1124	David Minster	Org. 6121 (electronic copy)
1	MS9957	Amanda Dodd	Org. 8253 (electronic copy)
1	MS0899	Technical Library	Org. 9536 (electronic copy)

